Crab By-Product Hydrothermal Carbonization and Hydrochar Characterization

by

Nadyana Incan, B.Eng.

A Thesis Submitted to the School of Graduate Studies

in partial fulfilment of the requirements of the degree of

Master of Engineering

Process Engineering

Faculty of Engineering & Applied Science

Memorial University of Newfoundland

January, 2024

St. John’s, Newfoundland, Canada

Abstract

In Atlantic Canada, fisheries and seafood processing are major industries contributing to the local economy. Shellfish industry, particularly snow crab, make up a significant waste stream from this industry. The high moisture content of the crab by-product makes it challenging to valorize. Hydrothermal carbonization (HTC), a hydrothermal process involving biomass in the presence of water, is a simple and effective means of valorizing high moisture biomass, which could negate all or part of the drying process. The main product of HTC is a solid called hydrochar, which has various applications (for example, fuel and bioadsorbent).

In this thesis, the hydrochar properties produced from snow crab (*Chionoecetes Opilio*) are studied to determine the effect of operating conditions on crab hydrochar and assess the best applications. Chapter 2 of this thesis includes a review of the literature on the existing hydrothermal carbonization of various feedstock from lignocellulosic non-lignocellulosic to marine biomass. The findings show that the valorization of marine biomass, especially crab by-products, is rarely studied. Moreover, many of the studies use pre-treatment methods such as deproteinization, deacetylation, or demineralization, which can be unsuitable and costly for remote locations of processing plants.

Chapter 3 is the bulk of the thesis experimental work and discussion. Crab hydrochar was synthesized from snow crab processing by-product using HTC over a range of temperatures (180 - 260 °C), residence times (0.5 – 3 h), and water to biomass ratios (2 - 4). In addition to the experiments performed using dried, ground RC, WC was also tested at specific operating condition to study the effects of drying. The hydrochar yield was determined, and feedstock and the hydrochar were compared via ash content (wt %, db), surface area (m^2/g), surface groups (FTIR), trace elements, pH, composition (CHN, wt%, db), and minerals (XRD). In general, the hydrochar (solid) yield decreased as water ratio and temperature increased, reflecting the feedstock's increased thermal and water decomposition. Hydrochar has a higher ash content than the feedstock, making it less desirable for fuel application. The increase in hydrochar BET surface area (maximum of 26 m^2/g at 260 °C, water ratio 3 and 30 min) and the presence of functional groups in the hydrochar showed potential to facilitate chemisorption as a bioadsorbent. The hydrochar also may suitable for soil amendment application due to its minerals content and soil pollutant adsorption capability.

Acknowledgment

The research presented in this thesis could not have been performed without the funding provided by the Ocean Frontier Institute (OFI), the Memorial University of Newfoundland School of Graduate Studies, and the Memorial University of Newfoundland Faculty of Engineering & Applied Science.

I would like to express my gratitude to my supervisors for this project, Dr. Kelly Hawboldt and Dr. Stephanie MacQuarrie. Their continued support and guidance in this project were the key aspect in creating this thesis and helping me grow as a researcher and as a person. Furthermore, I would like to thank Dr. Hawboldt for her encouragement while I am pursuing this research, with her support I am able to meet and work with a lot of great people during my study. I am very lucky to have been able to study under her supervision.

I would also like to extend gratitude towards the people in Memorial University's Core Research Equipment and Instrument Training (CREAIT) Network who helped to performed certain analysis, as well as Dr. Ali Shafiee and many people in Dr. MacQuarrie's team in Cape Berton University who helped performed Fourier-Transform Infrared Spectroscopy analysis. I extend sincere gratitude to Louisbourg Seafoods Limited for providing the crab by-product used in the experiments as well. Other individuals who may give advice and help me during my research include fellow students to whom I thanked, including David Hopkins, Zahra Ghanbarpour, Cedric Boschert, and work term student Daniel Kelly.

Getting through my study required more than academic support, and I have my closest people to thank for listening to and, at times, having to tolerate me over the past three years. I cannot begin to express my gratitude and appreciation for their kindness and support. Alex McNeil for his support during the time I spent at the University and writing this thesis. I would also like to thank Emma Brown who opened both her home and arms to me when I first arrived in the city and her friendship. Last, I would like to thank my mother and my best friend for her unwavering support throughout this thesis. Her moral support throughout this thesis was important in helping me complete this degree.

Table of Contents

List of Figures

List of Tables

List of Abbreviations

2FI	Two factor interactions
AICc	Akaike information criterion
ANOVA	Analysis of variance
ARC	Aquatic Research Cluster
BBD	Box–behnken design
BET	Brunauer-Emmett-Teller
DE	Design Expert
DoE	Design of experiment
EDS	Energy Dispersive Spectroscopy
FTIR	Fourier Transform-Infrared Spectroscopy
HTC	Hydrothermal carbonization
HTG	Hydrothermal gasification
HTL	Hydrothermal liquefaction
MHTC	Microwave hydrothermal carbonization
ICP-OES	Ion-coupled plasma optical emission spectroscopy
RC	Raw crab
RSM	Response surface method
SEM	Scanning electron microscope
WC	Wet crab
XPS	X-ray photoelectron spectroscopy
XRD	X-Ray diffraction

Chapter 1 - Introduction

Fisheries are critical economic driver in Atlantic Canada [1, 2]. Focusing on crab, in 2019, crab total landed product was 26.9 tonnes and increased to 38.4 tonnes in 2021 [3, 4]. However, up to 50 wt% of landed product lost as waste [5, 6]. This crab by-product is high in moisture content ranging from 50-78 wt% and it is decaying fast and has foul odour [7, 8, 9, 10]. The high moisture content led to costly wet waste disposal or drying pre-treatment. Furthermore, crab by-product degradation releases methane, ammonia, and nitrates which if not manage properly can pollute soil and air [10]. On top of that, remote location of processing plant poses a challenge to waste disposal [10]. Meanwhile this crab by-product still has some values. It consists of chitin, protein, lipid, and minerals which has potential for further valorisation [7, 11, 9, 12, 13, 14, 15, 16, 10, 17]. This is why, we need an economic and environmentally sustainable valorisation method that suited for high moisture waste stream.

Hydrothermal processing, where the biomass is thermally decomposed in the presence of water, is a potential treatment method that suitable for high moisture feedstock. Unlike other thermal processes (such as pyrolysis), hydrothermal processing could eliminate all or part of the drying pre-treatment and produce high-value compounds. Hydrothermal processes include hydrothermal carbonization (HTC), hydrothermal liquefaction (HTL), and hydrothermal gasification (HTG) [18, 19, 20, 21]. The main focus in this study is HTC, which produced a solid product called hydrochar. HTC was chosen due to its advantages compared to HTL, and HTG include: HTC is a milder process compared to HTL and HTG, and the process is well developed with large-scale HTC plants in operation [22, 23, 24]. The hydrochar product has various applications, from fuel to the treatment of wastewater and gas streams [24]. Furthermore, HTC research where marine biomass is the feedstock is limited and much of the work is on pretreated biomass/by-product. Enzymatic, deproteinization, deacetylation, or decalcification are commonly used as a pretreatment prior to HTC in shellfish [25, 26, 27, 28, 29]. The common pretreatment method is potentially suitable for recovering other value-added products. However, these pretreatments may be costly and compromising overall process feasibility.

1.1.Scope and Objectives

Research on the use of marine based feedstock as a hydrothermal carbonization (HTC) feedstock is limited, despite the abundance of crab by-product in seafood industry. This thesis seeks to study the production and use of hydrochar made from snow crab (*Chionoecetes Opilio*) as a potential valorisation effort. The objectives of the thesis are listed below:

- Study the effect of HTC process conditions variation (temperature, residence time, and water to biomass ratio) on crab by-product hydrochar
- Perform characterizations on the crab by-product hydrochar

1.2.Thesis Structure

Chapter 2 presents a literature review comparing hydrochar made from pulp and paper sludge and sewage sludge to marine-based (macroalgae and crustacean shell) HTC. The review begins by discussing the composition of sludges and marine-based materials, and how they are difference from each other. Then, HTC and hydrochar properties of well-studied material (pulp and paper sludge) are discussed followed by marine-based HTC and hydrochar in literature found to date. A modified version of this chapter will be submitted for publication.

Chapter 3 describes the production of crab by-product hydrochar in a 600 mL reactor and its properties are determined through characterization. The chemical and physical properties of the crab by-product hydrochar are determined using a variety of analysis to understand the material better. A modified version of this chapter will be submitted for publication.

Chapter 4 then provides a summary of the research performed in the previous chapters and provides conclusions and recommendations for the future of the field of study.

1.3.Co-Authorship Statement

The principal author of this thesis, Nadyana Incan, is the primary author on all chapters in this thesis and performed all experimental work and analysis except otherwise noted. Dr. Kelly Hawboldt, who acted as the principal supervisor on this thesis, served to provide technical

guidance, analytical support, and additional support in editing the thesis and is listed as a co-author on the manuscripts for chapters 2, 3, and 4. Dr. Stephanie MacQuarrie as the co-supervisor also provided technical guidance, analytical support, and editing for the work performed in chapters 2, 3 and 4, and is listed as a co-author in these chapters.

References

[1] Economic Analysis and Statistics and Fisheries and Oceans Canada, "Canada's Fisheries Fast Facts 2021," Economic Analysis and Statistics and Fisheries and Oceans Canada, Ottawa, 2022.

[2] Economic Analysis and Statistics and Fisheries and Oceans Canada, "Canada's Fisheries Fast Facts 2022," Economic Analysis and Statistics and Fisheries and Oceans Canada, Ottawa, 2023.

[3] Department of Fisheries and Land Resource Newfoundlad and Labrador, "Seafood Industry Year in Review 2019," Department of Fisheries and Land Resource Newfoundlad and Labrador, St. John's, 2020.

[4] Department of Fisheries and Land Resource Newfoundlad and Labrador, "Seafood Industry Year in Review 2021," Department of Fisheries and Land Resource Newfoundlad and Labrador, St. John's, 2022.

[5] Department of Fisheries and Land Resources, Newfoundland and Labrador, Canada, "Seafood Industry Year in Review 2019," [Online]. Available: https://www.gov.nl.ca/ffa/files/2019-SIYIR-WEB.pdf. [Accessed 12 August 2021].

[6] V. Sieber, M. Hofer, W. M. Brück, D. Garbe, T. Brück and C. A. Lynch, "ChiBio: An Integrated Bio-refinery for Processing Chitin-Rich Bio-waste to Specialty Chemicals," in *Grand Challenges in Marine Biotechnology*, P. H. Rampelotto and A. Trincone, Eds., Springer, Cham, 2018, pp. 555-578.

[7] M. Asunción Lage-Yusty, M. Vilasoa-Martínez and S. Álvarez-Pérez, "Chemical composition of snow crab shells (Chionoecetes opilio)," *CyTA - Journal of Food,* vol. 9, no. 4, pp. 265-270, 2011.

[8] V. Novikov, S. Derkach and I. Konovalova, "Chitosan Technology from Crustacean Shells of the Northern Seas," *KnE Life Sciences,* pp. 65-74, 2020.

[9] T. J. Beaulieu, P. Bryl and M.-É. Carbonneau, "Characterization of enzymatic hydrolyzed snow crab (Chionoecetes opilio) by-product fractions: A source of high-valued biomolecules," *Bioresource Technology,* vol. 100, no. 13, p. 3332–3342, 2009.

[10] M. Leffler, "Maryland Marine Notes (Archive) - Maryland Sea Grant - Treasure from Trash: Is There Profit in Crab Waste?," March April 1997. [Online]. Available: https://www.mdsg.umd.edu/maryland-marine-notes-archive.

[11] E. M. Aklog, H. Kaminaka, H. Izawa, M. Morimoto, H. Saimoto and S. Ifuku, "Protein/$CaCO_3$/Chitin Nanofiber Complex Prepared from Crab Shells by Simple Mechanical Treatment and Its Effect on Plant Growth," *International Journal of Molecular Sciences,* vol. 17, no. 10, p. 1600, 2016.

[12] W. J. Naczk, K. Brennan, C. Liyanapathirana and F. Shahidi, "Compositional characteristics of green crab (Carcinus maenas)," *Food Chemistry,* vol. 88, no. 3, p. 429–434, 2004.

[13] Y. I. Hajji, O. Ghorbel-Bellaaj, R. Hajji, M. Rinaudo, M. Nasri and K. Jellouli, "Structural differences between chitin and chitosan extracted from three different marine sources," *International Journal of Biological Macromolecules,* vol. 65, p. 298, 2014.

[14] C. Pires, A. Marques, M. Carvalho and I. Batista, "Chemical Characterization of Cancer Pagurus, Maja Squinado, Necora Puber and Carcinus Maenas Shells," *Poult Fish Wildl Sci,* vol. 5, no. 1, p. 1000181, 2017.

[15] B. S. Parthiban, A. Gopalakannan, K. Rathnakumar and S. Felix, "Comparison of the Quality of Chitin and Chitosan from Shrimp, Crab and Squilla Waste," *Current World Environment,* vol. 12, no. 3, p. 670–677, 2017.

[16] H. Ding, L. Lv, Z. Wang and L. Liu, "Study on the “Glutamic Acid-Enzymolysis” Process for Extracting Chitin from Crab Shell Waste and its By-Product Recovery," *Applied Biochemistry and Biotechnology ,* vol. 190, no. 3, p. 1074–1091, 2020.

[17] N. Yan and X. Chen, "Sustainability: Don't waste seafood waste," *Nature,* vol. 524, p. 155–157, 2015.

[18] S. Xiu, A. Shahbazi, V. Shirley and D. Cheng, "Hydrothermal pyrolysis of swine manure to bio-oil: Effects of operating parameters on products yield and characterization of bio-oil," *Journal of analytical and applied pyrolysis,* vol. 88, no. 1, pp. 73-79, 2010.

[19] Y. Matsumura, "Hydrothermal Gasification of Biomass," in *Recent Advances in Thermo-Chemical Conversion of Biomass*, 2015, pp. 251-267.

[20] A. M. Smith and A. B. Ross, "Production of bio-coal, bio-methane and fertilizer from seaweed via hydrothermal carbonisation," *Algal Research,* vol. 16, pp. 1-11, 2016.

[21] M.-M. Titirici, "Green Carbon," in *Sustainable carbon materials from hydrothermal processes*, Wiley, 2013, pp. 1-36.

[22] ipi.ag, "Hydrothermal carbonization: convert waste to energy," [Online]. Available: https://ipi.ag/en/htc-plant_14. [Accessed 13 October 2021].

[23] E. Bevan, J. Fu and Y. Zheng, "Challenges and opportunities of hydrothermal carbonisation in the UK; case study in Chirnside," *RSC Advances,* vol. 10, no. 52, pp. 31586-31610, 2020.

[24] M.-M. Titirici, A. Funke and A. Kruse, "Hydrothermal Carbonization of Biomass," in *Recent Advances in Thermochemical Conversion of Biomass*, 2015, pp. 325-352.

[25] S. Kannan, Y. Gariepy and G. S. V. Raghavan, "Optimization and Characterization of Hydrochar Derived from Shrimp Waste," *Energy & fuels,* vol. 31, no. 4, pp. 4068-4077, 2017.

[26] S. Kannan, Y. Gariepy and G. S. V. Raghavan, "Conventional Hydrothermal Carbonization of Shrimp Waste," *Energy & fuels,* vol. 32, no. 3, pp. 3532-3542, 2018.

[27] C. He, H. Lin, L. Dai, R. Qiu, Y. Tang, Y. Wang, P.-G. Duan and Y. S. Ok, "Waste shrimp shell-derived hydrochar as an emergent material for methyl orange removal in aqueous solutions," *Environment International,* vol. 134, 2020.

[28] S. Mikhail, *Microwave Hydrothermal Carbonization of Lobster Waste,* ProQuest Dissertations Publishing, 2020.

[29] X. Han, Z. Wu, Y. Yang, J. Guo, Y. Wang, L. Cai, W. Song and L. Ji, "Facile Preparation of a Porous Biochar Derived from Waste Crab Shell with High Removal Performance for Diesel," *Journal of Renewable Materials,* vol. 9, no. 8, p. 1377–1391, 2021.

Chapter 2 - Literature Review
Hydrothermal Carbonization of Wet Biomass

*A modified version of this chapter will be submitted for publication. It has been proofread and revised by Dr. Kelly Hawboldt and Dr. Stephanie MacQuarrie

Abstract

Thermochemical conversion of by-products of biomass processing can turn a carbon source into a carbon sink. However, conversion processes such as pyrolysis, gasification, and torrefaction require a dry feedstock and biomass residues high in water, such as fishery processing by-products and pulp and paper sludge, therefore require a costly drying step. Hydrothermal processes, such as hydrothermal carbonization (HTC), hydrothermal liquefaction (HTL), and hydrothermal gasification (HTG), offer a better choice as these processes use water as the medium. HTC has several advantages compared to the other types of hydrothermal processes, such as milder conditions, the process is well developed, and been implemented at an industrial scale. The main product of HTC is solid hydrochar which has applications from fuel to wastewater and gas treatment. In this paper a review of HTC applied to wet biomass feedstocks and impact of feedstock and operating conditions on hydrochar is explored. The review demonstrates that there is a wealth of HTC studies on pulp and paper sludge, sewage sludge, and macroalgae, however, very few studies on residues associated with fish processing. Given the volumes of fish waste generated, environmental impacts associated with disposal, limited re-use options due to biological contamination, the increasing focus on ocean health, and value of hydrochar, these residues are ideal candidates for HTC.

2.1. Introduction

Biomass residues (forestry, fishery, and agricultural) are typically treated as waste, which is costly with respect to disposal and loss of value from compounds bound in residues. Thermochemical conversion processes (e.g., pyrolysis, gasification, and torrefaction) can transform the residues into value-added products. However, these processes work best with "dry" biomass, and many biomass residues (e.g., fishery processing by-products and pulp and paper sludge) are often "wet", with water content ranging from 50-99 wt% [1, 2, 3, 4, 5]. The high-water content translates to high energy requirements and excessive water generated due to the drying required for thermochemical conversion.

Fishery processing by-products are particularly high in water due to the nature of the processing. Shellfish, and crab in particular, are critical economic drivers in Atlantic Canada [6], however up to 50 wt% of landed product is generated as processing by-product in the form of waste crab bodies [7]. The waste crab bodies are made up of 10–30 wt% chitin, 11–40 wt% protein,

and 20–50 wt% minerals, mainly calcium carbonate (dry weight) [4, 8, 9, 10, 11, 12, 13, 14, 15, 16]. The chitin can be extracted however, the industrial-scale process can be costly to build, typically requiring toxic chemicals with potential environmental hazards, and/or the product may have limited market due to the processing plants' location (i.e., rural/remote areas) [15, 17]. Crab processing by-products have foul odours and degradation releases methane, ammonia, and nitrates, which could pollute air and soil if not managed properly [15]. The forestry industry has similar issues with wet biomass, particularly the pulp and paper sludge [18]. Pulp and paper sludge is generally disposed of in landfills or incinerated [19, 20, 21]. Both disposal methods have disadvantages. The sludge must be dewatered to meet landfill disposal requirements, using large amounts of energy. The waste itself can contribute to global warming, soil pollution, groundwater contamination, and unnecessarily add to the landfill burden in a time of decreasing landfill capacity [20, 22]. The Canadian government also regulates sewage sludge disposal (semi-solid) to landfills, and it is prohibited in Newfoundland and Labrador (NL) due to its water content [23, 24]. Incineration can convert the sludge to energy, but again, the water must be removed (either prior to or during incineration), which requires excessive energy and associated impacts on air quality [19]. These issues are shared among other types of high-moisture biomass, such as crustacean processing waste, and macroalgae.

Economic and environmentally sustainable valorization of these wet biomass streams requires a process suited to high moisture feedstocks. Hydrothermal processing, where the biomass is thermally decomposed in the presence of water, is a potential treatment method that could eliminate all or part of the drying pretreatment and produce high-value compounds. Hydrothermal processes include hydrothermal carbonization (HTC), hydrothermal liquefaction or hydrothermal pyrolysis (HTL), and hydrothermal gasification (HTG) [25, 26]. The processes vary in residence time, temperature, and product yields [26]. HTC is a thermochemical process that operates between 180-250 °C [27, 28], while HTL and HTG operate between 300-400 °C and 400-600 °C, respectively [26]. The main product of HTC is solid (hydrochar), while the main product of HTL is liquid (bio-oil), and the primary product of HTG is gas composed of H_2, CH_4, and CO_2 [26]. The advantages of the HTC process compared to HTL, and HTG include: HTC is a milder process compared to HTL and HTG, and the process is well developed with large-scale HTC plants in operation [29, 30, 31]. More importantly, the hydrochar product has various applications, from fuel to the treatment of wastewater and gas streams [31]. In general, at the same residence time

and water:biomass ratio, as HTC temperature increases from 180-280 ^{o}C the hydrochar yield decreases [32, 33, 34, 1, 2, 35, 36, 27, 37]. The impacts of temperature and residence time have been extensively studied [1, 2, 3, 27, 32, 33, 35, 36, 37, 39, 41, 42], however studies on biomass to water ratio [40, 41, 42] are limited. Furthermore, HTC research where marine biomass is the feedstock is limited and the results are generally inconsistent. HTC on pulp and paper sludge has been more heavily researched.

HTC, which uses water as medium, is a good option to convert wet biomass into carbon rich material. Hydrochar has been targeted for use as; fuel (paper sludge, macroalgae, sewage sludge waste) [1, 2, 3, 27, 32, 33, 37, 38, 43], adsorption applications (sewage sludge, paper sludge, macroalgae, shrimp waste, and crab shell waste) [34, 44, 45, 46], or soil remediation [36]. Most studies focus on fuel applications due to the increase in carbon in hydrochar relative to the feedstock. The oxygen content is lower in the hydrochar relative to the feedstock resulting in a O/C and H/C ratios similar to solid fuels (e.g., coal). The low O/C may lower CO/CO_2 emissions during combustion relative to the feedstock. The lower H/C indicates the hydrochar is transformed into a stable aromatic compound. [47] The smaller pool of studies related to adsorbent applications compared to the fuel is attributed to the small surface area of hydrochar [34, 44, 45, 46]. However, a study on crab shell hydrochar for diesel adsorption application showed low surface area but high diesel adsorption capacity [45]. This shows that surface area is not be the only factor affecting adsorption application, and hydrochar surface functional groups may also have an impact. There's also a possibility for mineral/ash rich hydrochar with high nitrogen content (like macroalgae hydrochar) to be used for soil remediation [36].

To further explore the HTC option for wet biomass, the objectives of this paper are to; review; 1) compositions of wet biomass with a focus on sludge and shellfish processing by-products, and 2) HTC studies of Sludge and Marine Biomass consist of impact of feedstock and HTC conditions on hydrochar and based on this identify data gaps with respect to HTC and shellfish. The primary focus of this work is HTC of shellfish, however there is a lack of literature related to this area and therefore sludge (a well-studied HTC feedstock) was included to give a more comprehensive picture of conditions, trends, and hydrochar properties associated with HTC.

2.2. Types of Waste Wet Biomass

As indicated wet biomass can vary significantly in terms of water content. The properties of selected wet biomass are summarized in Table 2.1. Pulp and paper sludge moisture content can vary from 57 to 99 wt% depending on the sludge type [1, 2, 3]. There is no exact composition of pulp and paper sludge however, it mainly consists of organic fibres (cellulose, hemicellulose and/or lignin), inorganic fillers and coating materials such as kaolinite, limestone, and talc [48]. Sewage sludge contains approximately 70-90 wt% of water [49, 32, 34, 39, 50]. Typically, dewatered sewage sludge contains 50–70 % organic matter and 30–50 % mineral components (including 1–4 % of inorganic carbon), 3.4–4.0 % nitrogen, 0.5–2.5 % phosphorus, and other nutrients (unknown %) [51]. Studies on HTC and marine biomass include macroalgae and residues from crab, shrimp, and lobster processing [27, 35, 36, 38, 40, 41, 43, 44, 45, 46, 52, 58, 59, 60, 61]. As with other marine biomass, macroalgae is high in water (70–90 wt%). Macroalgae species vary widely in terms of composition, this is reflected in HTC studies involving where macroalgae was used where carbohydrates varied from 45–75 wt%, 7–35 wt% proteins, less than 5 wt% lipid, with minerals and vitamins making up the remainder on a dry basis. Crab shell moisture content varies from 50 to 70 wt% [4, 5] and shrimp processing residues between 70 to 80 wt% [41, 52]. As mentioned above, crab shells can vary as well in terms of composition depending on species and degree of processing; 20-40 wt% protein, 20–50 wt% calcium carbonate, and 15–40 wt% chitin (dry weight) [4, 8, 9, 10, 11, 12, 13, 14, 15, 16]. Shrimp processing by-product are as high as 80 wt% water, with the solid fraction varying from 33-40 wt% protein, 17-20 wt% chitin, and 34 wt% ash (dry weight) [53]. As discussed, each feedstock had different composition, such as lignocellulose-based pulp and paper sludge, carbohydrate-based macroalgae, and chitin-based crustacean shell. To consider, the different in composition may lead to different product properties since each has different degradation temperature [54, 55, 56, 57].

Table 2.1. Composition of selected wet biomass (wt%) – dry basis unless stated otherwise.

Sample	M	VM	FC	Ash	C	H	N	O	S	Lignin	Protein	Fat	Chitin	Lipids	Source
Municipal sewage sludge	-	-	-	33.14	36.33	5.9	4.23	12.81	-	-	-	-	-	-	[39]
Various Paper Mill Sludges:															[2]
PS	60.1*	-	--	16.0	34.6	4.7	0.3	44.4	BD	5.2	-	-	-	-	
DPS	63.5*	-	-	31.9	27.1	3.4	0.7	37.0	BD	10.0	-	-	-	-	
PSS1	64.1*	-	-	22.8	38.4	5.3	2.3	30.3	0.9	20.2	-	-	-	-	
PSS2	76.5*	-	-	4.5	42.8	6.1	0.7	45.8	0.2	17.6	-	-	-	-	
PFR	57.1*	-	-	19.5	39.8	5.3	0.6	34.6	0.3	22.6	-	-	-	-	
PTS	98.7*	-	-	17.1	23.9	3.9	0.6	48.4	6.2	20.4	-	-	-	-	
Paper Board Mill Sludge	-	62.5	7.4	30	29.69	4.34	3.28	31.65	1.04	-	-	-	-	-	[3]
Paper Sludge-PSS:															[1]
Lab scale	76*	62.1	3.9	34.1	31.3	4.6	2.2	27.8	-	-	-	-	-	-	
Pilot scale	76.4*	62.1	10.9	27	34.8	4.3	4	29.9	-	-	-	-		-	
Fibre sludge	72*	-	-	-	37.6	6.46	5.64	-	1.27	-	-	-	-	-	[34]
Biosludge	90*	-	-	-	37.8	6.04	0.25	-	0.12	-	-	-	-	-	
Paper sludge	-	47.38	5.18**	47.44	22.65	3.22	1.32	24.25	1.07	-	-	-	-	-	[37]
Seaweed	10.46	63.29	12.44	24.28	33.76	4.19	2.33	34.75	0.69	-	-	-	-	-	[36]
Seaweed (*Eucheuma Cottonii*)	11.21	47.41	27.82	13.58	21.11	4.26	0.35	57.73	2.97	-	-	-	-	-	[40]
Sea Lettuce	92	70.79	29.21	34.92	26.33	4.38	2.61	31.76	-	-	-	-	-	-	[60]
Red Seaweed (*Gracilaria lemaneiformis*)	-	70.8	11	18.2	33.5	5.2	1.3	60	-	-	9.3	-	-	0.92	[42]
Macroalage waste (algal meal)	-	-	-	7.7	43.99	5.95	5.21	36.13	1.02	-	-	-	-	-	[61]
Snow crab shell (*Chionoecetes opilio*)	72*	-	-	28.5	-	-	-	-	-	-	34.2	17.1	-	-	[4]
King crab shell*	68	-	-	17	-	-	-	-	-	-	8.6	-	5.5	0.9	[5]
Snow crab shell*	53.8	-	-	15.1	-	-	-	-	-	-	25.7	-	4.9	0.5	
Red snow crab shells	-	-	-	-	-	-	-	-	-	-	16	-	30	-	[8]
Snow crab by-products	77.8*	-	-	-	-	-	-	-	-	-	42.87	-	16.24	14.82	[9]
Various crab shells	-	-	-	62.90 - 74.97	-	-	-	-	-	-	13.2 - 20.7	-	10.3-16.4	-	[12]

Waste shrimp shell	-	-	-	4.97	43.51	7.60	5.45	38.47	-	-	-	-	-	-	[46]
Shrimp waste	80.16	80.86	-	14.22	43.09	6.91	11.47	37.93	-	-	-	-	-	-	[41]
Shrimp waste	68.75	81.96	-	14.56	42.39	5.69	11.91	39.24	-	-	-	-	-	-	[52]
Lobster waste	74.9	46.6	-	26	30.29	5.53	5.01	59.18	-	-	-	-	-	-	[58]

M: moisture content; FC: fixed carbon; VM: volatile matter; C: carbon content; H: hydrogen content; N: nitrogen content; O: oxygen content; S: sulfur content

BD: below detection limit; PS: Primary sludge (PS); DPS: De-inking paper sludge (DPS); PSS: Mixture primary and secondary sludge; PFR: Preliminary fibre rejects (PFR); PTS: Pre-thickened sludge (PTS)

*wet basis, per wet sample weight; ** Fixed carbon% = 100% - volatile matter% - ash%

2.3. Hydrothermal Carbonization (HTC) studies of Sludge and Marine Biomass

In this section the HTC of sludge (pulp and paper, sewage) feedstocks and marine biomass are discussed. The more comprehensively studied sludge will be discussed first followed by marine biomass including macroalgae, shrimp, lobster, and crab shell.

2.3.1. Sewage Sludge

There are ample number of studies regarding sewage sludge HTC and Table 2.2 summarizes the relevant sewage sludge HTC studies. In a study by Chao et al. (2013), 10.3 g of dewatered sewage sludge (85.7 wt% moisture) was treated using HTC at 200 °C for 4, 6, 8, 10, and 12 h [32]. The hydrochar yields ranged from 53 to 61 wt% (db) and increased with residence time [32]. Longer residence times decreased volatile matter, nitrogen, and sulfur content in the hydrochar, while fixed carbon and ash content increased [32]. The fixed carbon increased from 5.47 wt% to 8 wt% from 4 to 10 h but greater than10 h carbon content flattened (8.13 wt% at 12 h). In another study of sewage sludge by Kim et al. (2014), the HTC temperature was varied from 180 to 280 °C with a residence time of 30 min at a 1:1 (volume) sludge to water ratio [33]. The hydrochar yields decreased from 94 to 80 wt% (db), fixed carbon content increased from 8.37 to 12.7 wt%, and volatile matter decreased (47.28-62.28 wt%) as temperature increased. Carbon content increased (39.98 to 48.45 wt%) and oxygen (5.92 to 4.13 wt%), sulfur (0.24 to 0.01 wt%), and nitrogen (7.18 to 4.94 wt%) decreased with temperature increase [33]. As a result, the H/C and O/C ratios of the sewage sludge hydrochars were 11-49% and 3-27% lower than their feedstock, approximating properties closer to lignite [33]. The H/C ratio indicates aromaticity (stability), lower values indicate a more stable aromatic structure. The decrease in O/C (polarity) indicates the hydrochar is less polar than the feedstock, polarity can inform soil and adsorption applications. In a study by Zhang et al. (2014), HTC experiments were performed on 80 wt% moisture sewage sludge underwent HTC (190 and 260 °C and 1, 6, 12, 18 and 24 h) [39]. As

temperature and residence time increased, (or reaction intensity) the same trends were observed as previous studies except nitrogen and hydrogen which were relatively constant [39]. The higher heating value (HHV) varied little with temperature and time (16.7-18.3 MJ/kg) or compared to the feedstock (at 17.55 MJ/kg) [39].

Table 2.2. Sewage Sludge HTC Summary (wt%) – dry basis unless stated otherwise

Sample	M* (wt%)	biomass:water (wt:wt)	T(°C)	t (h)	Mixing	Result	Source
Municipal sewage sludge	80	As it is	190, 260	1 - 24	none	• Ash: 46.65-51.85 wt%; ash content steadily increased with residence time at temperature of 190°C yet at 260°C ash content increased up to 12hr HTC then decreased • C: 35.92-38.6 wt%; increased as temperature and residence time increased • H: 4.93-5.31 wt%; hydrochar H content decreased from its feedstock and mostly constant with temperature increased and residence time • O**: 3.12-7.96 wt%; decreased as temperature and residence time increased; the decrease was more severe at 260°C • N: 1.73-1.92 wt%; hydrochar N content decreased from its feedstock and mostly constant as temperature and residence time increased Molar Ratio: • H/C: 1.63-1.71; slightly decreased as temperature increased, mostly constant with residence time • O/C: 0.07-0.17; decreased as temperature and residence time increased • HHV: 16.74-18.33 MJ/kg; HTC impact on HHV is not significant due to the decreased (feedstock 17.55) of HHV at 190°C and only increased at 260°C after 18 h	[39]
Sewage sludge	70	Diluted to 78 wt%	180 - 260	2	none	• Solid yield: 70-83 wt%; increased in temperature, decreased solid yield • FTIR of 260°C hydrochar: the presence of aluminosilicates; intensification of C-H asymmetric and asymmetric peak; decreased in O-H peak • Fibre sludge hydrochars surface areas at all temperatures were approximately between 20-30 m^2/g • Surface area increased as temperature increased up to 220°C; then collapsed at 260°C • Sewage sludge hydrochars' pH was acidic	[34]
Dewatered sewage sludge	85.7	As it is, 10.3 g	200	4 - 12	none	• Solid yield: 53.9- 60.4 wt%; longer residence time, increased solid yield • Ash: 43.89-46.69 wt%; increased with longer residence time • VM: 45-50.64 wt%; decreased with longer residence time • FC: 5.35-8.31 wt%; increased with longer residence time • C: 32.5-33.2 wt%; slightly decreased with longer residence time • H: 4.1- 4.4 wt%; slightly decreased with longer residence time • O: 16.9- 18.5 wt%; decreased with longer residence time • N: 2.1-2.2 wt%; hydrochar N content decreased from its feedstock and constant as residence time increased Molar Ratio: • H/C: 1.53-1.60; slightly decreased with residence time • O/C: 0.39-0.42; slightly decreased with residence time • HHV: 14.74-15.09 MJ/kg; slightly decreased with longer residence time, residence time impact on HHV is not significant • HHV***: 27.55-28.52% MJ/kg; HHV increased from feedstock, yet residence time impact on HHV is not significant	[32]

Anaerobically digested sludge	-	300:300 (mL:mL)	180 - 280	0.5	200 rpm	• Solid yield: 80.4-93.9 wt%; increased in temperature, decreased solid yield • Ash: 29.35-40.02 wt%; increased as temperature increased • VM: 47.28-62.28 wt%; decreased as temperature increased • FC: 8.37-12.7 wt%; increased as temperature increased • C: 39.98-48.45 wt%; increased as temperature increased • H: 4.13- 5.92 wt%; decreased as temperature increased • O: 42.47- 46.68 wt%; decreased as temperature increased • N: 4.94-7.18 wt%, decreased as temperature increased Molar Ratio: • H/C: 1.01 and 1.99; decreased with as temperature increased • O/C: 0.65 and 0.90; decreased with as temperature increased • HHV: 17.3-22.4 MJ/kg; increased as temperature increased	[33]
Dewatered sewage Sludge	80	50:100 (g:g)	148 - 248 (423 - 523 K)	5 min	Stirred	• Ash: 26.6-33.9 wt increased as temperature increased • VM: 58.1 -66.1 wt%; decreased as temperature increased • FC:7.3-8 wt%; increased as temperature increased Ultimate analysis (d.a.f) • C:50.7-54.2 wt%; increased as temperature increased • H: 7.2-7.7 wt%; slightly decreased as temperature increased • N: 3.5-4.8 wt%; hydrochar N content decreased from its feedstock and mostly constant as temperature increased • O: 33.8-37.7 wt%; decreased as temperature increased • HHV: 15.3-17.4MJ/kg; decreased as temperature increased	[49]
Sewage sludge	89.32	1:9 (g/mL)	270	2	Stirred	Feedwater pH variation = 2, 3, 5, 7, 9, 11 and 12 • Solid yield: 50.12-57.37wt%; pH has little effect on the yield • Ash: 66.12-81.79wt%; decreased with the increase of pH	[50]

*M = per wet/fresh feedstock weight

**O=100%-(H_2O%+Ash%+C%+H%+N%)

***dry ash-free

While temperature and residence time are key factors, the properties of the water (ratio, pH etc) are also critical as it will determine if any additional water is required. Liu et al. (2020) studied the impact of the feed-water pH on sewage sludge hydrochars produced at 270 °C and 2 h [50]. As water pH increased from 2 to 11, the ash content decreased from 81.79 to 66.12 wt% and then plateaued. The pH had a negligible effect on other measured properties (yield, moisture content, and pH of hydrochar surface) [50]. Further analysis of the surface showed alkaline conditions favour formation of N-containing groups (including amides, pyridines, indoles, cyanogens, and furan) and ketones, while acidic conditions favour formation of alicyclic hydrocarbons, siloxanes, acid, and alcohols [50]. Published work indicates that the sewage sludge to water ratio does not have a significant impact on the hydrochar properties (Table 2). In general, properties are within 20% of each other (at similar temperature and time), regardless of the sewage sludge:water ratio.

(Fourier transform infrared) FTIR spectra of dewatered sewage sludge hydrochar showed little change of functional group with residence time 4-12 h at 200 °C [32]. The study by He et al. (2013) was proposed that hydrochars at 200 °C showed a less intense OH peak attributed to

dehydration [32]. The study also proposed that the intensity of peaks attributed to C=O associated to carboxylic groups and ketone and amide groups were reduced, likely due to decarboxylation reactions [32]. In the same study, the presence of C-H and -C=C associated with aromatic carbons was noted in the raw sewage sludge and its hydrochar. Increasing HTC temperature (180-280 °C, 30 min), was proposed to showed similar trends in a separate study of sewage sludge HTC [33]. In addition, the study proposed that the N-O peak intensity decreased as temperature increased [33]. It was also noted the O-H and C=O functional groups in the hydrochars were less intense compared to feedstock. It was proposed that the decrease in intensity was due to dehydration and decarboxylation reactions [33]. However, it should be noted FTIR is not a quantitative analysis and therefore relating intensity to density of functional groups is difficult to justify without additional analysis, particularly in complex matrices such as hydrochar.

Dewatered sewage sludge hydrochars (HTC at 200 °C) morphologies showed a more porous material compared to the feedstock and the porosity increased with residence time [32]. This trend is consistent with HTC of pulp and paper sludge [1, 3, 34]. He et al. (2013) proposed that the increase in hydrochar porosity could reduce the drying time of hydrochar at ambient temperature [32].

Surface areas of sewage sludge hydrochars produced at 190 and 260 °C for 1-24 h were between 1 to 17 m^2/g [39]. At 190 °C the surface area increased with time up to 6 h. At residence times greater than 6 h, the surface area dropped from 8.70 m^2/g to ~2-4 m^2/g. At 260 °C surface area increased with time up to 12 h (17.30 m^2/g) and decreased at longer times (1.22-5.27 m^2/g) [39]. It is possible that this was a result of pore collapse under prolonged heating.

Thermogravimetry-Derivative Thermogravimetry (TGA-DTG) studies of dewatered sewage sludge feedstock overall show shifts in volatile mater with time and temperature. In a study by He et al. (2013), the dewatered sewage sludge feedstock DTG had only one peak at 310 °C (volatile matter) [32]. Under HTC treatment (200 °C for 4, 6, 8, 10, or 12 h), as time increased, the 310 °C peak decreased and a second peak formed [32]. The 310 °C peak was proposed to be depolymerization reactions (150 to 350 °C) and the second peak was attributed to further volatile matter degradation and char combustion (between 300 to 590 °C) [32]. This change mirrored the increase in fixed carbon content and decrease in volatile matter content [32].

2.3.2. Pulp and Paper Sludge

Pulp and paper mill sludge reviewed in this work includes: dried sludge [2, 3, 37], dewatered paper sludge [1], or fresh sludge [34]. Pulp and paper HTC studies are summarized in Table 2.3.

Table 2.3. Pulp and Paper Mill Sludge HTC Summary (wt%) – dry basis unless stated otherwise.

Sample	M* (wt%)	biomass:water (wt:wt)	T(°C)	t (h)	Rpm	Result	Source
Paper Board Mill Sludge	-	1:9	200	10	none	• Hydrochar pH 5.79 After HTC: • FC: 15.6 wt% • VM: 44.5 wt% • Ash: 39.9 wt% • C: 32.77 wt% • H: 3.13 wt% • N: 3.32 wt% Molar ratio: • H/C: 1.13 • O/C: 0.45 • Hydrochar surface area increased from 0.75 m^2/g to 3.74 m^2/g • HTC made hydrochar more porous; microspheres diameter 31.1-49.2 nm (from 100nm); carbon nanotubes were observed • HHV: 18.39 MJ/kg	[3]
Six different Paper Mill Sludge:		1:9	180 - 260	0.5	180	• Increased in temperature: decreased solid yield, increased liquid and gas yield, increased HHV • General trend after HTC: Hydrochars carbon content increased compared to feedstock Hydrochars ash content increased compared to feedstock Hydrochars oxygen content decreased compared to feedstock Hydrochars hydrogen content decreased compared to feedstock	[2]
PS	60.1					• Solid yield: 30.3-96.2 wt% • Liquid yield: 3.8-58.1 wt% • Gas Yield: 0-11.6 wt% • HHV: 15-22.8 MJ/kg Feedstock to 260°C hydrochar comparison • Ash: 16→33.1 wt% • C: 34.6→ 44.3 wt% • H: 4.7→3.8 wt% • N: 0.3 → 0.2 wt% • O: 44.4→18.5 wt%	
DPS	63.5					• Solid yield: 58.4-91.7 wt% • Liquid yield: 8.3-33.9 wt% • Gas Yield: 0- 7.2 wt% • HHV: 11.4-13 MJ/kg feedstock to 260°C hydrochar comparison • Ash: 31.9→46 wt% • C: 27.1→ 22.2 wt% • H: 5.3→4.2 wt% • N: 0.7 → 0.4 wt% • O: 37→29.6 wt%	
PSS1	64.1					• Solid yield: 54.1 -81.2 wt% • Liquid yield: 18.3- 38.8 wt% • Gas Yield: 0- 7.1 wt%	

						• HHV: 21.7- 27.4 MJ/kg feedstock to 260°C hydrochar comparison • Ash: 22.8→36 wt% • C: 38.4→ 40.5 wt% • H: 3.4→1.8 wt% • N: 2.3 → 2.1 wt% • O: 30.3→16 wt%	
PSS2	76.5					• Solid yield: 41.1 -90.9 wt% • Liquid yield: 9.1- 49.9 wt% • Gas Yield: 0-9 wt% • HHV: 19.6- 28.9 MJ/kg feedstock to 260°C hydrochar comparison • Ash: 4.5→5.2 wt% • C: 42.8→ 62.2 wt% • H: 6.1→5.7 wt% • N: 0.7 → 1.6 wt% • O: 45.8→25 wt%	
PFR	57.1					• Solid yield: 45.4-93.2 wt% • Liquid yield: 6.8- 42.9 wt% • Gas Yield: 0-10.7 wt% • HHV: 18.5- 25.2 MJ/kg feedstock to 260°C hydrochar comparison • Ash: 19.5→26.8 wt% • C: 39.8→ 57.6 wt% • H: 5.3→5.5 wt% • N: 0.6 → 0.6 wt% • O: 34.6→9.2 wt%	
PTS	98.7					• Solid yield: 43.8 -87.5 wt% • Liquid yield: 8- 52 wt% • Gas Yield: 0-4.1 wt% • HHV: 18.6- 31.5 MJ/kg Feedstock to 260°C hydrochar comparison • Ash: 17.1→50.5 wt% • C: 23.9→ 40.2 wt% • H: 3.9→4.3 wt% • N: 0.6 → 0.4 wt% • O: 48.4→3.3 wt%	
Fibre Sludge (bleached and unbleached fibres)	72	Diluted to 81wt% water	180 - 260	2	none	• Solid yield: 35 -90 wt%; decreased as temperature increased • Material rich in lignocellulosic (fibre) experienced more yield loss as temperature increased • FTIR of 260°C hydrochar: the presence of carbonate; intensification of C=C aromatic peak; intensification of C-H asymmetric and asymmetric peak; decreased in O-H peak • Fibre sludge hydrochars surface areas at all temperatures were approximately below 10 m^2/g • Surface area increased as temperature increased up to 220°C; then collapsed at 260°C • Fibre sludge hydrochars' pH was basic	[34]
Biosludge (pulp and boxboard wastewater mixed with low-fibre wastewater, pH adjustment, chlorate reduced and aerated)	90	As it is	180 - 260	2	none	• Solid yield: 44 -54 wt%; decreased as temperature increased • FTIR of 260 hydrochar: the presence of kaolinite; intensification of C=C aromatic peak; intensification of C-O-C peak; intensification of C-H asymmetric and asymmetric peak; decreased in O-H peak • Biosludge hydrochars surface areas were approximately between 5-35m^2/g • Surface area increased as temperature increased up to 220°C; then collapsed at 260°C • Biosludge hydrochars' pH was acidic	

Mixture of primary and secondary sludge	76 After dewatered: 71.9%	-Lab scale: 1:1 (wt/wt) dewatered sludge:water -Pilot scale: dewatered sludge:steam 351.1kg:138kg	Lab-scale: 180 - 240 Pilot-scale: 197	0.5	stirred	• Solid yield** decreased as temperature increased • Lab-scale solid yield approximately 20-25 wt% • Pilot-scale solid yield 12% • Characteristic (ultimate analysis, HHV, atomic ratio) of hydrochars from lab-scale and pilot are similar • FC: 5.3-10.1 wt%; increased as temperature increased • VM: 56.5-62 wt%; decreased as temperature increased • Ash: 34.3-37.2 wt%; slightly increased as temperature increased and slightly drop from 37.2 wt% at 200°C to 35.8 wt% at 240°C • C: 31.7-35.6 wt%; increased as temperature increased • H: 3.9-4.2 wt%; remained the same as temperature increased • O:22.4-27.8 wt%; decreased as temperature increased • N: 1.4-2 wt%; remained stable as temperature increased Molar ratio: • H/C: 1.42-1.59; decreased as temperature increased • O/C: 0.47-0.66; decreased as temperature increased • HHV: 13.4– 14.7 MJ/kg; slight increased as temperature increased **wet basis	[1]
Paper sludge	-	10g:150mL	180 - 300	0.5	300	• VM, H, O, N content decreased as temperature increased; the opposite effect on FC, C, and ash content • FC**: 6.13 -7.01 wt% • VM: 26.76-39.06wt% • Ash: 54.81-66.23 wt% • C: 19.11-20.91 wt% • H: 1.71-2.6 wt% • O: 11.91-20.11 wt% • N: 0.42-0.78 wt% Molar Ratio: • H/C: 1.07-1.49; decreased as temperature increased • O/C: 0.47-0.72; decreased as temperature increased • HHV: 8.853 – 9.412 MJ/kg; decreased as temperature increased	[37]

*M = per wet/fresh feedstock weight

**Fixed carbon%=100% -volatile matter% -ash%

***O%=100%-C%-H%-N%-S%-Cl%-ash%

Hydrochar yields in the table vary from 70-90 wt% (dry basis, db) at temperatures between 180-240 °C and then drop to 30-40 wt% at temperatures above 260 °C [2, 37, 34]. Liquid and gas yields increased with temperature, with liquid yields increasing from 3 to 60 wt% and gas yields from 0 to 12 wt% [2]. The hydrochar elemental composition of the pulp and paper sludge had similar trends with respect to temperature and time as the sewage sludge. The hydrochars showed 2-20 wt% increase in carbon content compared to the feedstock [1, 2, 3]. The oxygen and hydrogen decreased, and subsequently H/C and O/C ratio were lower in hydrochar relative to feedstock. Pulp and paper sludge H/C varied from 1.3-1.8 while the hydrochars varied from 0.9-1.5; the feedstocks O/C varied from 0.67-1 and the hydrochars O/C from 0.1-0.66 [1, 37]. As noted above this indicates the hydrochars are transformed into aromatic compound with low polarity. The increase in concentration ash (non reacting) in de-inking paper sludge (DPS), preliminary fibre

rejects (PFR), and pre-thickened sludge (PTS) is reflected in the higher yield [2]. The concentration of non-reacting compounds (ash) in DPS, PFR and PTS hydrochar were between 26.8 -50.5 wt%, higher than other types pulp and paper mill hydrochars (PS,PSS1,PSS2) with ash content between 5.2 -35 wt% (treated at 260 °C and 0.5 h) [2]. Oumabady et al. (2020) studied the impact of temperature and residence time on HTC of paper board mill sludge (from effluent treatment plant) [3]. Temperature, water:biomass ratio, and time were optimized for adsorbent uses by maximizing surface area and pore volume and for fuel by minimizing H/C ratio and O/C ratios. The resulting optimum that satisfied both was 200°C with 10 h holding time using a 1:9 biomass to water ratio. The paper board mill sludge feed pH was slightly acidic at 6.36 and became more acidic after the HTC process (pH of 5.79) [3]. In a related study by Niinipuu et al. (2020), hydrochars from fibre sludge (unbleached and bleached fibre) had pH values ranging from 7 to 7.8, whereas hydrochar produced from biosludge had pH ranging from 5.5 to 6 [34], highlighting the impact of composition on hydrochar properties even between "similar" feedstocks. The wood bleaching process is a basic process whereas biosludge is typically rich in organic compounds which more easily degrade into acids during HTC. In addition, the bleached fibre contains carbonate which is basic in nature while the biosluge contains kaolinite which is acidic (Table 2.3).

The residence time is particularly important with respect to the decomposition of lignin. Lignin in the sludge can vary considerably (5.2-22.6 wt%) [2]. In a study of HTC over 30 min at 260 °C, the lignin showed little decomposition resulting in an increased concentration in the hydrochar relative to the feedstock (19.7 wt% to 87.8 wt%) [2]. The fibre resistance to decomposition was reflected in a study by Areeprasert et al. where a mixture of primary and secondary sludge hydrochar showed remaining fibrous material at temperatures between 180-240 °C treated over 30 min [1]. In longer residence time studies using fibre sludge, fibre material was still visible (2 h residence time between 180-260 °C) [34]. The study suggested longer residence times are required to degrade lignocellulosic material in the sludge [34].

At the biomass to water ratios studied (Table 2.3) there is not substantial impact on the hydrochar properties. As with the sewage sludge, properties fall within 20% of each other regardless of the biomass to water ratio. As noted is Table 2.3, the hydrochar ash content and composition is dominated by feedstock.

As with the sewage sludge, FTIR showed that peaks associated with OH and C=O were less intense in pulp and paper hydrochars relative to the feedstock. This was proposed to be attributed to dehydration and decarboxylation reactions [1, 3, 37]. There were also peaks related to C-H and C-O-C proposed for the raw paper sludges and its hydrochars in various studies [1, 3, 34]. Besides the functional groups, the mixture of primary and secondary sludge hydrochars FTIR spectra was proposed to have a peak related to Si-O [1]. The same study also proposed that the primary and secondary paper sludge hydrochars showed stable traces of additive substances such as kaolinite (weak bands at 3697 and 3620 cm^{-1}) and calcium carbonate (peak at 875 cm^{-1}) [1]. The same additives are also proposed in fibre sludge hydrochar (calcium carbonate at 1416 cm^{-1} and 872 cm^{-1}) and biosludge (low fibre wastewater) hydrochar (kaolinite at 3620–3695 cm^{-1}) [34].

As with sewage sludge the surface area initially increases with temperature and then plateaus or decreases. For instance, the surface area of fibre sludge hydrochar increased as temperature increased to 220 °C with 2 h residence time (up to 5 m^2/g) [34]. At temperatures greater than 220 °C the surface area decreased (1.4 m^2/g at 260 °C) [34]. Relative to the feedstock the surface area increased slightly. For instance, paper broad mill sludge hydrochar (200 °C, 10 h) increased to 3.75 m^2/g from the feedstock of 0.75 m^2/g however surface area is not notable [3]. Other studies show a similar order of magnitude increase in surface area from feedstock to hydrochar, paper sludge hydrochar treated between 180 to 240 °C and 30 min increased from a feedstock value of 13.73 m^2/g to 35.49-50.70 m^2/g [37]. As temperature was further increased to 270 and 300 °C (30 min) there was no impact. In general paper sludge hydrochar show higher surface area (5-51.01 m^2/g) compared to sewage sludge hydrochar (1-17 m^2/g) treated at similar conditions.

Surface morphology changes between feedstocks and hydrochar were evident after HTC. Studies show that the paper sludge hydrochar became more homogenous and porous compared to the feedstock [1, 3, 34]. The lignocellulosic material degradation in the samples increased with temperature which was indicated by gradual disappearance of fibrous material in the hydrochar [1, 3, 34]. As noted above, fibrous material made up of cellulose, hemicellulose, and mainly lignin that degrade over a temperature range higher than HTC temperatures studied (above 280 °C). To compare with paper sludge, Niinipuu et al. (2020) also studied paper mill biosludge with a much lower fibre content (not quantified) [34]. The low fibre content in the biosludge resulted in

hydrochar without fibrous material. The size of hydrochars particles is not commonly mentioned in the literature, in a study of paper broad mill sludge (200 °C,10 h) the hydrochar diameter ranged from 31.1 nm to 49.2 nm, much lower than the feedstock (1 μm). Further investigation with TEM displayed a spherical shape of the hydrochar with nanotubes [3].

TGA-DTG pyrolysis curves of various paper sludge hydrochars showed a common peak at 310-400 °C, associated with cellulose and hemicellulose degradation [2]. For primary and secondary sludge mixtures, this was the only peak observed. For paper sludge hydrochars from DPS, PFR, and PTS, there was a minor peak at 640-780 °C due to lignin decomposition. Primary and de-inked primary sludge had another major peak at 750 °C due to the chemicals in the feedstock [2].

In a study of different types of paper mill sludges hydrochars, generated at 260 °C over 30 min, showed increased carbon and decreased oxygen content compared to the feedstocks (Table 3); this translated to improved HHV (dry ash-free) [2]. The feedstocks HHV ranged from 13 to 19 MJ/kg while the hydrochars varied from 22 to 31 MJ/kg [2]. The Van Krevelen's diagram showed that the hydrochars produced had similar properties to coal [2]. However, this relatively small increase in HHV must be compared to the energy required for conversion and other parameters such as sludge disposal/treatment costs. Areeprasert et al. (2014) studied laboratory scale HTC (180-240 °C, 30 min) and produced hydrochars with a negligible change in HHV (13.1 to 13.6 MJ/kg) compared to its feedstock (12.7 MJ/kg) [1]. Compared to sewage sludge hydrochar HHV, pulp and paper sludge hydrochars HHV were higher. TGA using air has been used to study the combustion of hydrochar. PTS-260 °C hydrochar had a more rapid mass loss at 190-350 °C due to high volatile matter when compared to coal. Mixing 50:50 PTS-260 °C hydrochar and coal resulted in TG and DTG behaviour similar to coal. Co-combustion of paper board mill sludge hydrochar with coal was studied in [3]. The result showed a decrease in moisture and ash in the coal-hydrochar mixtures. TGA was also used to study the impact of volatile matter (higher HTC temperatures) in the hydrochar [37] The decrease in volatile matter led to higher ignition temperature (from 274 to 311°C) and a more stable flame. As HTC temperatures increased from 180 to 300°C (Table 3) the burnout temperature (temperature where fuel is completely consumed) increase from 748 to 763 °C. [37]. In a comparison of ignition temperature and burnout temperature of paper sludge hydrochars to coal, the paper sludge hydrochars ignition temperature

(262.0- 380.4 °C) was lower than coal (466.7 °C) while burnout temperature (557.1- 788.7 °C) was higher (627.8 °C). This low ignition temperature and higher burn out temperature indicate the hydrochars were less thermally stable than coal [2]. In the same study [2], hydrochar and coal were mixed and ignition temperature and burnout temperatures showed similar properties to coal. The mixed hydrochar and coal showed the potential application as alternative energy/fuel.

2.3.3. Macroalgae/Seaweed

HTC of macroalgae has been shown to remove alkali metals and chlorine, thus reducing slagging and fouling when the hydrochar was used for combustion/pyrolysis [27]. HTC also improved the macroalgae porosity, making it a potential adsorbent or soil amendment. HTC studies related to macroalgae are outlined in Table 2.4.

Table 2.4. Macroalgae HTC Summary (wt%) – dry basis unless stated otherwise.

Sample	M* (wt%)	biomass:water (wt:wt)	T(°C)	t (h)	rpm	Result	Source
Seaweed waste (fresh seaweed from surface seawater)	-	1:9	180 - 220	0.5 - 2	Stirred prior HTC	• Solid yield (mass dried solid after HTC/mass of dried feedstock): 30.5-46.9 wt%; decreased as temperature and residence time increased • Solid yield**wet basis (mass solid after HTC/mass of feedstock): 25.6-40.2 wt%; decreased as temperature and residence time increased • Liquid yield (mass liquid after HTC/ total mass of feedstock): 54-68.5 wt%; increased as temperature and residence time increased • Gas Yield (=100-(solid yield**+liquid yield)): 4.7-6.55 wt%; nearly constant as temperature and residence time variation • FC: 17.75- 24.15 wt%; increased as temperature and residence time increased • VM: 54.15- 61.02 wt%; decreased as temperature and residence time increased • Ash: 20.14- 21.79 wt%; nearly constant as temperature and residence time variation • C: 43.17-48.49 wt%; increased as temperature and residence time increased • H: 4.27-4.95 wt%; nearly constant as temperature and residence time variation • O: 22.21-28.70 wt%; remained constant at ~27-28 wt% at temperature 180-200°C regardless of the residence time, but it decreased considerably from ~28.5 wt% at 200 °C to 25.13 and 22.21 wt% at 220 °C, as residence time increased • N: 2.63-2.91 wt%; nearly constant as temperature and residence time variation Molar Ratio: • H/C: 1.1-1.4; decreased as temperature and residence time increased • O/C: 0.42-0.5; decreased as temperature and residence time increased	[36]

						• HHV: 13.81-18.93 MJ/kg; increased as temperature and residence time increased	
Three species of macroalgae; *L. digitata* *L. hyperborea* *A. esculenta*	80-89%	24:220 (g:mL)	200, 250	1	none	• Solid yield: 18.4-39 wt% • Increased temperature resulted in decreased solid yield • Ash: 3.6-21.2 wt%; compared to its feedstock ash content decrease at a temperature of 200 °C yet increased when temperature increased to 250 °C • C: 50.2- 67.1 wt%; increased as temperature increased • H: 4.9-6.2 wt%; increased as temperature increased • O: 17.3-26.6 wt%; decreased as temperature increased • N: 2.4-3.5 wt%; hydrochar's N content increased from its feedstock and mostly constant with temperature increased Molar Ratio: • H/C: 0.9-1.31; increased as temperature time increased • O/C: 0.20-0.34; decreased as temperature time increased • HHV: 21-27.5 MJ/kg; increased with temperature increased	[27]
Various macroalgae: *Saccharina latissima* *Fucus serratus*	-	1:10 (g:mL)	150 - 250	1	none	• Solid yield: 22-44.7 wt% • Increased temperature resulted in decreased solid yield • FC: 16.1-19.2 wt%; increased as temperature increased • VM: 61.8- 73.1 wt%; decreased as temperature increased • Ash: 10.8-19.1 wt%; increased as temperature increase • C: 41.1-54.6 wt%; increased as temperature increased • H: 3.7- 4.4 wt%; stable as temperature increased • O: 15-26.1 wt%; decreased as temperature increased • N: 2.2-3 wt%; decreased as temperature increased • HHV: 16.9-22.3 MJ/kg; increased as temperature increased	[35]
Eucheuma Cottonii	-	1:20, 1:10, 1:5	250, 275	0.5 - 1.5	none	• Hydrochar produced: 4.64 - 25.145 g (unknown feedstock weight) • Increased in temperature and residence time resulted in decreased hydrochar produced • Decreasing water used increased the hydrochar produced • Compounds found in the liquid product: benzene, cyclopentane, heptane, methylcyclohexane, 2,5-dimethylhexane, toluene, cis-1,3 dimethylcyclohexane, cyclohexane, diacetone alcohol, levulinic acid • The surface area of 250 °C-30mins hydrochar was 12.35 m^2/g after activation with heat and CO_2	[40]
Sea Lettuce	92	250 mL slurry / as it is	150 - 220	0.5 - 2	-	• Solid yield (mass of dry char/dry solid in slurry): 9.51-24.43 wt% • Increased temperature and residence time resulted in decreased solid yield • Solid yield**wet basis (mass solid after filtration/mass of initial slurry): ~6-24 wt%; decreased as temperature and residence time increased • Liquid yield (mass of liquid after filtration/ mass of initial slurry): 73.09-89.18 wt% • Gas yield (100-liq yield%-solid yield**%): 2-8 wt% • FC: 12.22-20.64 wt%; decreased as temperature and residence time increased • VM: 79.36-89.32 wt%; increased as temperature and residence time increased • Ash: 17.23-23.03 wt%; increased as temperature and residence time increased • C: 36.50-44.71 wt%; increased as temperature and residence time increased • H: 4.56-5.99 wt%; stable as temperature and residence time increased • O: 24.56 -34.67 wt%; decreased as temperature and residence time increased • N: 1.76-3.01 wt%; decreased as temperature and residence time increased Molar Ratio: • H/C: 1-1.5; decreased as temperature and residence time increased	[60]

						O/C: 0.6-0.9; decreased as temperature and residence time increased	
Red seaweed (Gracilaria lemaneiformis)	-	1%,3%,5%,10% (biomass to water / w:v)	160 - 200	20 min	-	Microwave Hydrothermal Carbonization Temperature effect (160 – 200℃) - 20 min, ratio 3%, 0.4 M H_2SO_4 • Solid yield: 31.4-20.8 wt% • Decreased in temperature resulted in decreased solid yield • FC: 28.4-37.9 wt%; increased as temperature increased • VM: 54.7-57.4 wt%; decreased as temperature increased • Ash: 10.9-14.3 wt%; decreased as temperature increased • C: 48.8-57.8 wt%; increased as temperature increased • H: 5.2-6 wt%; stable as temperature increased • O: 35.2-44 wt%; decreased as temperature increased • N: 1-1.9 wt%; slightly decreased as temperature increased • HHV: 18.8-24.7 MJ/kg; increased as temperature increased Ratio effect (1-10%) - 20 min, 180℃, 0.2 M H_2SO_4 • Solid yield: 28.8-34.1 wt% • increased in biomass weight resulted in increased solid yield • FC: 30.1-31.2 wt%; similar in value as biomass weight increased • VM: 55.2-56.1 wt%; similar in value as biomass weight increased • Ash: 13.3-13.9 wt%; similar in value as biomass weight increased • C: 51.2-56 wt% (ratio 1-5), 53.8 wt% at ratio of 10 • H: 5.4-5.7 wt%; similar in value as biomass weight increased • O: 39.7-41.9 wt%; similar in value as biomass weight increased • N: 1.2-1.3 wt%; similar in value as biomass weight increased • HHV: 21.5-23.7 MJ/kg (ratio 1-5), 20.5 MJ/kg at ratio of 10 Acid concentration effect (0-0.6M H_2SO_4) - 20 min, 180℃, ratio 3% • Solid yield: 24.6-32.1 wt% • increased in acid concentration resulted in decreased solid yield • FC: 24.4-37.6 wt%; increased as acid concentration increased • VM: 51.3-59.9 wt%; decreased as acid concentration increased • Ash: 11.1-15.1 wt%; decreased as acid concentration increased • C: 45.6-55.9 wt%; increased as acid concentration increased • H: 5.8-6 wt%; similar in value as acid concentration increased • O: 37.2-46.6 wt%; decreased as acid concentration increased • N: 1.1-1.9 wt%; slightly decreased as acid concentration increased • HHV: 17.9-23.3 MJ/kg (increased as acid concentration increased from 0, 0.1, to 0.2 M), stable at 23.2-23.3 as acid concentration increased from 0.2 to 0.6 M	[42]
Macroalgae waste (red seaweed waster from agar production plant)	-	30% solids	200, 230	2, 6	-	• Solid yield: 52.3-60 wt%; basis was not specified • Increased temperature and residence time resulted in decreased solid yield • Ash: 10.41-13.59 wt%; increased as temperature and residence time increased • C: 50.73-55.08 wt%; increased as temperature and residence time increased • H: 5.24-5.47 wt%; stable as temperature and residence time increased • O: 20.33-27.58 wt%; decreased as temperature and residence time increased • N: 4.35-4.86 wt%; stable as temperature and residence time increased Molar Ratio: • H/C: 1.17-1.29; decreased as temperature and residence time increased	[61]

		• O/C: 0.28-0.41; decreased at 230°C as residence time increased, but stable at 200 • HHV: at 200°C decreased from 21.11 to 20.75 MJ/kg; at 230°C increased from 20.74 to 23.25 MJ/kg

*M = per wet/fresh feedstock weight

In a study of HTC of seaweed, the temperature and residence time were varied between 180-220 °C and 30-120 min at biomass to water mass ratio of 1:9. Solid yields varied from 25-40 wt%, liquids from 54-69 wt%, and gas yields from 4-7 wt% (wet basis/total feedstock) [36]. As temperature increased the liquid yield increased and solid yield decreased while gas yield remained stable [36]. Increasing residence time showed the same trend but to a lesser degree [36]. In a study by Shrestha et al. (2021) sea lettuce (common green seaweed) with a 92 wt% moisture content was treated using HTC between 150-220 °C with residence time between 30-120 min) [60]. The solid yield ranged on a wet basis from 6 to 22 wt%, liquid yield from 73.09-89.18 wt%, and gas yield from 2-8 wt%. As temperature increased (at a constant residence time) the solid yield decreased approximately 60%, as residence time was increased (at constant temperature) the solid yield decreased by 3-28% (depending on temperature) [60]. Compared to the seaweed [36], the yields (wet basis) of sea lettuce study showed the same trends and similar values. In another study, red algae waste from an agar production plant (70% water) underwent HTC between 200-230°C over 2-6 h with hydrochar yields from 52.3-60 wt% (basis was not specified) which decreased as temperature and residence time increased [61]. Compared to sewage sludge and pulp and paper sludge solid yields which varied from 40-90 wt% [2, 37, 34, 32, 33], dry basis, generally macroalgae yields were lower (20-40 wt%, dry basis) within the same range operating conditions.

In a more extensive study by Cao et al. (2019) red algae (*Gracilaria lemaneiformis*) were subjected to microwave-assisted hydrothermal carbonization (MHTC) with and without the addition of sulfuric acid [42]. In MHTC with only water at 180 °C, 20 min, and 3% biomass, the solid yield was 32.1 wt% (db) and as sulfuric acid concentration increased from 0.1 to 0.6 M the solid yield gradually decreased from 28.1 to 24.6 wt% (db). Increasing temperature at a fixed acid content and biomass:water ratio, dropped the hydrochar yield from 31.4 to 20.8 wt% (db) while carbon content increased from 48.8 to 57.8 wt% (Table 2.4) [42].The same study also varied biomass to water ratio (biomass to water (w/v) 1-10, 20 min, 180 °C, 0.2 M H_2SO_4). Increasing

the ratio resulted in an increase in yield and carbon content and carbonization became unfavorable at ratio of 10 [42]. Prakorso et al. (2018) studied *Eucheuma Cottonii* for HTC and varied the biomass to water ratio (1:5, 1:10, 1:20), temperature (250 and 275 °C) and residence time (30 to 90 min) [40]. As with previous studies, as the ratio increased the hydrochar yield increased [40].

Overall higher HTC temperatures and/or longer residence times reduced oxygen content in the hydrochars and increased fixed carbon and overall carbon wt% (Table 2.4) [36, 27, 35, 60, 61]. The change in elemental composition showed H/C and O/C ratios of the hydrochars to be similar to peat, and both ratios approach the lignite region as HTC temperature and time increased [36]. This indicates that macroalgae hydrochars have potential as fuel [36] as indicated above, low H/C indicate stability which is important for transport and low O/C leads to a cleaner burning.

Macroalgae are high in mineral content relative to sludge, particularly calcium and magnesium. According to Patel et al. (2021), the inorganic yield (ratio of inorganic content in the hydrochar to inorganic content in the raw seaweed) × solid yield] in the macroalgae hydrochar decreased as temperature and residence time increased compared to the feedstock, except for phosphorous and manganese [36]. The hydrochar mineral content (phosphorous, potassium, calcium, magnesium, boron, phosphorous and manganese) decreased as residence time increased when reaction temperature was 180 °C. However, at 200 °C and 220 °C, the minerals concentration increased as residence time increased with the exception of potassium and boron which continued to decrease [36]. The increase is possibly due to organic materials degradation and dissolution into the liquid phase at higher temperature and residence time thereby concentrating the inorganics in the solid. The highest mineral content in the hydrochar was calcium (1.39-2.13 wt%) followed by potassium (0.81-1.31%) and magnesium (0.64-0.81 wt%) with other elements less than 0.6 wt% [36]. In work by Kantarli et al. (2019) the fate of alkali/earth metals in marcoalgae HTC treatment was studied [43]. Alkali (Na, K) and alkaline earth metals (Mg) decreased (<0.01- 0.56 wt%) relative to the feedstock (0.72-7.96 wt%) [43]. Calcium was concentrated in the hydrochar, increasing from 1.03-3.77 wt% in the feedstock to 5.35-9.27 wt% [43]. Drawing any conclusions about the fate of inorganics undergoing HTC is difficult as it will be a function of the temperature, time, pH, and water content as well as the relative solubility of the inorganic in water. Mineral content in marine species is highly variable even within the same species, as proximate composition is also a function of the maturity of the species [27]. Smith and Ross [27] investigated

the seasonal effect on hydrochar quality of three species of macroalgae: *Laminaria digitata, Laminaria hyperborean,* and *Alaria esculenta*. Macroalgae harvested in the fall showed the highest char yield due to the high carbon content in the feedstock, while spring harvested macroalgae hydrochar showed the highest ash due to high mineral content in the feedstock [27].

The composition of HTC liquid of macroalage HTC also has been studied. The *Eucheuma cottonii* HTC liquid at 275 °C with 30 min residence time showed the presence of alkanes, aromatic, alcohol (diacetone), and organic acid (levulinilic acid), with particularly high toluene content (63.01% of the total area via GC-MS), followed by benzene (14.53% of the total area) [40]. In another study, Patel et al. (2021) analyzed the mineral content in waste macroalgae HTC liquid (180-220 °C, 120 min) and identified high levels of potassium (14-16 wt%), followed by magnesium (~5 wt%), and calcium (3-4 wt%) [36]. As discussed above, the solubility of the compounds factors into its fate. potassium was the most soluble of the elements studied and phosporus is the least soluble (< 0.1 wt% in liquid). HTC liquid products of various macroalgae had mineral content and organic carbon and it was proposed that the liquid could be treated to collect the minerals for fertilizer or treated by anaerobic digestion to produce energy such as methane/hydrogen [27].

HTC liquids (150-260 °C, 1h) of *Saccharina latissimi* and *Fucus serratus* were acidic at low temperatures and increased to below neutral with temperature (pH 4.8 to 6.74). The acidic nature of HTC liquid was proposed to be due to high fatty acids concentrations. The increase in pH with temperature was attributed to an increase in phenolic compounds (0.16 to 0.25 mg/L) and/or solubilization of alkaline ash into the liquid [35]. *Gelidium Sesquipedale* (red algae) hydrochars were only slightly acidic and slightly increased as temperature (200-230 °C) and residence time (2-6 h) increased from a pH low of 6.04 to a high of 6.58. The trend in pH was attributed to simple sugars and hemicellulose degradation to organic acids at lower HTC temperatures [61]. On the other hand, at higher HTC temperature lignin degradation produces less acidic phenolic compounds resulting in a slightly higher pH [61].

TGA-DTG was used to assess material thermal stability, degradation temperature, proximate composition, and use as a solid fuel. Kantarli et al. (2019) studied three species of macroalgae: *Fucus serratus* (FS)*, Alaria esculenta* (AE), and mixed species of *Cystoseria sp.* and *Laurencia sp.* (BS) [43]. HTC was performed over a range of temperatures (200-250 °C), 30 min,

water content of 75 wt%. Raw macroalgae analysis under a nitrogen atmosphere showed a DTG peak related to moisture loss at approximately 100 °C, a major peak between 200-250 °C (carbohydrate and protein decomposition), and a minor peak at approximately 600-700 °C due to alkali carbonates decomposition [43]. Comparing the feedstock to hydrochars, the peak at 100 °C was reduced in the hydrochars showing the moisture indicative in HTC and the second peak shifted to higher temperature (300–350 °C), which is related to char degradation, indicating that HTC converted biomass into char like product [43].This was similar to sludge peaks, with the breadth of the peak varying due to the different organic materials in the feedstocks. The DTG third peak was where we saw the variability in the feedstock composition. For comparison, hydrochar from pulp and paper sludge had a major peak at 750°C due to chemicals (such as additives, coagulants, flocculants, and minerals) and lignin [2], macroalgae hydrochar was at 600-700 °C due to minerals decompositions [43], and sewage sludge does have a second peak [32].

In order to assess fuel potential, the hydrochar was studied under oxygen/air atmospheres in TGA experiments [43]. In air, one to two peaks were present in macroalgae hydrochars (i) a peak associated with fixed carbon at 350-400 °C for all hydrochars studied and (ii) a peak associated with the formation and oxidation of volatiles at 250-300 °C present in AE and FS hydrochars. The two peaks overlapped for BS hydrochar [43]. The peak associated with fixed carbon combustion moved from ~450°C in the feedstock to ~300-350°C in the hydrochars due to increased fixed carbon content [43].

In studies where HHV was assessed, increasing temperature and residence time yielded higher HHV. The increased in HHV likely due to increase in carbon content and decreased in volatile matter and ash content as temperature and residence time increased [36]. In studies of *Sargassum horneri* HTC, the HHV increased with residence time (30 to 120 min). The HHV was 13.81-16.63 MJ/kg, 16.39-18.12 MJ/kg, and 17.55-18.93 MJ/kg at 180, 200, and 220 °C respectively, compared to the feedstock at 12.21 MJ/kg [36]. Hydrochars produced from *Sargassum horneri* combined with citric acid as a catalyst produced hydrochars with HHV of 19 to 25.1 MJ/kg; the feedstock HHV was 17.4 MJ/kg [38]. As the residence time increased from 2-16 h, HHV increased from 21.4 to 23.6 MJ/kg and temperature changes between 180-200 °C had no effect. Above 200ºC, HHV increased (up to a value of 23.8 MJ/kg) [38]. HTC of red seaweed combined using sulfuric acid catalysis (20 min reaction time) showed an increase in HHV (18.8 to

24.7 MJ/kg) at much lower temperatures (160 to 200 °C). Given the feedstock HHV was lower than [41] at at 12.5 MJ/kg this represents a much larger increase in HHV [42]. In another study, red algae waste from agar production plant (HHV 18.49 MJ/kg) treated at 200-230 °C and 2-6 h resulted in hydrochars with slightly higher HHVs (20.74-23.25 MJ/kg [61]. Similar to sewage sludge hydrochar HHV, the macroalgae hydrochars were comparable to lignite HHV (15 to 18 MJ/kg) [62].

A study of surface morphologies of *Sargassum horneri* showed microsphere formation in the hydrochar after treatment at 190 °C with residence times of 4 to 8 hours [38]. Zeng et al. (2018), studied *Sargassum horneri* hydrochar surface morphologies (HTC at 180 °C, 2 h) before and after KOH activation [44]. The activated hydrochar did not have microspheres, but the hydrochar became more porous with a honeycomb pattern after activation. Round shape microspheres and structure like fibres were present in heat-activated *Eucheuma Cottonii* hydrochar (250 °C, 30 min) [40]. The red algae waste hydrochar in [56] showed a thick fibre structure when treated at 200 °C for 2 h. Increasing the HTC time to 6 h resulted in a cracked surface with thinner fibre structure [61]. Further temperature increase to 230°C over 2 h resulted in a honeycomb structure on the surface and the hydrochar became more porous when time increased to 6 h. Despite the improvement in surface morphologies, some fibre structure remained and was attributed to lignocellulosic [38]. As previously mentioned in the paper sludge section, the complete degradation of lignocellulosic material requires temperatures exceeding 300 °C, and these studies explain the remaining fibrous material observed in SEM (Scanning electron microscope) [1, 34].

The surface area of macroalgae has been studied in acid catalyzed HTC or thermally/chemically activated hydrochars. Xu et al. (2013) showed surface areas 0.6 to 31.8 m^2/g (180-210 °C for 2-16 h) in acid-catalyzed *Sargassum horneri* hydrochars [38]. Heat-activated *Eucheuma Cottonii* hydrochar had a surface area of 12.35 m^2/g (HTC conditions of 250 °C for 30 min) [40]. Compared to commercial activated carbon, the hydrochar surface area is low [38]. Zeng et al. produced high surface hydrochar from macroalgae (*S. honeri*), for CO_2 adsorption, by KOH activation [44]. At 180 °C for 2 h with no KOH treatment, the surface area was 26.64 m^2/g. Under the same conditions and KOH activation, the surface area increased to 1221 m^2/g. The *Sargassum horneri* hydrochars (both unactivated and activated) were then compared for CO_2 adsorption. The adsorption capacities of the unactivated char were 36 mg/g and increased to 101.7 mg/g using

activated char [44]. In the study of waste hydrochars, BET surface areas between 5.9 to 12.7 m^2/g were obtained (the feedstock surface area was not indicated) [61]. At 200 °C, the surface area increased from 5.9 to 10.3 m^2/g as residence time increased from 2 to 6 h [61]. As the temperature increased from 200 to 230 °C (at 2 h) the surface area increased to 12.7 m^2/g. However, further increases in time increases (2 to 6 h at 230 °C) showed a lower surface area of 10.1 m^2/g [61]. It should be noted, overall, these changes in surface area are small, however, the study does demonstrate, as with other feedstocks, high temperatures combined with long residence times tend to decrease surface areas. The decrease in surface areas is likely due to pore collapse or condensing aromatic structure [34]. Generally, the surface areas of macroalgae hydrochar – without activation (5.9-12.7 m^2/g) were similar to sewage sludge hydrochar (1-17 m^2/g) [39].

Similar to biomass based sludges, macroalgae hydrochars FTIR show decreased O-H intensities compared to the feedstock [40, 61]. Mendez et al. (2019) proposed that as the temperature or reaction time increased, the C=O peak reduced (ketone, amide, and carboxylic groups) [61]. In contrast, peaks associated with C=C in aromatic structures increased due to decarboxylation and aromatization [61]. C-O-C and C-O stretching intensified at 200 °C HTC but decreased at 230 °C HTC; the study proposed this was due to a reduction in the O/C atomic ratio of 0.41 and 0.28-0.38, respectively [61]. Again, any comparison of "intensity" is not a reflection of quantity. Without additional analysis, particularly in complex matrices such as hydrochar, assessing trends in functional groups is difficult. A study of Sargassum *horneri* treated using $Fe(NH_4)_2(SO_4)_2 \cdot 6H2O$ catalyst (1.96 g) and 1:4 (mass biomass:mL of water) at 180 °C for 2 h resulting in hydrochar with weak O-H, C=C, and N-H peaks [44]. The N-H peak detected may related to the catalyst used. Further, HTC with KOH activation hydrochars only showed peaks associated with O-H and C=C this was proposed due to reaction between hydrochar and KOH [44]. Sea lettuce hydrochars produced at 150-200 °C and 1 h showed O-H, C-H, C=C, and C-O functional groups similar to the feedstock [60]. *Sargassum horneri* hydrochars also showed O-H, C-H, C=O/C=C, and C-O/C-C functional similar to the feedstock [38].

2.3.4. Shrimp

As noted above, crustaceaFn waste differs from macroalgae and sludge in the form of the carbohydrate that dominates (chitin vs lignocellulose) and higher mineral content. Kannan et al.

(2015; 2017; 2018), studied HTC and microwave-assisted hydrothermal carbonization (MHTC) of raw seafood waste and seafood waste pretreated (via mineral and/or protein removal). Both finfish and shrimp waste were studied [59, 52, 41]. In the first paper, waste MHTC was conducted at 150-180 °C with residence times between 1-2.5 h on raw and pretreated samples as a screening study. For the raw feed (i.e., no pretreatment in form of protein or mineral removal) the authors claimed no conversion to hydrochar was observed) [59]. However, data to support this was not provided. This could be due to the complex nature of the feedstock (as proposed by authors). However, the polysaccharide in shrimp is chitin versus cellulose/hemicellulose, chitin does not show significant degradation at temperatures below 300°C [54]. The protein in the feed can hydrolyze at the studied temperatures yet typically requires longer reaction times [63]. MHTC of pretreated feedstock, where the material was treated via acid and bases (1-3 days at pH 3-5 or 1-3 days at pH 9-12), did not show hydrochar formation but again no data was shown to indicate how this was assessed [59]. The study suggested that this result was due to the poor digestibility of seafood waste in acidic or alkali conditions [59]. The pretreatment was modified to an enzymatic treatment using a mixture of lipid/protein/carbohydrate acting enzymes to break down the biomolecules into their monomers to facilitate polymerization reactions in MHTC [59]. Enzymatic pretreatment did result in hydrochar (yield 38wt% db) from shrimp waste at MHTC of at 150 °C for 1 h [59]. Building on these screening experiments, Kannan et al. (2017) focused on the MHTC shrimp shells using enzymatic pretreatment [41]. The yield of the enzymatic pretreated shrimp waste hydrochars was approximately 18.5-35.4 wt% (db) at temperatures between 150-210 °C and residence times between 60-120 min. In the screening experiment, the biomass to water ratio did not affect hydrochar yield when the temperature and residence time was constant at 180 °C and 60 min. Hydrochar yield increased as temperature increased from 120 to 180 °C (at 60 min and biomass to water ratio 1), but then plateaued from 180 to 210 °C [41]. Increasing the MHTC time from 60 to 120 min (constant at 180 °C and biomass to water ratio 1) increased hydrochar yield [41]. The study proposed that the “trends”, or lack thereof, in hydrochar yield is likely due to the complex macromolecular structure of the shrimp waste [41]. To better define the relationships a statistical analysis through the Response Surface Method (RSM) was performed with hydrochar yield as a function of temperature and residence time. The analysis showed significant interaction between temperature and residence time and the interactions [41]. Further, the RSM plot showed hydrochar yield increased with temperature and residence time increased up until a certain point

and then started to decrease, showing a parabolic RSM plot [41]. The maximum yield predicted by the RSM surface optimization was approximately 42 wt% (db) at 184 °C and 112 min [41]. Hydrochar elemental analysis showed an increase in carbon with increase in temperature and residence time and corresponding decrease in oxygen (Table 2.5). This work was continued with HTC by Kannan et al. (2018) [52] , again using enzymatically pretreated shrimp waste under the same conditions as the MHTC experiment [41]. The hydrochar yield of HTC of shrimp shell was in the same range as the MHTC experiments (18.79-28.65 wt%db). Analysis by RSM showed the same trends in residence time and temperature on yield as the previous MHTC study [41]. The hydrochar yield predicted was a better match to the with a predicted maximum yield of 29 wt% (db) at 186 °C and 120 min. The trends in carbon and oxygen are the same as MHTC (Table 2.5). It was also observed that there was little difference (percentage difference < 20%) in the C, H, N, and O content between MHTC and HTC hydrochars at the same conditions [52, 41]. The only apparent difference was that MHTC resulted in a higher maximum hydrochar yield at similar conditions [52].

Wu et al. (2022), studied HTC of dried raw shrimp shell between 120- 280 °C and a residence time of 2 h (water to biomass ratio not specified). Hydrochar was observed but no yield was reported [64]. The TGAs of the feedstock to the hydrochars indicate the temperature peak for thermal decomposition shifted from 337.87 °C for the feedstock to between 356-399 °C for the hydrochars. This was proposed to indicate the formation of a more stable aromatic structure in the hydrochar [64]. The study proposed that the shrimp hydrochar showed dehydration/moisture loss at 30-150 °C, devolatilization of organic compounds (protein/chitin) at 180-580 °C, and thermal degradation of $CaCO_3$ at 580-900 °C [64]. The 580-900 ºC mass loss rate peak shifted to a higher temperature as HTC temperature increased. It was proposed this was due to the crystalline transformation of $CaCO_3$ [64]. At 580-900 °C, the mass loss peak related to $CaCO_3$ was similar to macroalgae hydrochar mass loss at 600-700 °C due to minerals decomposition [43].

It is worth noting that in Kannan et al. (2015) study of MHTC of raw (no pretreatment) shrimp, no hydrochar was reported (as noted above) [58]. This may be due to differences in what researchers considered “hydrochar” vs unreacted solid.

The hydrochar carbon in Wu et al. (2022) study ranged from16.03-20.73 wt% (Table 2.5). The hydrochar carbon decreased from 20.73 wt% at 120 °C to 16.03wt% at 200 °C. As HTC

temperature increased from 200 °C to 280 °C carbon increased to 19.5wt% [64]. The HTC temperature also had little influence on hydrogen and sulphur content (no feedstock elemental content reported) potentially due to high mineral content. The feedstock ash was 27.58 wt% (no hydrochar proximate and mineral composition reported) [64]. The nitrogen content decreased as temperature increased (Table 2.5). The decrease in nitrogen was proposed due to increasing degree of deacetylation at higher temperatures [64]. The nitrogen decrease may also be due to the hydrolysis of proteins, given that the HTC temperature was still below 300 °C and below chitin degradation temperatures, but this cannot be confirmed.

Chen et al. (2022), conducted HTC on dried shrimp at 220 ºC over 24 h in acidic water (2 M HCL) (1 g shrimp/10 mL water) [65]. The acid-assisted HTC was proposed to enhance the hydrolysis process and remove the impurities/minerals in the feedstock [65]. The removal of minerals was demonstrated by the absence of $CaCO_3$ peaks (XRD) in hydrochars [65]. The shrimp hydrochar yield was 3.1 wt% (db) with 68.1 wt% carbon, 5.2 wt% nitrogen, and 2.8 wt% hydrogen [65]. It was proposed that shrimp HTC had low yield due to strong protein hydrolysis rather than carbonization reaction [65].

Enzymatic pretreated shrimp produced MHTC hydrochars were cracked flat-like structures with visible microspheres (no BET surface area reported) [41]. Similar surface morphologies were reported in pretreated shrimp HTC hydrochar [52]. Similarly, In He et al. (2020), hydrochard from pretreated shrimp shell waste (HTC of 180 °C and 12 h), compact flat-like surface morphologies were observed and a surface area of 4.27 m^2/g was reported [46]. The flat-like surface morphologies were possibly due to minerals in the hydrochar. The hydrochar was subsequently washed with acetic acid to remove the calcium carbonate and transforming the hydrochar surface area into a more porous material and increasing the surface area to 12.65 m^2/g. This is still a low surface area given the extent of processing involved [46]. The acid-washed hydrochar, was studied for methyl orange adsorption. The maximum adsorption capacity was reached within 150 min (755.08 mg/g at 310 K at a solution pH of 4) [46]. In a related study, minerals were removed simultaneously with HTC from shrimp in an acid-assisted HTC (220 °C and 24 h). As with the previous work, the result was porous irregular shaped particles in the hydrochar with a surface area of 26.8 m^2/g [65]. The higher surface area compared to the study in [61] was possibly due to higher temperature and longer residence times and/or combining the acidic treatment with HTC [65]. In

the Wang et al. study (2022), the BET surface area of shrimp hydrochar without pretreatment HTC was 4.03-14.63 m^2/g [64]. The surface area (at constant 2 h HTC) increased from 120 to 240 °C and then decreased from 260 to 280 °C [64]. The study proposed the decrease in surface area was due to pore collapse at higher temperatures [64]. Overall, the surface area of shrimp hydrochars from pretreated shrimp or acid-assisted HTC still resulted in low surface area, similar to shrimp HTC without any additional treatment.

For the HTC experiments involving the raw (no pretreatment) shrimp, the functional groups in the feedstock and hydrochar were compared via FTIR analysis [64]. The feedstock showed peaks associated with N-H, C-H, carbonate C-O, amide 1, and amide 2 [64]. Amide 1 is a primary amide (with single carbon attached to nitrogen) and amide 2 is a secondary amide (with two carbons attached to nitrogen) [66]. The nitrogen functional group detected in raw shrimp was possibly from chitin. The shrimp hydrochar peaks were associated with O-H, N-H, C-H, C=O, carbonate C-O, amide 1, and amide 2 [64], which similar to the feedstock. The carbonate C-O indicated $CaCO_3$ in feed and hydrochars and was validated by XRD analysis [64]. XPS (X-ray photoelectron spectroscopy) analysis on hydrochar showed the presence of -C-(C,H)/C=C related to hydrocarbon/aromatic structure [64]. Additionally, the XPS showed the presence -C-(O,N) and -C=O related to amide/alcohols/carbonyls/carboxylates [64]. The presence of C=H and C=O in XPS analysis was also found in FTIR.

In other studies, FTIR analysis of raw (no pretreatment) shrimp showed peaks associated with O-H, C=C, N-H, and C-S [41, 52]. FTIR analysis of hydrochars produced from pretreated shrimp in MHTC at 150-210 °C, water ratio 1:1, and 60-120 min showed similar functional groups with the untreated shrimp feedstock: O-H, C=C, N-H, and C-S [41]. This work proposed there was C-H peaks in the pretreated shrimp MHTC hydrochar [41]. The mode of thermal treatment, conventional vs MHTC did not impact peaks identified for the pretreated shrimp hydrochars. [52]. Another shrimp hydrochar from the HTC of deproteinized and deacetylated shrimp feedstock, followed by hydrochar acid washing, showed peaks associated with O-H, C=O, and C-H aliphatic groups which were also present in the untreated raw shrimp shell [46]. XPS analysis of pretreated acid-washed hydrochar concluded that the hydrochar contained a long aliphatic chain and had abundant nitrogen functional groups (e.g. 27.25% of –HN–C=O and 53.60% of $–NH_2$) [46]. In another study by Chen et al. (2022), combining HTC and acid treatment, FTIR analysis on the

shrimp hydrochar (acid assisted HTC, 220 °C for 24 h) showed peaks similar to [46]. The study also proposed the presence of aromatic C=C, N–H, and C–N peaks [65]. In the same study, XPS analysis found spectra possibly associated with pyrrolic N at 400.1–400.2 eV, pyridinic N at 398.5–398.7 eV, and Quaternary N at 401.5–401.8 eV [65], which supported the proposed nitrogen containing functional groups in the FTIR.

FTIR of untreated shrimp hydrochar showed peaks related to $CaCO_3$ [64]. Compared with treated shrimp HTC, no peak was associated with carbonate in the other acid-washed or acid-assisted HTC hydrochar [46, 65]. This was understandable since the carbonate was gone due to the acid involved. Other than the carbonate, overall, shrimp and its hydrochar (treated or untreated) showed similar spectra, with O-H, C-H, C=O, and nitrogen-containing functional groups such as C-N or N-H. Different from sludges and macroalgae hydrochar [1, 3, 37, 32, 33, 38, 61], shrimp HTC studies discussed above propose FTIR peaks related to the nitrogen functional group [46, 41, 52, 65] which related to chitin.

Kannan, et al. (2020) [67] also studied the liquid product in the work above on from pretreated (protein removal) shrimp shell [41, 52]. Visually the liquid was light yellow to dark amber in color, with pH of 6-7 [67]. The identified components in HTC and MHTC liquid were categorized into 3 major groups: diketopiperazines (DKP), pyrazines, and pyrrolidine derivatives [67]. MHTC liquid composition showed no change when temperature varied. On the other hand, HTC liquid showed a shift in composition; at low HTC temperature (120-180 °C), dipeptides and cyclic ketones were present in the HTC liquid while at 210 °C piperidinones and acids were present. MHTC did not indicate dipeptides, cyclic ketones, piperidinones, and acids indicating the mode of heat transfer may impact the liquid composition [67]. The liquid product (HTC and MHTC) was mainly composed of nitrogen containing compounds (such as DKPs, pyrazines and pyrrolidines) produced from proteins [67]. Pyrazines were proposed to form via the Maillard reaction (reaction of protein derived products (amino acids) and carbohydrates) [67].

Table 2.5. Selected Crustacean Shells HTC Summary (wt%) – dry basis unless stated otherwise.

Sample	M* (wt%)	biomass:water (wt:wt)	T(°C)	t (h)	rpm	Result	Source

Shrimp	[41]	1:1	150 - 210	1 - 2	none	Enzymatic pretreated feedstock Microwave HTC • Solid yield: 18.53-35.4 wt% • Total fixed carbon**: 2.23-13.34 wt%; increased with temperature and residence time • VM: 63.73-70.08 wt%; decreased as temperature and residence time increased • Ash: 21.41-25.15 wt%; decreased as temperature and residence time increased • C: 39.02 -49.23 wt%; increased with temperature and residence time • H: 5.45-6.23 wt%; slightly increased with temperature and residence time, but at 210 °C H content constant at ~5.8% • O: 39.9-50.67 wt%; decreased as temperature and residence time increased • N: 4.54 -5.69 wt%; stable with temperature and residence time variation Mass ratio: • H/C: 0.11-0.14; decreased as temperature and residence time increased • O/C: 0.79-1.3; decreased as temperature and residence time increased • HHV: 18.26-23.22 MJ/kg; increased with temperature and residence time	[41]
Shrimp	[52]	1:1	150 - 210	1 - 2	none	Enzymatic pretreated feedstock Conventional HTC • Solid yield: 18.79-28.65 wt% • Total fixed carbon**: 36-39.36 wt%; increased with temperature and residence time • VM: 34.71-43.3 wt%; decreased as residence time increased but slightly increased with temperature. Hydrochars VM are lower than the feedstock (81.96wt%) • Ash: 19- 23.7 wt%; no correlation with temperature and residence time. Hydrochars ash content are higher than the feedstock (14.56%) • C: 41.61-50.36wt%; increased with temperature and residence time • H: 5.53-5.9wt%; no correlation with temperature and residence time. • O: 37.47-47.57wt%; decreased as temperature and residence time increased N: 5.19-6.52wt%; stable with temperature and residence time variation Mass ratio: • H/C: 0.11-0.14; decreased as temperature and residence time increased • O/C: 0.79-1.4; decreased as temperature and residence time increased • HHV: 19.20-24.2 MJ/kg; increased with temperature and residence time	[52]
Shrimp	[64]	Unknown	120-280	2	none	• C: 16.03-20.73 wt%; no correlation as temperature • H: 1.21-1.86 wt%; no correlation with temperature • N: 0.09 – 2.63 wt%; decreased as temperature increased • S: 0.06-0.35 wt%; no correlation with temperature	[64]
Shrimp	[65]	(4+x[a])g:40mL	220	24	Stirred prior HTC, no RPM	Shrimp HTC, HCl assisted • C: 68.1 wt% • H: 5.2 wt% • N: 2.8 wt%	[65]
Lobster	[58]	1:1	150-210	1-2	none	Enzymatic pretreated feedstock Microwave HTC • Solid yield: 38.21-50.6 wt% • Total fixed carbon**: 4.42-19.7wt%; increased with temperature and residence time • VM: 37.1- 47.1 wt%; decreased with temperature and residence time • Ash: 30.1-52.8 wt%; decreased with temperature and temperature. Hydrochar ash contents are higher than feedstock (26%) • C: 33.6-36.4 wt%; increased with temperature and residence time • H: 3.17-4.29 wt%; no correlation with temperature and residence time. • O: 55.3-60.1 wt%; decreased as temperature and residence time increased N: 2.86-4.28 wt%; increased with temperature and residence time	[58]

						Mass ratio: • H/C: 0.09-0.12; decreased as temperature and residence time increased • O/C: 1.57-1.79; decreased as temperature and residence time increased • HHV: 8.28-15.3 MJ/kg; increased with temperature and residence time	
Crab Shell	[68]	4g:40mL	220	3	none	Activated at 800 °C Activated Crab Shell • C: 81.39 wt% • H: 2.47 wt% • O: 10.57 wt% • N: 2.27 wt% • S: 1.09 wt%	[68]

*M = moisture = calculated from fresh feedstock weight

**Total carbon (%) = 100- (Moisture content (%) + Volatile matter (%) + Ash content (%))

x^a = glucose addition for HTC feedstock: 0-4 g

2.3.5. Lobster

With respect to other crustacean species, one study on lobster MHTC was found on the effect of MHTC conditions and hydrochar characterization [58]. The lobster waste was pretreated via enzymatic hydrolysis (viscozym/lipase/protease) followed by MHTC following method by Kannan, et al. (2015) [59]. The study was done at three MHTC temperatures (150 °C, 180 °C, and 210 °C) and residence times (60, 90, and 120 mins) with biomass to water weight ratio of 1:1. RSM was conducted on the data with temperature and residence time as factors, and hydrochar yield as the response. The analysis showed that residence time and the interaction between temperature and residence time had a significant effect on hydrochar yield. Hydrochar yield increased as temperature and residence time increased, up until a maximum value after which the hydrochar yield drops, resulting in an inverted parabola surface plot [58]. These trends were similar to similar to pretreated shrimp MHTC and HTC discussed previously [41, 52]. The maximum hydrochar yield by RSM optimization was 52 wt% at 203 °C and 60 min. The raw lobster waste had 46.6 wt% volatile matter, 74.9 wt% moisture, 30.29 wt% fixed carbon, and 26 wt% ash. Produced hydrochars had a lower volatile matter and moisture content and higher fixed carbon and ash content relative to the feedstock (Table 2.5). The hydrochar total fixed carbon content increased from 4.02 wt% to 19.7 wt% and ash decreased from 52 to 32 wt% as MHTC temperature and residence time increased from 150 to 210 °C and 60 min to 120 min [58]. Volatile matter decreased only marginally (<0 5 wt%) with residence time (60 min to 120 min) at 150°C and 180°C. This was also true of moisture content, decreasing from 1.72 to 0.42 wt% at 150°C and from 1.75 to 0.57 wt% at 180 °C. At 210 °C, the volatile matter increased from 37.1 to 47.1 wt% as residence time increased from 60 min to 120 min. At 210 °C, the volatile matter increased from

37.1 to 47.1 wt% as residence time increased from 60 min to 120 min which was unexpected. There was no explanation as to why; however, the study proposed that further investigation was needed to see the trend at a higher temperature since the increase in the volatile matter was undesirable as it would increase environmental impact and pollution. Comparing shrimp [41] using the same pre-treatment and MHTC conditions, lobster hydrochar had higher yield and ash content and lower carbon content than shrimp hydrochar. This could be due to higher unreacted minerals or chitin content. Since chitin degrades at a much higher temperature than HTC conditions this will lead to unreacted chitin staying in the solid leading to higher solid yield.

The hydrochars (residence time 60-120 min and temperature 150-210℃) had carbon content ranging from 33-36 wt%, nitrogen from 3-4 wt%, hydrogen from 2-4 wt%, and oxygen from 55-60 wt% [58]. Generally, the hydrochar carbon increased and oxygen decreased (not unexpected given O is determined by difference). as temperature and residence time. These trends resulted in lower O/C and H/C atomic ratios of hydrochars [58] similar to sludge hydrochar. The lower O/C ratio illustrated that decarboxylation reactions occurred, while lower H/C ratios demonstrated dehydration reactions during MHTC [58].

The MHTC transformed light pink lobster waste into brown/black coloured hydrochar [58], not unexpected given that the process would impact thermally labile carotenoids. Additionally, surface morphologies analysis showed the transformation of feedstock into porous plate-like structures hydrochar [58]. The pores became more pronounced as the MHTC temperature and residence time increased. Microspheres were detected at 180 °C and 210 °C MHTC [58]. The hydrochar HHV fluctuated, ranging from 8-15.3 MJ/kg lower or only slightly higher than the feedstock 14.4 MJ/kg. The hydrochars FTIR showed an O-H peak intensity reduction compared to the feedstock [58], it was proposed that the dehydration reaction occurred as proposed in HTC of sludges [1, 3, 37, 32, 33], and macroalgae [38, 61] studies. MHTC was proposed to intensified aliphatic carbons and out-of-plane bend of aromatic C-H functional groups peaks in the hydrochars [58].

2.3.6. Crab

Studies on crab shell HTC have emerged recently. The studies were more focused on pretreated crab shell/activated hydrochar (activating agent, acid, applied during HTC or post-

HTC). The crab shell hydrochar characterization was limited to the surface area, functional groups, and crystallinity [45, 68, 69].

A study by Han et al. (2021) [45], produced hydrochar from decalcified and deproteinized crab shell waste. After pretreatment, the powdered crab shell was mixed with 50% acetic acid (w/v = 1:1) as an activating agent and carbonized at 180 °C for 10 h. After HTC, the feedstock transformed into porous hydrochar and the hydrochar increased to 17.01 m^2/g from the feedstock of 9.57 m^2/g [45]. The surface area of crab hydrochar was low but slightly higher than shrimp hydrochar surface area of 4.27-12.65 m^2/g [46]. Acetic acid improved the HTC reaction, as the acid reacts with calcium carbonate, washing the hydrochar and exposing more pores in the process [46]. In another study by Wu et al. (2022), crab shell powder was hydrothermally treated (5 g sample and 30 mL water) at 180, 200, and 220 °C over 12 h [69]. The hydrochar was then activated at 800 °C (no method outlined in paper). The BET surface area the hydrochar was low and showed no change between 180 °C and 220 °C (4.254 to 4.701 m^2/g) [69]. Compared to Han et al. (2020) [54] , the hydrochar surface area was lower, possibly due to pore collapse at high activation temperature or the acetic acid treatment. Peng et al. (2019), studied HTC at 220 °C for 3 h on crab shell (4 g) mixture with 40 mL of purified water [68]. The dried hydrochar product was then activated with KOH in a N_2 atmosphere at 700 °C, 3h). The KOH-activated crab shell hydrochar surface area was 2109 m^2/g [68]. Overall, studies of unactivated crab shell hydrochar was comparable with macroalgae, and shrimp hydrochar (1-17 m^2/g) [39, 61, 64] .

XRD analysis of crab shell and hydrochars were done in some of the aforementioned studies. XRD analysis showed that compared to feedstock, crab shell hydrochar treated at 180 °C for 10 h (with acetic acid) showed less intense $CaCO_3$ peaks while the peaks related to chitin intensified [45]. The chitin may have been concentrated due to mineral loss/ decalcification pretreatment. However, as noted previously, XRD intensity alone cannot be directly linked to quantity. The work by Wu et al. (2022) on crab shell and activated hydrochar showed almost identical $CaCO_3$ peaks [69]. No chitin peaks were identified in the crab shell or activated hydrochar. The absence of chitin in the crab shell is unexpected since there was no pretreatment on the crab shell which would result in a breakdown of chitin crystalline structure and therefore not present in XRD. The KOH-activated crab shell hydrochar XRD had no identifiable peaks,

likely due to amorphous structure of hydrochar resulting from the extensive acid washing done in this study to remove the crystalline $CaCO_3$ [68].

Functional groups identified for crab shell were O-H, X-H (halogen), C-H and oxygen-containing groups such as R-N=C=O and C=O [45]. The acetic acid HTC crab shell hydrochar (180 °C, 10 h) showed the same functional groups. The crab shell hydrochar by Wu et al. (2022) (220 °C, 12 h) also showed peaks associated to O-H similar to the feedstock [69]. Overall, the crab shell hydrochar FTIR spectra was similar to the feedstock. The O-H, C-H, and C=O functional groups in the crab shell and the hydrochar were similar to the sludges (sewage and pulp and paper) [1, 3, 37, 32, 33], the macroalgae hydrochar [38, 61], and the shrimp and lobster HTC studies discussed above [46, 41, 52, 65].

SEM analysis of activated crab shell hydrochar (180-220 °C, 12 h, activated at 800 °C) showed plate-like structure in the original crab shell was broken, nanospheres formed and became more apparent as HTC temperature increased from 180 to 220 °C. EDS (Energy Dispersive Spectroscopy) was used to calculate the atom % of hydrochar produced at 220 °C and 12 h and showed 79.21 % C, 10.05 % Ca, and 9.09% O (crab shell composition not indicated) [69].

Studies in crab shell HTC are limited with respect to breadth or characterization and range of HTC conditions studied [45, 68, 69]. In terms of application, studies have focused on adsorption applications [45, 69] or potential for electrochemical energy storage [68]. Carbon based material is proposed to be a good candidate for electrochemical energy storage due favourable electrical conductivity, high stability, and low cost. Crab shell nitrogen content was shown to improve electrochemical reactivity and electrical conductivity. However, the crab shell hydrochar itself needed to be improved by combining it with other biomass (e.g. rice husk), to enhance porosity and facilitate a more active site for electrolyte ion transfer [68].

2.4. Conclusion

Studies on crustacean shell HTC were limited compared to sludges and macroalgae. Additionally, many crustacean shell HTC studies pretreated the feedstock extensively (such as enzymatic hydrolysis, protein removal, or carbonate removal). Furthermore, the characterization of the crustacean and its hydrochar was limited, especially on crab shell and crab shell hydrochar.

Shrimp and lobster (M)HTC did a handful of characterization (such as ultimate analysis, FTIR, XRD, XPS, and BET). On the other hand, crab shell HTC characterization was limited to BET, FTIR, and XRD.

Regarding FTIR, the common functional groups present in crustacean shell and their hydrochar were O-H, C-H, C=C, C-O, and some proposed a presence of nitrogen functional groups (such as N-H and amides I/II). The functional groups in the crustacean shell hydrochar were similar to the feedstock, unlike some reduction or intensification of certain peaks reported in some sludges and macroalgae FTIR. However, as discussed throughout the paper, FTIR is a qualitative analysis. Thus, the reduction or intensification of peaks related to quantity is not advisable. The only difference observed in the crustacean shell hydrochar compared to sludges and macroalgae HTC was the proposed nitrogen functional groups (possibly from chitin and protein). XRD of crustacean feedstock showed the presence of calcium carbonate. In the hydrochar, depending on pretreatment or any acid treatment, the calcium carbonate peaks may or may not be present. As for sludges and macroalgae, XRD was not studied.

The surface area of crustacean shell hydrochar was comparable with sewage sludge and macroalgae hydrochar at below 30 m^2/g. Meanwhile, pulp and paper sludge hydrochar were higher at 30-50 m^2/g. However, the hydrochar surface area is still low considering commercial activated carbon or any activated biomass hydrochar (can be ~1000 m^2/g). Nevertheless, crustacean shell hydrochar (such as shrimp and crab shell) had been studied for adsorption and showed a good result. Thus, surface area might not be the only factor deciding the adsorption performance; the crab shell hydrochar diesel adsorption had a high capacity despite the low surface area, as previously mentioned in the earlier section. The functional group might play an important part in adsorption performance.

Generally, HTC increased hydrochar carbon and fixed carbon content for all feedstock. Conversely, oxygen, hydrogen, nitrogen, sulphur, and volatile matter content decreased by temperature and residence time increased. According to the studies, the reactions during HTC were dehydration and decarboxylation reactions. The reactions also translate into a decrease in H/C and O/C ratio. The decrease in H/C and O/C showed that the HTC transformed biomass into a more stable solid rich in aromatic compounds that burn cleaner if used as fuel. However, as discussed above, the study on ultimate analysis in crustacean shell HTC was limited. Moreover, the existing

studies did pretreatment, which may show a different trend from untreated crustacean shell HTC. Thus, there is still a gap in knowing the effect of HTC conditions on crustacean shell hydrochar ultimate composition. Moreover, the composition of chitin-based crustacean shell differs from lignocellulosic-based pulp and paper sludge and carbohydrate-based macroalgae. Each material has a different degradation temperature, and depending on HTC conditions, it may affect the ultimate composition and distribution.

Furthermore, on HTC conditions, as discussed, temperatures and residence time effects have been studied extensively. However, the effect of biomass to water ratio is barely discussed. As discussed, Kannan et al. (2017) varied biomass to water ratio on shrimp HTC, but it was found that the ratio did not affect the hydrochar yield [41]. Prakorso et al. (2018) also studied the ratio effect on macroalgae HTC and concluded that increased water during HTC reduced solid product [40]. Other studies on pulp and paper sludge and sewage sludge did not study biomass-to-water ratio. However, observation on studies discussed above showed that the hydrochars properties vary within 20 wt% regardless of biomass to water ratio. Even so, studying the water ratio effect may be an interesting aspect of crustacean shell HTC. It has been studied from macroalgae HTC that there was a possibility that some minerals were transferred to the liquid medium during HTC, and since it was known that calcium carbonate was the main inorganics in the crustacean shell. Thus, water to biomass may affect the crustacean HTC hydrolysis and dissolution of minerals.

It is proven that HTC could transform biomass into hydrochar for possible fuel or adsorbent applications or electrochemical energy storage. As discussed in the review, this potential application can be seen from hydrochar composition, properties, and surface area. There was a good amount of research on sewage sludge, pulp and paper sludge, and macroalgae HTC, yet very little on shrimp, lobster and crab shells (including the product characterization and applications). Most of the crustacean HTC studies used pretreatment on the feedstock to break down the protein, lipid, and carbohydrates or remove the protein and carbonate. Furthermore, some studies used unconventional methods, microwave HTC or adding catalyst instead of conventional HTC. This needs to look more into since the processing plants' location (i.e., rural/remote areas) might be unsuitable for microwave HTC due to the equipment and upscaling, and additional pretreatment can add cost, including catalyst usage. Looking back at the abundance of fishery processing by-products and the pollution the waste can cause, there is plenty of room to study the HTC process

application for shellfish. There are gaps in research, such as only a few papers studied shellfish, no study on biomass to water ratios, more study on temperature and residence time needed especially for crab shell, further studies on HTC without pretreatment and hydrochar characterization, and possible applications of the hydrochars.

References

[1] C. Areeprasert, P. Zhao, D. Ma, Y. Shen and K. Yoshikawa, "Alternative Solid Fuel Production from Paper Sludge Employing Hydrothermal Treatment," *Energy & fuels,* vol. 28, no. 2, pp. 1198-1206, 2014.

[2] N. Saha, A. Saba, P. Saha, K. McGaughy, D. Franqui-Villanueva, W. J. Orts, W. M. Hart-Cooper and M. T. Reza, "Hydrothermal Carbonization of Various Paper Mill Sludges: An Observation of Solid Fuel Properties," *Energies,* vol. 12, no. 5, p. 858, 2019.

[3] S. Oumabady, P. S. Sebastian, S. P. Kamaludeen, M. Ramasamy, P. Kalaiselvi and E. Parameswari, "Preparation and Characterization of Optimized Hydrochar from Paper Board Mill Sludge," *Nature Reserach,* vol. 10, no. 1, p. 773, 2020.

[4] M. Asunción Lage-Yusty, M. Vilasoa-Martínez and S. Álvarez-Pérez, "Chemical composition of snow crab shells (Chionoecetes opilio)," *CyTA - Journal of Food,* vol. 9, no. 4, pp. 265-270, 2011.

[5] V. Novikov, S. Derkach and I. Konovalova, "Chitosan Technology from Crustacean Shells of the Northern Seas," *KnE Life Sciences,* pp. 65-74, 2020.

[6] Department of Fisheries and Land Resources, Newfoundland and Labrador, Canada, "Seafood Industry Year in Review 2019," [Online]. Available: https://www.gov.nl.ca/ffa/files/2019-SIYIR-WEB.pdf. [Accessed 12 August 2021].

[7] V. Sieber, M. Hofer, W. M. Brück, D. Garbe, T. Brück and C. A. Lynch, "ChiBio: An Integrated Bio-refinery for Processing Chitin-Rich Bio-waste to Specialty Chemicals," in *Grand Challenges in Marine Biotechnology*, P. H. Rampelotto and A. Trincone, Eds., Springer, Cham, 2018, pp. 555-578.

[8] E. M. Aklog, H. Kaminaka, H. Izawa, M. Morimoto, H. Saimoto and S. Ifuku, "Protein/$CaCO_3$/Chitin Nanofiber Complex Prepared from Crab Shells by Simple Mechanical Treatment and Its Effect on Plant Growth," *International Journal of Molecular Sciences,* vol. 17, no. 10, p. 1600, 2016.

[9] T. J. Beaulieu, P. Bryl and M.-É. Carbonneau, "Characterization of enzymatic hydrolyzed snow crab (Chionoecetes opilio) by-product fractions: A source of high-valued biomolecules," *Bioresource Technology,* vol. 100, no. 13, p. 3332–3342, 2009.

[10] W. J. Naczk, K. Brennan, C. Liyanapathirana and F. Shahidi, "Compositional characteristics of green crab (Carcinus maenas)," *Food Chemistry,* vol. 88, no. 3, p. 429–434, 2004.

[11] Y. I. Hajji, O. Ghorbel-Bellaaj, R. Hajji, M. Rinaudo, M. Nasri and K. Jellouli, "Structural differences between chitin and chitosan extracted from three different marine sources," *International Journal of Biological Macromolecules,* vol. 65, p. 298, 2014.

[12] C. Pires, A. Marques, M. Carvalho and I. Batista, "Chemical Characterization of Cancer Pagurus, Maja Squinado, Necora Puber and Carcinus Maenas Shells," *Poult Fish Wildl Sci,* vol. 5, no. 1, p. 1000181, 2017.

[13] B. S. Parthiban, A. Gopalakannan, K. Rathnakumar and S. Felix, "Comparison of the Quality of Chitin and Chitosan from Shrimp, Crab and Squilla Waste," *Current World Environment,* vol. 12, no. 3, p. 670–677, 2017.

[14] H. Ding, L. Lv, Z. Wang and L. Liu, "Study on the “Glutamic Acid-Enzymolysis” Process for Extracting Chitin from Crab Shell Waste and its By-Product Recovery," *Applied Biochemistry and Biotechnology ,* vol. 190, no. 3, p. 1074–1091, 2020.

[15] M. Leffler, "Maryland Marine Notes (Archive) - Maryland Sea Grant - Treasure from Trash: Is There Profit in Crab Waste?," March April 1997. [Online]. Available: https://www.mdsg.umd.edu/maryland-marine-notes-archive.

[16] N. Yan and X. Chen, "Sustainability: Don't waste seafood waste," *Nature,* vol. 524, p. 155–157, 2015.

[17] F. M. Kerton, Y. Liu, K. W. Omari and K. Hawboldt, "Green chemistry and the ocean-based biorefinery," *Green Chemistry,* vol. 15, no. 4, pp. 860-871, 2013.

[18] NRCAn, "Overview of Canada's forest industry," 16 July 2020. [Online]. Available: https://www.nrcan.gc.ca/our-natural-resources/forests-forestry/forest-industry-trade/overview-canadas-forest-industry/13311. [Accessed 15 March 2021].

[19] T. Mahmood and A. Elliott, "A review of secondary sludge reduction technologies for the pulp and paper industry," *Water research (Oxford),* vol. 40, no. 11, pp. 2093-2112, 2006.

[20] T. Wajima and J. F. Rakovan, "Removal behavior of phosphate from aqueous solution by calcined paper sludge," *Colloids and surfaces. A, Physicochemical and engineering aspects,* vol. 435, pp. 132-138, 2013.

[21] A. Haile, G. G. Gelebo, T. Tesfaye, W. Mengie, M. A. Mebrate, A. Abuhay and D. Y. Limeneh, "Pulp and paper mill wastes: utilizations and prospects for high value-added biomaterials," *Bioresources and bioprocessing,* vol. 8, no. 1, pp. 1-22, 2021.

[22] Environment and Climate Change Canada, "Canadian: Solid waste diversion and disposal," 20 December 2018. [Online]. Available: https://www.canada.ca/en/environment-climate-change/services/environmental-indicators/solid-waste-diversion-disposal.html. [Accessed 4 October 2021].

[23] L. Giroux, "State of Waste Management in Canada," Canadian Council of Ministers of the Environment, 2014. [Online]. Available: https://www.nswai.org/docs/State_Waste_Mgmt_in_Canada.pdf. [Accessed 4 October 2021].

[24] Goverment of Newfoundland and Labrador: Department of Environment and Conservation, Pollution Prevention Division, "Waste Management: Environmental Standards for Municipal Solid Waste Landfill sites," May 2010. [Online]. Available: https://www.gov.nl.ca/ecc/env-protection/waste/. [Accessed 4 October 2021].

[25] S. Xiu, A. Shahbazi, V. Shirley and D. Cheng, "Hydrothermal pyrolysis of swine manure to bio-oil: Effects of operating parameters on products yield and characterization of bio-oil," *Journal of analytical and applied pyrolysis,* vol. 88, no. 1, pp. 73-79, 2010.

[26] Y. Matsumura, "Hydrothermal Gasification of Biomass," in *Recent Advances in Thermo-Chemical Conversion of Biomass*, 2015, pp. 251-267.

[27] A. M. Smith and A. B. Ross, "Production of bio-coal, bio-methane and fertilizer from seaweed via hydrothermal carbonisation," *Algal Research,* vol. 16, pp. 1-11, 2016.

[28] M.-M. Titirici, "Green Carbon," in *Sustainable carbon materials from hydrothermal processes*, Wiley, 2013, pp. 1-36.

[29] ipi.ag, "Hydrothermal carbonization: convert waste to energy," [Online]. Available: https://ipi.ag/en/htc-plant_14. [Accessed 13 October 2021].

[30] E. Bevan, J. Fu and Y. Zheng, "Challenges and opportunities of hydrothermal carbonisation in the UK; case study in Chirnside," *RSC Advances,* vol. 10, no. 52, pp. 31586-31610, 2020.

[31] M.-M. Titirici, A. Funke and A. Kruse, "Hydrothermal Carbonization of Biomass," in *Recent Advances in Thermochemical Conversion of Biomass*, 2015, pp. 325-352.

[32] C. He, A. Giannis and J.-Y. Wang, "Conversion of sewage sludge to clean solid fuel using hydrothermal carbonization: Hydrochar fuel characteristics and combustion behavior," *Applied energy,* vol. 111, pp. 257-266, 2013.

[33] D. Kim, K. Lee and K. Y. Park, "Hydrothermal carbonization of anaerobically digested sludge for solid fuel production and energy recovery," *Fuel,* vol. 130, pp. 120-125, 2014.

[34] M. Niinipuu, K. G. Latham, J.-F. Boily, M. Bergknut and S. Jansson, "The impact of hydrothermal carbonization on the surface functionalities of wet waste materials for water treatment applications," *Environmental Science and Pollution Research volume ,* vol. 27, p. 24369–24379, 2020.

[35] A. E. Brown, G. L. Finnerty, M. A. Camargo-Valero and A. B. Ross, "Valorisation of macroalgae via the integration of hydrothermal carbonisation and anaerobic digestion," *Bioresource technology,* vol. 312, pp. 123539-123539, 2020.

[36] N. Patel, B. Acharya and P. Basu, "Hydrothermal Carbonization (HTC) of Seaweed (Macroalgae) for Producing Hydrochar," *Energies,* vol. 14, no. 7, p. 1805, 2021.

[37] Y. Lin, X. Ma, X. Peng, S. Hu, Z. Yu and S. Fang, "Effect of hydrothermal carbonization temperature on combustion behavior of hydrochar fuel from paper sludge," *Applied Thermal Engineering,* vol. 91, pp. 574-582, 2015.

[38] Q. Xu, Q. Qian, A. Quek, N. Ai, G. Zeng and J. Wang, "Hydrothermal Carbonization of Macroalgae and the Effects of Experimental Parameters on the Properties of Hydrochars," *ACS Sustainable Chemistry & Engineering,* vol. 1, no. 9, p. 1092–1101, 2013.

[39] J.-h. Zhang, Q.-m. Lin and X.-r. Zhao, "The Hydrochar Characters of Municipal Sewage Sludge Under Different Hydrothermal Temperatures and Durations," *Journal of Integrative Agriculture,* vol. 13, no. 3, pp. 471-482, 2014.

[40] T. Prakoso, R. Nurastuti, R. Hendriansyah, J. Rizkiana, G. Suantika and G. Guan, "Hydrothermal Carbonization of Seaweed For Advanced Biochar Production," *MATEC Web of Conferences,* vol. 156, p. 05012, 2018.

[41] S. Kannan, Y. Gariepy and G. S. V. Raghavan, "Optimization and Characterization of Hydrochar Derived from Shrimp Waste," *Energy & fuels,* vol. 31, no. 4, pp. 4068-4077, 2017.

[42] L. Cao, I. K. Yu, D.-W. Cho, D. Wang, D. C. Tsang, S. Zhang, S. Ding, L. Wang and Y. S. Ok, "Microwave-assisted low-temperature hydrothermal treatment of red seaweed (Gracilaria lemaneiformis) for production of levulinic acid and algae hydrochar," *Bioresource Technology,* vol. 273, pp. 251-258, 2019.

[43] I. C. Kantarli, M. Pala, Y. Yildirim, J. Yanik and M. H. Abreu, "Fuel characteristics and combustion behavior of seaweed-derived hydrochars," *Turkish journal of chemistry,* vol. 43, no. 2, p. 475–491, 2019.

[44] G. Zeng, S. Lou, H. Ying, X. Wu, X. Dou, N. Ai and J. Wang, "Preparation of Microporous Carbon from Sargassum horneri by Hydrothermal Carbonization and KOH Activation for CO2 Capture," *Journal of Chemistry,* 2018.

[45] X. Han, Z. Wu, Y. Yang, J. Guo, Y. Wang, L. Cai, W. Song and L. Ji, "Facile Preparation of a Porous Biochar Derived from Waste Crab Shell with High Removal Performance for Diesel," *Journal of Renewable Materials,* vol. 9, no. 8, p. 1377–1391, 2021.

[46] C. He, H. Lin, L. Dai, R. Qiu, Y. Tang, Y. Wang, P.-G. Duan and Y. S. Ok, "Waste shrimp shell-derived hydrochar as an emergent material for methyl orange removal in aqueous solutions," *Environment International,* vol. 134, 2020.

[47] International Biochar Initiative, "About the IBI Biochar Standards," 2019. [Online]. Available: https://biochar-international.org/wp-content/uploads/2019/01/IBI_Biochar_Standards_V2.1_Final1.pdf.

[48] M. Hojamberdiev, Y. Kameshima, A. Nakajima, K. Okada and Z. Kadirova, "Preparation and sorption properties of materials from paper sludge," *Journal of Hazardous Materials,* vol. 151, no. 2, p. 710–719, 2008.

[49] T. Namioka, Y. Morohashi, R. Yamane and K. Yoshikawa, "Hydrothermal Treatment of Dewatered Sewage Sludge Cake for Solid Fuel Production," *Journal of Environment and Engineering,* vol. 4, no. 1, pp. 68-77, 2009.

[50] X. Liu, Y. Zhai, S. Li, B. Wang, T. Wang, Y. Liu, Z. Qiu and C. Li, " Hydrothermal carbonization of sewage sludge: Effect of feed-water pH on hydrochar's physicochemical properties, organic component and thermal behavior," *Journal of hazardous materials,* vol. 388, pp. 122084-122084, 2020.

[51] A. Rorat, P. Courtois, F. Vandenbulcke and S. Lemiere, "Sanitary and environmental aspects of sewage sludge management," *Industrial and Municipal Sludge,* p. 155–180, 2019.

[52] S. Kannan, Y. Gariepy and G. S. V. Raghavan, "Conventional Hydrothermal Carbonization of Shrimp Waste," *Energy & fuels,* vol. 32, no. 3, pp. 3532-3542, 2018.

[53] R. H. Rødde, A. Einbu and K. M. Vårum, "A seasonal study of the chemical composition and chitin quality of shrimp shells obtained from northern shrimp (Pandalus borealis)," *Carbohydrate polymers,* vol. 71, no. 3, pp. 388-393, 2008.

[54] Z. Sebestyén, E. Jakab, A. Domán, P. Bokrossy, I. Bertóti, J. Madarász and K. László, "Thermal degradation of crab shell biomass, a nitrogen-containing carbon precursor," *J Therm Anal Calorim,* vol. 142, p. 301–308, 2020.

[55] M. M. Nassar and G. D. M. MacKay , "Mechanism of Thermal Decomposition of Lignin," *Wood and Fiber Science,* vol. 16, no. 3, pp. 441-453, 1984.

[56] T. Gagić, A. Perva-Uzunalić, Z. Knez and M. Škerget, "Hydrothermal Degradation of Cellulose at Temperature from 200 to 300 °C," *Industrial & engineering chemistry research,* vol. 57, no. 18, pp. 6576-6584, 2018.

[57] Y. Yang, M. Zhang, A. I. Alalawy, F. M. Almutairi, M. A. Al-Duais, J. Wang and E.-S. Salama, "Identification and characterization of marine seaweeds for biocompounds production," *Environmental technology & innovation, ,* vol. 24, p. 101848, 2021.

[58] S. Mikhail, *Microwave Hydrothermal Carbonization of Lobster Waste,* ProQuest Dissertations Publishing, 2020.

[59] S. Kannan, Y. Gariepy and G. S. V. Raghavan, "Optimization of Enzyme Hydrolysis of Seafood Waste for Microwave Hydrothermal Carbonization," *Energy & fuels,* vol. 29, no. 12, pp. 8006-8016, 2015.

[60] A. Shrestha, B. Acharya and A. A. Farooque, "Study of hydrochar and process water from hydrothermal carbonization of sea lettuce," *Renewable energy,* vol. 163, pp. 589-598, 2021.

[61] A. Méndez, G. Gascó, B. Ruiz and E. Fuente, "Hydrochars from industrial macroalgae “Gelidium Sesquipedale” biomass wastes," *Bioresource technology,* vol. 275, pp. 386-393, 2019.

[62] P. Breeze, "Chapter 2 Coal Types and the Production and Trade in Coal," in *Coal-fired Generation*, Academic Press, 2015, p. 10.

[63] J. Csapá, Z. Csapó-Kiss, L. Wágner, T. Tálos, T. G. Martin, S. Folestad, A. Tivesten and S. Némethy, "Hydrolysis of proteins performed at high temperatures and for short times with reduced racemization, in order to determine the enantiomers of d- and l-amino acids," *Analytica chimica acta,* vol. 339, no. 1, pp. 99-107, 1997.

[64] R. Wu, Y. Li, X. Pang, Z. Hu and X. Jian, "Insight into evolution of chemical structure and mineralogy to reveal the mechanism of temperature-dependent phosphorus release from hydrochars," *Industrial Crops and Products,* no. 185, p. 115101, 2022.

[65] Z. Chen, H. Jia, Y. Guo, Y. Li and Z. Liu, "Nitrogen-doped hydrochars from shrimp waste as visible-light photocatalysts: Roles of nitrogen species," *Environmental Research,* vol. 208, p. 112695–112695, 2022.

[66] J. Coates, "Interpretation of Infrared Spectra, A Practical Approach," in *Encyclopedia of Analytical Chemistry*, R. Meyers, Ed., Chinchester, John Wiley & Sons Ltd, 2000, p. 10815–10837.

[67] S. Kannan, I. Burelle, V. Orsat and G. S. Vijaya Raghavan, "Characterization of Bio-crude Liquor and Bio-oil Produced by Hydrothermal Carbonization of Seafood Waste," *Waste and Biomass Valorization,* vol. 11, no. 7, pp. 3553 - 3565, 2020.

[68] L. Peng, Y. Liang, J. Huang, L. Xing, H. Hu, Y. Xiao, H. Dong, Y. Liu and M. Zheng, "Mixed-Biomass Wastes Derived Hierarchically Porous Carbons for High-Performance Electrochemical Energy Storage," *ACS Sustainable Chemistry & Engineering,* vol. 7, no. 12, p. 10393–10402, 2019.

[69] J. Wu, J. Yang, P. Feng, L. Wen, G. Huang, C. Xu and B. Lin, "Highly efficient and ultra-rapid adsorption of malachite green by recyclable crab shell biochar.," *Journal of Industrial and Engineering Chemistry,* p. 206–214, 2022.

Chapter 3 - Hydrothermal Carbonization of Snow Crab Processing By-Product: Hydrochar Characterization

*A modified version of this chapter will be submitted for publication. It has been proofread and revised by Dr. Kelly Hawboldt and Dr. Stephanie MacQuarrie.

Abstract

Fishery processing (crab) is an important industry in Atlantic Canada. However, up to half of the landed product ends as processing by-product with over 70 wt% water content. Often regarded as a "waste" this by-product has applications in soils, wastewater treatment, and other industries, an area of research largely unexplored. Hydrothermal carbonization (HTC) converts biomass into a more stable and useable material (hydrochar) and uses water as a medium. This valorization not only creates a profit stream but also reduces the environmental impacts of the crab by-product treatment and disposal. In this work, HTC hydrochar from snow crab (*Chionoecetes opilio*) processing by-product/feedstock is characterized with respect to key properties in an effort to delineate potential end use applications and the impact of process parameters (temperature, residence time, and water to biomass ratio) on these properties. The temperature range was 180-260 ℃, residence time of 0.5-3 h, and water to biomass ratio of 2-4 (wt:wt). The solids yield decreased as water ratio and temperature increased (time did not impact yield to the same extent). The hydrochar ash content increased from 33-45 wt% as water ratio and temperature increased to the maximums studied in this work. XRD analysis showed that the hydrochar retained chitin and $CaCO_3$. Trace analysis showed calcium was the most abundant mineral in the feedstock and hydrochar, consistent with the XRD $CaCO_3$ peak. Compared to the feedstock (11 m^2/g), the hydrochar BET surface area increased with temperature and water ratio, reaching a maximum of 26 m^2/g at 260 °C, water ratio 3 and 30 min. However, increasing the time to 3 h reduced the surface area to 13.47 m^2/g. Hydrochar carbon content is similar or slightly higher than the feedstock due to competing polymerization reaction and $CaCO_3$ dissolution. Nitrogen decreased as temperature increased possibly due to protein degradation. Hydrochar and feedstock showed similar functional groups. The functional groups in the hydrochar have potential to facilitate chemosorption as a bioadsorbent.

3.1. Introduction

Shellfish harvesting in general and crab in particular, are critical economic drivers in Atlantic Canada [1]. Full utilization of the crab is important not only from an environmental perspective but also for overall industry sustainability. Up to 50 wt% of the landed product ends up as processing by-product (shell and residual meat) [2]. The by-product is 50-70 wt% moisture, and the dry matter is approximately 10–30 wt% chitin, 11–40 wt% protein, and 20–50 wt%

minerals (mainly calcium carbonate) [3, 4, 5, 6, 7, 8, 9, 10, 11, 12]. If not managed properly, the by-products degradation can lead to emissions of greenhouse gases, ammonia, and nitrates, which could pollute air and water [11]. The common methods of disposal are landfill and incineration. These methods could lead to pollution, landfill burden, and the need for excessive drying prior/during incineration [13, 14, 15]. The by-product has potential applications in soils and materials. However, the high moisture content means in order to valorize the by-product processes must either be able to tolerate high water or drying is required. Hydrothermal methods which use temperature and sub/supercritical water in the process, are ideal for wet biomass. Hydrothermal carbonization (HTC), where the process occurs at temperature ranges from 180-250 °C (self-generated pressure by water vapor) can be more attractive from a process intensity perspective compared to higher temperature and pressure hydrothermal process such as hydrothermal liquefaction (HTL) and hydrothermal gasification (HTG). In addition, HTC is well developed with some large-scale HTC plants in operation [16, 17, 18, 19]. HTC has been studied using feeds such as; pulp and paper sludge, sewage sludge, and macroalgae, [e.g., 20-36]. There is limited work in HTC and applications of shellfish processing by-products [23, 37, 38, 39, 40, 41, 42, 43, 44, 45]. The primary product of HTC (solid hydrochar) has been studied for applications in: fuel (paper sludge, macroalgae, sewage sludge waste) [21, 20, 22, 24, 28, 30, 32, 46, 47], adsorption (sewage sludge, paper sludge, macroalgae, shrimp waste, and crab shell waste) [23, 25, 33, 43], and soil remediation [27]. Most hydrochar studies focus on fuel applications, due to the fact that the bulk of the studies use a feedstock that produces a high carbon material and therefore a high heating value. The high ash content of shellfish based hydrochar make solid fuel a less feasible route due to fouling and slagging during combustion. Adsorption is less well studied in part due to the low surface area of hydrochar relative to other carbon solids (e.g., biochar) [23, 25, 33, 43]. However, surface area is not the only factor in adsorption capacity. A study on crab shell hydrochar for diesel adsorption application showed low surface area but high diesel adsorption capacity [43]. The study proposed that the adsorption mechanism was chemisorption which involves electron exchange between the functional group in the hydrochar and diesel [43]. Mineral/ash-rich hydrochar with high nitrogen content (like macroalgae hydrochar) is also appealing as soil amendment [27]. Thus, shellfish based hydrochar may have applications in soils or as an adsorbent but require analysis of surface functional groups, mineral content, and ultimate and trace element content to determine applicability.

The impacts of temperature and residence time on HTC products have been studied [e.g., 20, 21, 22, 24, 26, 27, 28, 30, 31, 46, 47]. However, research focused on raw marine biomass/by-product is limited with much of the work focused on pretreated biomass/by-product. Pretreatments include deproteinization, deacetylation, or demineralization are commonly used prior to HTC in shellfish [23, 38, 39, 42, 43]. While this is useful on potentially recovering other value-added products, these pretreatments are often costly and may impact overall process feasibility. Further, in the bulk of these studies, there is little study of the impact of water to biomass ratio (important in optimizing hydrochar properties and process water management) and the interaction between water, temperature, and time on hydrochar properties. All of these factors will determine the feasibility of HTC as a method to valorize shellfish processing by-product and potential applications. This works seeks to cover this research gap by studying the impacts of HTC conditions (temperature, residence time, and water to biomass ratio) on crab by-product hydrochar properties and provide data that can be used in HTC processing of crab and potential hydrochar applications. Properties assessed include elemental composition, ash content, pH, trace element, FTIR, XRD, and surface area. Elemental and ash analysis are typically used to assess fuel applications [20, 21, 22], while elemental, ash, and trace element analysis may indicate suitability for soil amendment [19, 27]. Surface functionality (FTIR, pH), structure (XRD), and surface area (BET) are important in assessing adsorption applications [23, 43, 45].

3.2. Material and Methodology

3.2.1. Materials

Snow crab processing by-product was supplied by Louisbourg Seafoods Limited, Nova Scotia, Canada. The snow crab processing by-product was kept frozen at -30°C. For experiments requiring dried crab (to study water to biomass ratio), the snow crab processing by-product was dried at 100 °C for 1080 minutes and ground to a particle size of less than 2.0 mm. For experiments requiring snow crab shell processing by-product as received (69 wt% water), the by-product (bodies and legs) was hammered into smaller pieces and then ground with a food processor for a maximum of 1 to 2 min to ensure the sample was still frozen (to minimize moisture loss). For consistency, the dried snow crab processing by-product will herein be mentioned as raw crab (RC), and snow crab processing by-product will refer to as wet crab (WC).

3.2.2. Hydrothermal Carbonization (HTC) of Snow Crab Processing By-Product

The ranges of HTC temperature, time, and water to biomass ratios were selected based on an extensive literature review [25, 38, 39, 42] and are outlined in Table 3.1.

Table 3.1. Experiment Conditions

Parameter			
Temperature (℃)	180	220	260
Residence time (h)	0.5	1.75	3
Water to biomass ratio (wt/wt) (R)	2:1	3:1	4:1

HTC experiments were performed in a 600 mL 4625 Series Parr reactor without mixing (Appendix Figure A1). Two sets of experiments were performed, one set using Design of Experiment (DoE) to determine number of experiments and HTC run conditions (water ratio/temperature/residence time). In these experiments the sample was dried, ground and then mixed with specified water to biomass ratio (further will be refer as water ratio). A second set of experiments were performed where the WC was used without any treatment at 68.99 wt% water (only utilizing the water/moisture in the sample). The second set was done to determine if drying had any effect on hydrochar. The HTC of wet crab hydrochars are referred as HWC.

For the experiments where samples were dried, 60 g of dried sample was mixed with ultrapure water (18.2 MΩ-cm) in the reactor with the specified water fraction. The reactor was heated to the desired temperature and held constant for the specified residence time. The time needed to reach 180 °C was ~40 mins, 220 °C was ~70 mins, and 260 °C was ~90 mins. The reactor was cooled by immersing in cold water for 10-20 mins. The experiments were done in duplicate, except for HC. The solid product was separated from the liquid by vacuum filtration. The liquid product was stored in a glass bottle and the wet solid hydrochar dried in the oven at 105 °C for 24 h. The dried sample was then weighed and stored in a glass jar for further analysis in a storage fridge. The hydrochar yield was calculated as:

$$\text{Yield (wt\%, db)} = \frac{g\ dried\ hydrochar}{g\ dried\ crab\ shell} * 100\% \qquad \text{(Eq. 1)}$$

3.2.3. Design of Experiment (DoE)

Box–behnken design (BBD) was used in the DoE (Design Expert® software V13 (DE)). BBD design was selected to study the influence of each factor and their interactions with less runs required when compared to Central Composite Design (CCD). The input factors were water to biomass ratio (A), temperature (B), and residence time (C). This resulted in 15 runs, as shown in Table 3.2. In addition to standard runs design by BBD, confirmation run (HC) generated by DE was included in the table. The HWC also done to see the difference between using wet and dried material, as previously mentioned.

In the DE software the best model is determined based on F-value, p-value, adjusted and predicted R^2 (within 0.2 difference), and Akaike information criterion (AICc, backward selection direction). The factors water to biomass ratio (A), temperature (B), residence time (C), 2 factor interactions (2FI), and quadratic effects were included in the model if the p-value was < 0.05. To maintain hierarchy of the model, factors with p-values > 0.05 were included in the model if their 2FI or quadratic effect were significant. [49]

Table 3.2. Response Surface Method BBD Runs (H1-15), Confirmation Run (HC), and Wet Crab HTC Run (HWC) Conditions.

Run/Sample Name	R	T (°C)	t (h)
H1	3	220	1.75
H2	4	260	1.75
H3	4	220	0.5
H4	2	220	3
H5	3	260	3
H6	3	180	3
H7	3	180	0.5
H8	2	220	0.5
H9	2	180	1.75
H10	2	260	1.75
H11	3	220	1.75
H12	4	220	3
H13	3	220	1.75
H14	3	260	0.5
H15	4	180	1.75
HC	2.42	260	1.75
HWC	2.22	260	1.75

3.2.4. Feedstock and Hydrochar Property Analysis.

3.2.4.1. Moisture Content

WC moisture content was measured using a Mettler Toledo Moisture analyzer HB43-S (readability 0.01%).

3.2.4.2. Ash analysis

The ash content was determined by placing 1.0 g of sample in a muffle furnace at 750 °C for 6 h. The process was repeated using a 1-h intervals of heating until the loss of mass was less than 0.0005 g. [50] The ash content was calculated as:

$$\text{Ash content (wt\%, db)} = \frac{g\ ash}{g\ dried\ sample} * 100\% \qquad \text{(Eq. 2)}$$

The ash for the hydrochars were adjusted to reflect the yield (wt%):

$$\text{Ash content, relative to the feedstock } \left(\frac{g\ ash\ in\ hydrochar}{g\ dried\ crab\ shell}, db\right) = \frac{g\ ash\ in\ hydrochar\ (g)}{g\ dried\ hydrochar\ (g)}\ x\ \frac{yield\ (wt\%, db)}{100} \qquad \text{(Eq. 3)}$$

3.2.4.3. Ultimate analysis

Ultimate analysis (carbon, hydrogen, and nitrogen) was conducted at the Aquatic Research Cluster (ARC) at Memorial University of Newfoundland using a Perkin-Elmer 2400 Series II CHN analyzer elemental analyzer (accuracy ≤0.3%).

3.2.4.4. FTIR

Fourier-Transform Infrared Spectroscopy (FT-IR) was performed at Cape Berton University (CBU), Sydney, Nova Scotia, Canada. using a Nicolet Summit Mid-Infrared FTIR spectrometer (KBr method). The sample was ground into a fine powder prior to use. The wavelength used is from 4000 cm^{-1} to 400 cm^{-1} with a resolution of 4 cm^{-1}, average scans 16 or 32.

3.2.4.5. XRD

X-Ray Diffraction (XRD) analysis was performed using a Rigaku Ultima IV diffractometer at MUN's TERRA Facility. The instrument was operated at 40 kV, 44 mA with 0.02° step change. The range analyzed was between 5°-100° (2θ/minute). Diffractogram peaks were then matched to existing databases using Materials Data Incorporated (MDI) JADE software V8.8.

3.2.4.6. Surface area

Surface area analysis by Brunauer-Emmett-Teller (BET) was conducted with a Micromeritics Tristar II Plus. The sample was degassed using FlowPrep 060 at 120 ºC for 24 h, under nitrogen flow, then N_2 was used as an adsorbate at a temperature of 77 K (-196 ºC).

3.2.4.7. Acid digestion and Trace Elements Analysis (ICP-OES)

Trace element analysis (ICP-OES) is performed to see trace elements (metals) in the RC and selected hydrochars. Chemicals used in this experiment were 68 wt% nitric acid, 30 wt% hydrogen peroxide, and 37 wt% hydrochloric acid from ACP Chemicals for acid digestion. Prior to trace analysis, the sample matrix needs to be destroyed by acid digestion leaving only the target analyte. Samples with a mass of 0.1 g were first measured and added to a plastic digestion vial with 1 mL of 68 % HNO_3 and 1.0 mL of 30 % H_2O_2 and left to flux on a hotplate at 60 ºC for 48 h, after which the mixture was dried down. The procedure was then repeated until no effervescence occurred when adding the acid and hydrogen peroxide, and the solution was clear. After, the solution was evaporated and 6M HCl was added to the remaining solids. When the solution appeared clear and did not effervesce, the solution was dried and 5 mL of 6M HCl was added to the remaining solid. The HCl solution was left to flux at 100 ºC for 24 h. After 24 h, the solution was dried again, and 5 mL diluted nitric acid (~2 wt%) was added to transform the metals back to nitrate form. The final solution was sent to Memorial University's Micro-Analysis Facility for trace element analysis using a Perkin-Elmer 5300 DV Inductively Coupled Plasma Optical Emission Spectroscopy (ICP-OES) device. The trace elements concentration was in mg/L. The trace element content in the sample (RC and selected hydrochars) were calculated with equation 4. Trace element content was corrected with yield (wt%, db) to calculate the hydrochar trace element relative to the feedstock (equation 5).

$$\text{Trace element, x } \left(\frac{g}{g\ dried\ sample}\right) = \left[C_x \left(\frac{mg}{L}\right) - C_{blank} \left(\frac{mg}{L}\right)\right] * \frac{V\ (L)}{g\ dried\ sample} \quad \text{(Eq 4)}$$

$$\text{Trace element } \left(\frac{g\ x\ in\ dried\ hydrochar}{g\ dried\ crab\ shell}\right) = \text{Trace element, x } \left(\frac{g\ x\ in\ dried\ hydrochar}{g\ dried\ hydrochar}\right) x \frac{yield\ (wt\%,db)}{100} \quad \text{(Eq 5)}$$

Where x is the element (e.g., Ca, Mg, Na, etc.), C_x is trace element of x element in mg/L, C_{blank} is trace element from blank vial in mg/L, and V is volume of last addition of diluted nitric (5 mL) in L (0.005 L).

3.2.4.8. pH

Liquid product and hydrochar pH were measured using Accumet AB200 by Fischer science with an Accumet 13-620-631 pH electrode. The liquid product pH measurement was measured undiluted. The hydrochar pH was measured by mixing 2 g of hydrochar with and 20 mL ultrapure water (18.2 MΩ-cm) in a beaker glass. Before hydrochar pH measurement, the hydrochar mixtures were agitated at speed knob 3 for 30 mins using VWR OS-500 agitator.

3.2.4.9. TGA

Thermogravimetric Analysis (TGA) is performed to see sample thermal degradation profile in the RC and RC hydrochar. The RC analysis was performed at Cape Berton University (CBU), Sydney, Nova Scotia, Canada (TA Instrument model Q500 TGA) at 20 mL/ min of Nitrogen ramp at 10 °C/min to 800 °C. The RC hydrochar analysis was performed at MUN's Centre for Chemical Analysis, Research and Training (TA Instruments TGA55) at 60 mL/ min of Nitrogen ramp at 15 °C/min to 750 °C and switched to air for 15 min to calculate ash content. The RC hydrochar HTC condition was at 220 °C, water ratio 3, and 1.75 h residence time in the oven.

3.3. Result and Discussion

3.3.1. Feedstock Characterization

The WC moisture content was approximately 69 wt%, similar to other crab by-product feedstocks in related studies [3, 5, 48, 51]. Visually, the WC was greyish in color with white orange shell fragments. The RC was heterogenous, consisting of white orange shell particles, fine particles, and dried leftover meat (Figure 3.1).

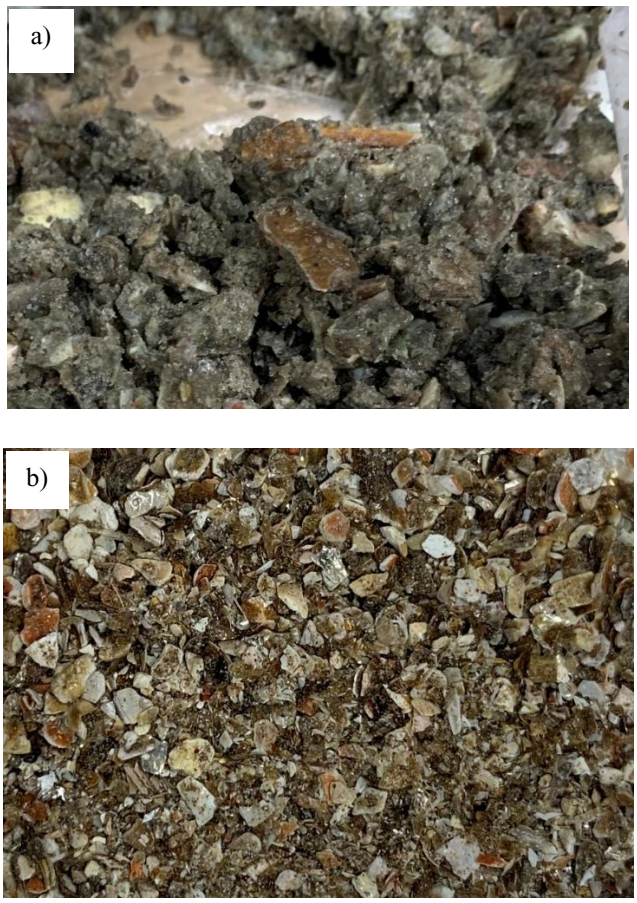

Figure 3.1. Ground a) Wet Crab (WC), and b) Raw Crab (RC).

The RC in this study (Table 3.1) had similar C, H, N, ash, and pH with feedstock analyzed in Dai et al. (2017) [52]. The RC N content (wt%) also similar to snow crab N content (~ 5.5 wt%, db) by Burke and Kerton (2023) [51]. The crab ash content (32.15 wt%) was at the lower end of range from other studies (28.5-74.97 wt%) [3, 8, 44, 51]. The BET surface area was 11.48 m^2/g, which was similar to Han et al. (2021) at 9.57 m^2/g and slightly higher compared to Dai, et al. (2017) at 6 m^2/g [43, 52]. Variability in RC is expected as the crab species, season, and extent of processing impacts the by-product. FTIR, XRD, and trace element analysis, will be discussed in hydrochar sections.

Table 3.3. Raw Crab Properties

Properties	This Study (< 2 mm)	[52] (<0.18 mm)
C (wt%)	29.80	26.97
N (wt%)	6.02	5.15
H (wt%)	4.11	3.6
Ash (wt%)	32.15 ± 1.32	33.16
BET (m^2/g)	11.48 ± 0.511	6
pH	8.81 ± 0.01	10.23

wt% in db unless state otherwise

3.3.2. Hydrochar Production

Overall, RC and WC hydrochar are brown and as the HTC temperature increased the colour turned darker (Fig 3.2). The particle size of WC fed to the HTC unit is larger than the RC due to the difference in grinding method (Fig 3.2).

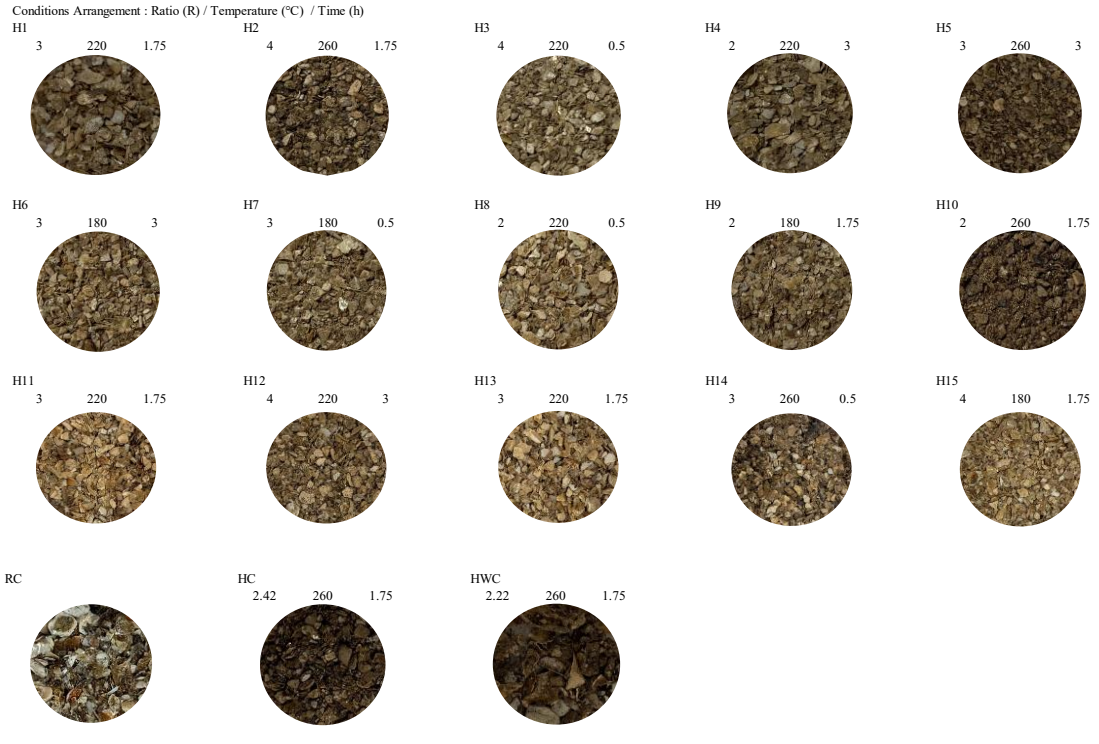

Figure 3.2. HTC Hydrochar Physical Appearance.

The liquid's colour changes with temperature increase, gradually transitioning from dark brown colour into a clearer orange colour (Figure 3.3). This could be the result of pigments partitioning into the liquid phase at higher temperatures. The change in colour might also related to water ratio, as the light-coloured liquid was found at ratio 2 and 3, but not at 4. However, more study on the HTC liquid is needed in order to understand the composition of liquid.

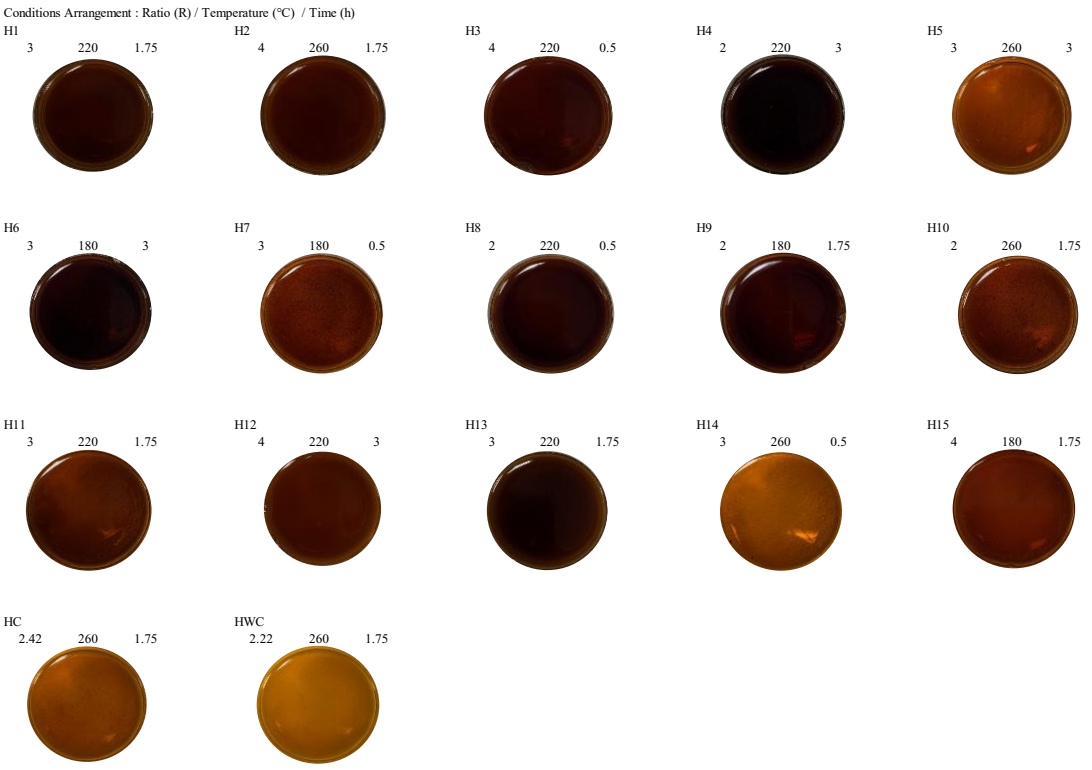

Figure 3.3. HTC Liquids Appearance.

The hydrochar yields as a function of reaction conditions are summarized in Table 3.4. From Figure 3.4, it can be seen that yield decrease is affected by increases in temperature and residence times. At a constant water ratio, increasing temperature from 180 to 260 °C decreases yield by up to 16 %. At all temperatures, the yield decreased with increasing water ratio.

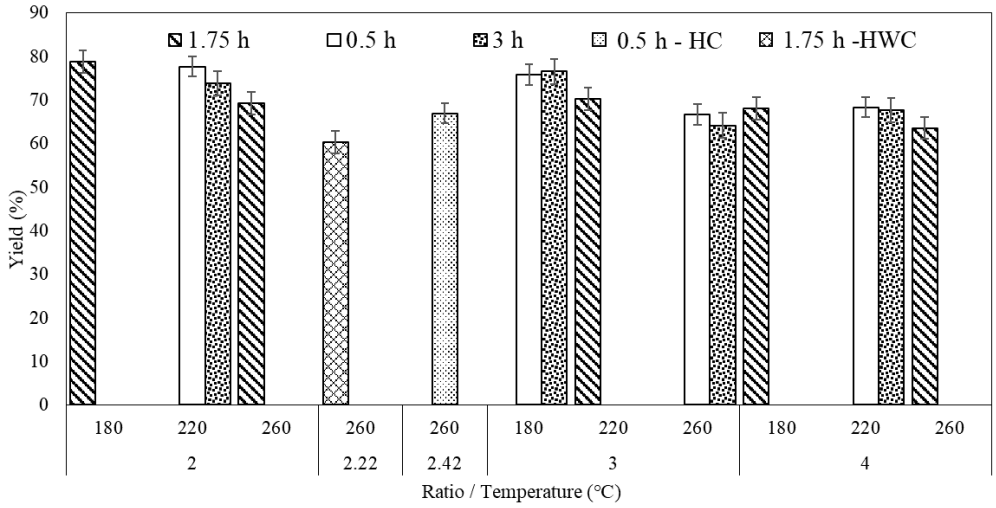

Figure 3.4. Hydrochar yield (wt%) as a function of time, temperature, and water ratio.

At 260 °C and 1.75 h, the HWC (water ratio 2.22) yield was 60.3 wt% which is lower than the dried crab HTC yield at a similar water ratio (water ratio 2), at 69.2 wt%. The differences in water ratio from 2 to 2.22 or 10 % relative increase in water, resulted in yield decrease by 18.4 %. The decrease may be attributed the higher heterogeneity of crab samples in the WC vs RC. When the material is dried the overall mass/volume of sample is much lower and it is therefore less difficult to obtain a representative sample from the material. For instance, the RC for each HTC run was obtained from the same batch, and the yield difference in duplicates (H1-H15) was between 0.1-8.2 %.

The crab hydrochar yields were higher at approximately 70-80 wt% (db) than studies where feedstock was pretreated enzymatically (shrimp and lobster) where yields varied from approximately 28-50 wt% (db). Note that solid yield decrease represents increased conversion of the material. Temperatures in these studies varied from 150-210 °C, residence time of 1-2 h, and water ratio of 1 [38, 39, 42]. The lower yield may be due to the lower amount of protein in the enzymatic pretreated hydrochars. The enzymatic process breaks down the proteins into smaller peptides, potentially increasing the protein fraction in dissolution into the water phase [38, 39, 42, 53].

Table 3.4. Summary of Snow Crab Processing By-Product HTC Yield and Hydrochar Properties

Sample	R	T (°C)	t (h)	Solid Yield (wt%)	Ash (wt%)	BET (m^2/g)	dry basis, db		
							C (wt%)	N (wt%)	H (wt%)
RC	-	-	-	-	32.15 ± 1.32	11.48 ± 0.05	29.80	6.02	4.11
H1	3	220	1.75	70.8 ± 0.03	39.21 ± 1.36	20.16 ± 0.13	26.69	3.33	2.83
H2	4	260	1.75	63.6 ± 0.03	43.23 ± 1.42	20.26 ± 0.11	25.71	2.58	2.40
H3	4	220	0.5	69.1 ± 0.03	36.64 ± 1.33	22.12 ± 0.16	23.37	3.14	2.56
H4	2	220	3	73.8 ± 0.03	37.71 ± 1.25	20.22 ± 0.13	23.21	2.42	2.19
H5	3	260	3	64.2 ± 0.03	42.11 ± 1.42	13.47 ± 0.14	31.80	3.63	3.35
H6	3	180	3	76.6 ± 0.03	34.76 ± 1.30	19.23 ± 0.16	30.76	5.11	3.93
H7	3	180	0.5	75.8 ± 0.03	35.85 ± 1.34	13.58 ± 0.13	29.85	5.08	4.52
H8	2	220	0.5	77.7 ± 0.03	36.11 ± 1.33	16.63 ± 0.11	31.70	4.74	3.90
H9	2	180	1.75	78.7 ± 0.03	33.56 ± 1.33	15.68 ± 0.15	33.79	6.27	4.18
H10	2	260	1.75	69.2 ± 0.03	39.48 ± 1.35	14.53 ± 0.15	28.93	3.16	2.95
H11	3	220	1.75	69.9 ± 0.03	39.87 ± 1.36	24.39 ± 0.14	29.43	3.73	3.50
H12	4	220	3	67.7 ± 0.03	40.80 ± 1.34	24.62 ± 0.14	28.80	3.60	3.32
H13	3	220	1.75	70.2 ± 0.03	40.37 ± 1.37	25.25 ± 0.12	29.35	3.68	3.49
H14	3	260	0.5	66.7 ± 0.03	41.57 ± 1.39	26.30 ± 0.13	27.99	3.35	2.97
H15	4	180	1.75	68.1 ± 0.03	37.31 ± 1.31	26.67 ± 0.17	24.09	3.23	2.64
HC	2.42	260	0.50	67.0 ± 0.03	36.96 ± 1.21	19.04 ± 0.13	26.72	2.47	2.76
HWC	2.22	260	1.75	56.5 ± 0.03	40.53 ± 1.23	16.17 ± 0.08	31.31	3.46	3.51

R: water ratio (wt:wt)

3.3.3. Hydrochar Characterization

3.3.3.1. Ash Content

The RC and crab hydrochar ash content is summarized in Table 3.4. The hydrochars ash content was up to 34 % higher compared to the RC. From Figure 3.5, it can be seen that ash content increased is affected by temperature and water ratio increase. At all water ratios, hydrochar ash content increased with HTC temperature by up to 17 %. At all temperature, the hydrochar ash content increased with water ratio by up to 11 %.

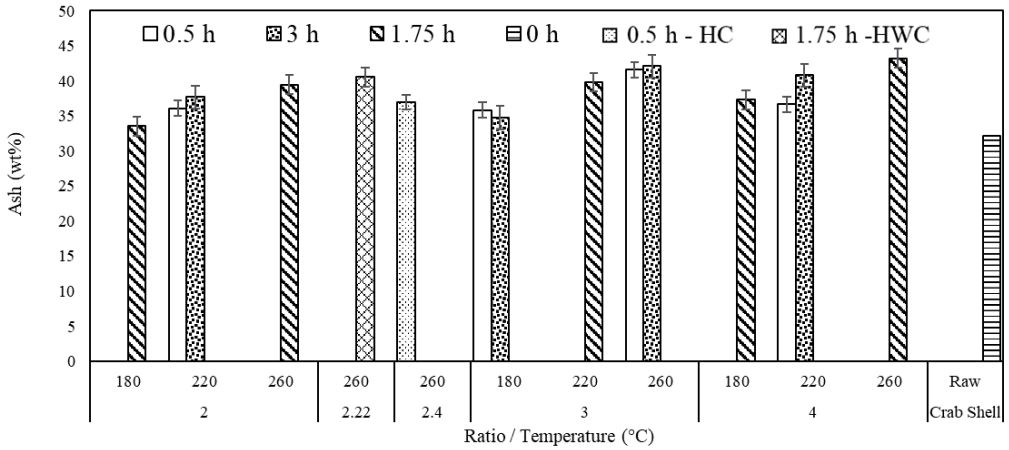

Figure 3.5. Ash Content (wt%) of Raw Crab and Hydrochar as a function of time, temperature, and water ratio.

To compare with the initial ash in the RC, equation 3 was used to calculate the ash in the hydrochar relative to the initial feedstock. The hydrochar ash content was by up to 34 % lower than the RC ash content at 0.332 $g_{ash}/ g_{raw\ crab}$ (Appendix Table A1 and Figure A2). The lowest hydrochar ash content (0.432 $g_{ash}/ g_{raw\ crab)}$, compared to the initial feedstock was hydrochar at water ratio 4, 260 °C, and 1.75 h. The lower ash content in hydrochar relative to the initial feedstock indicates some soluble minerals transfer into the liquid product during HTC [27]. As such, the lowest ash content was found at highest water ratio 4 and highest temperature 260 °C showing the combination of high water ratio and temperature led to increased mineral dissolution [54].

3.3.3.2. TGA

TGA analysis was performed on RC and RC hydrochar. The RC hydrochar HTC condition was 220 °C, water ratio 3, and 1.75 h residence time. The TGA and DTG graph of RC and RC hydrochar can be seen in Figure 3.6 below.

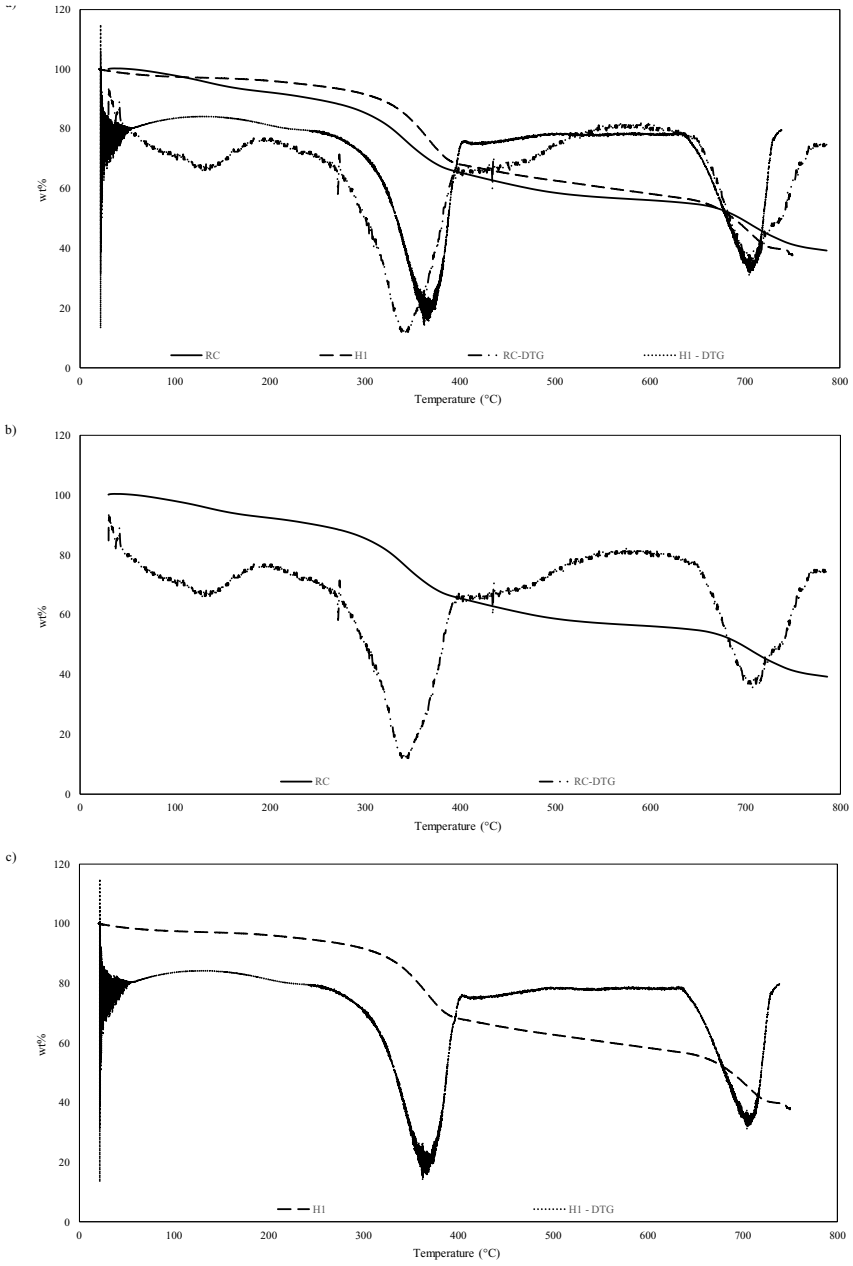

Figure 3.6. TGA (wt%) and DTG (mass loss rate, wt%/min) of a) RC and RC hydrochar overlapped, b) RC, and c) RC hydrochar, as a function of temperature.

The peak of mass loss rate at approximately 100 °C was due to moisture loss. The second peak at approximately 350 °C was associated with chitin degradation [55]. The RC hydrochar second peak shifted to a higher temperature at approximately 366 °C from the RC at 344 °C. The temperature shift to a higher temperature was possibly due to a more stable aromatic structure in the hydrochar [40]. The third peak at approximately 700 °C was associated with the thermal degradation of calcite [52]. The ash content of the hydrochar based on the TGA was 37.68 wt% (db) was approximately the same as the muffle furnace value (39.81 wt%, db).

3.3.3.3. XRD

XRD analysis comparing the RC and selected hydrochars are summarized in Figure 3.7.

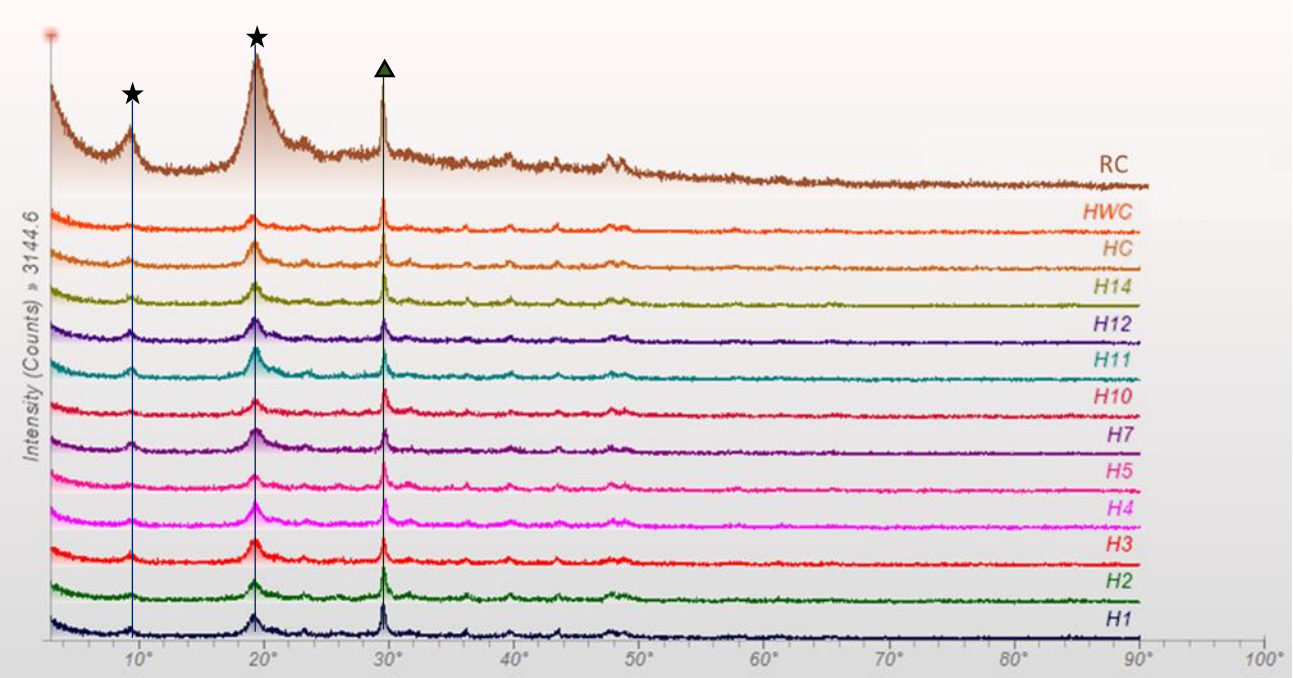

Figure 3.7. XRD analysis on crab shell and selected hydrochar; star: chitin peaks and triangle: $CaCO_3$ peak.

The raw crab had two peaks at approximately 10° and 20° associated to chitin, this was consistent with chitin peak found by [43, 56, 57]. The third major peak at approximately 30° was associated to $CaCO_3$ [43, 45]. Overall, the chitin and $CaCO_3$ peaks are still visible in the hydrochar

although the intensity is reduced compared to the RC. Reduced intensity cannot be directly correlated to quantity. However, the ratios of peaks can give an indication of the relative decrease or increase of chitin and $CaCO_3$ (Figure 3.8 and Peak Data in Appendix Table A2). As temperature and time increase at a water ratio of 2 we see a decrease in the chitin:$CaCO_3$ ratio. At temperatures below 280 °C chitin is relatively stable and therefore the increasing ratio is reflecting the increasing concentration in $CaCO_3$ due to reduction in proteins in solids due to hydrolysis (outlined in detail in section 3.3.3). At water ratios 3 and 4, the ratio of chitin:$CaCO_3$ increases with time and temperature, likely a result of increased dissolution of $CaCO_3$ in the water. The high noise indicates low crystallinity with amorphous material in the RC and hydrochars. An effort to reduce noise by reducing interval and grounding sample into finer particle had been done, nevertheless there was no improvement, indicating the RC and hydrochar $CaCO_3$ is amorphous in structure.

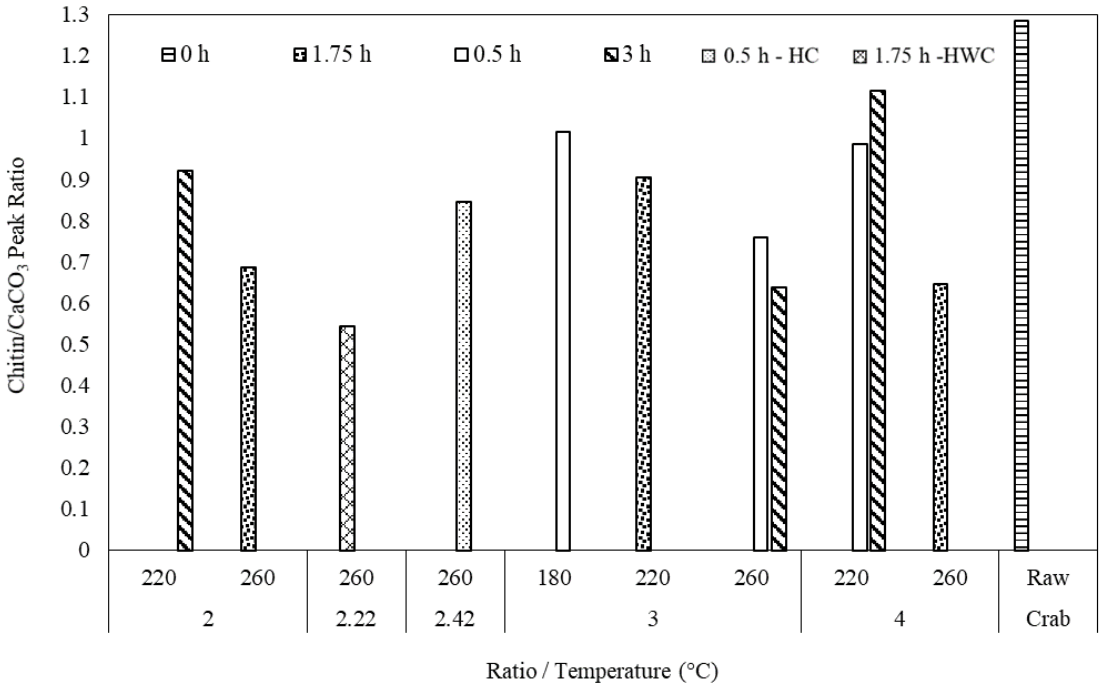

Figure 3.8. Crab Shell and Hydrochar XRD Chitin/CaCO3 peak ratio.

3.3.3.4. Trace Elements

Calcium was the most abundant element in the RC and its hydrochar (Table 3.5). This was consistent with XRD strong $CaCO_3$ peak discussed in the previous section. The second and third

highest elements, phosphorus and magnesium are 6 and 15 times lower than Ca. The increase in temperature from 180 to 260 °C at 3 h and water ratio of 3 (H6 and H5) appears to have concentrated trace elements, increasing by 40 %. The higher concentration elements (Ca, Na, P, and Mg) increased from 10-20 %. The same trend was observed as residence time increased from 0.5 (H14) to 3 h (H5) at constant temperature (260 °C) and water ratio (3).

Overall, the mineral content in the hydrochar increased compared to the RC. As with the ash, the relative mineral content in hydrochar was calculated via equation 5. Relative mineral content decreased in the hydrohar when compared to RC. This can be seen when the trace element concentrations were corrected by hydrochar yield as presented in Table 3.5. This possibly due to minerals transfer to water during HTC, the dissolution of minerals to the water can be seen from minerals present in the HTC liquid, including but not limited to calcium (from $CaCO_3$), (Appendix, Table A3).

Table 3.5. RC and Hydrochar Trace Elements

A. Concentrations in mg/g of dried sample

Element \ Sample*	RC	±	H6	±	H14	±	H5	±
Ca	138.3	2.1	151.1	2.2	175.6	2.5	174.5	2.8
P	23.2	0.8	25.5	0.8	29.5	1.0	27.6	1.0
Mg	10.4	0.1	11.0	0.2	12.8	0.2	12.4	0.2
Na	6.1	0.3	5.3	0.3	4.7	0.2	6.3	0.3
S	5.2	0.3	4.5	0.2	4.8	0.2	5.5	0.3
Sr	2.2	0.1	2.4	0.1	2.8	0.1	2.7	0.1
K	3.2	0.2	2.3	0.1	2.0	0.1	2.9	0.1

B. Concentrations Corrected by Yield in mg/g of dried raw crab

Element \ Sample*	H6	±	H14	±	H5	±
Ca	115.6	1.7	117.1	1.7	112.0	1.8
P	19.5	0.6	19.7	0.6	17.7	0.6
Mg	8.5	0.1	8.5	0.1	8.0	0.1
Na	4.1	0.2	3.2	0.2	4.1	0.2
S	3.5	0.2	3.2	0.2	3.5	0.2
Sr	1.9	0.0	1.8	0.0	1.7	0.1
K	1.7	0.1	1.3	0.1	1.9	0.1

*Sample: R- T (°C)- t (h)

H6: 3-180-3; H14: 3-260-0.5; H5: 3-260-3

3.3.3.5. FTIR

FTIR a qualitative analysis tells the functional groups present in the sample. The FTIR plots are presented in Figure 3.9 and compiled studies on FTIR peak identification is presented in Table 3.6.

Table 3.6. FTIR Functional Group Identification

Bands (cm^{-1})	Sample	Functional Group	Sources
3200-3700	RC, H1-15, HWC, HC	O-H	[58]
3200-3570		O-H	[59]
3300-3600		O-H	[60, 61]
3450		O-H	[45]
3424		O-H	[4]
3273.2 and 3259.6		O-H	[43]
3440		O-H	[62]
3424		OH	[4]
3459	RC, H1-H15 HWC, HC	N-H	[4]
3380-3400 +3325-3345		aliphatic N-H	[59]
3460-3510+ 3380-3415		aromatic N-H	[59]
2880	RC, H1-15, HWC, HC	C-H	[62]
2800-3000		C-H	[58]
2800-2950		C-H	[60, 61]
1610–1550/1420–1300	RC, H1-15, HWC, HC	Carboxylate (carboxylic acid salt)	[59]
1250-1600		C=O	[58]
1250-1601		C=O	[60, 61]
peak 1500		C=O	[60, 61]
1668.4		C=O	[43]
1612		C=C	[45]
1660 and 1630 cm−1	RC, H1-15, HWC, HC	C-O stretching of the acetamido moieties (amide I)	[62]
1580 cm−1		deformation of N-H bonds of the amino groups (amide II)	[62]
1652 and 1621		amide 1	[4]
1554		amide 2	[4]
1680–1630		Amide	[59]
1660 and 1630 cm−1		C-O stretching of the acetamido moieties (amide I)	[62]
1410–1490/860–880	RC, H1-15, HWC, HC	Carbonate ion	[59]
1410		C-O	[58, 63]
1080		$CO3^{2-}$	[58]
1450 and 870		derived from CaCO3	[4]
1070.4 and 1072.4		X-H due to amine/ester	[43]

950-1200	C-O and C-OC	[62]
871	C-O	[58, 63]

RC FTIR (Figure 3.9.a), showed peaks of groups related to chitin [64, 65, 66]: 3444 cm^{-1} associated to O-H, at 3273 cm^{-1} associated to N-H [4, 59, 62], 2967 and 2920 cm^{-1} indicated C-H functionality [58, 60, 61], 1620 cm^{-1} associated to C=O [43, 58, 60, 61], 1508 cm^{-1} from amide 2 [59], and 1020-1150 cm^{-1} associated to C-O [59, 62]. Amide 2 is a result of deformation of primary amides NH_2 and a mixed vibration of secondary amides N-H bending and C-N stretching [67]. The N-H, C=O, and amide 2 peaks can due to protein in the RC [66], however since those peaks also found in chitin and RC is a heterogenous mixture the peaks are likely overlapped. There were also peaks at 1407 cm^{-1} and small peak at 868 cm^{-1} are the functional groups related to the carbonate ion from $CaCO_3$ in the RC [59, 68]

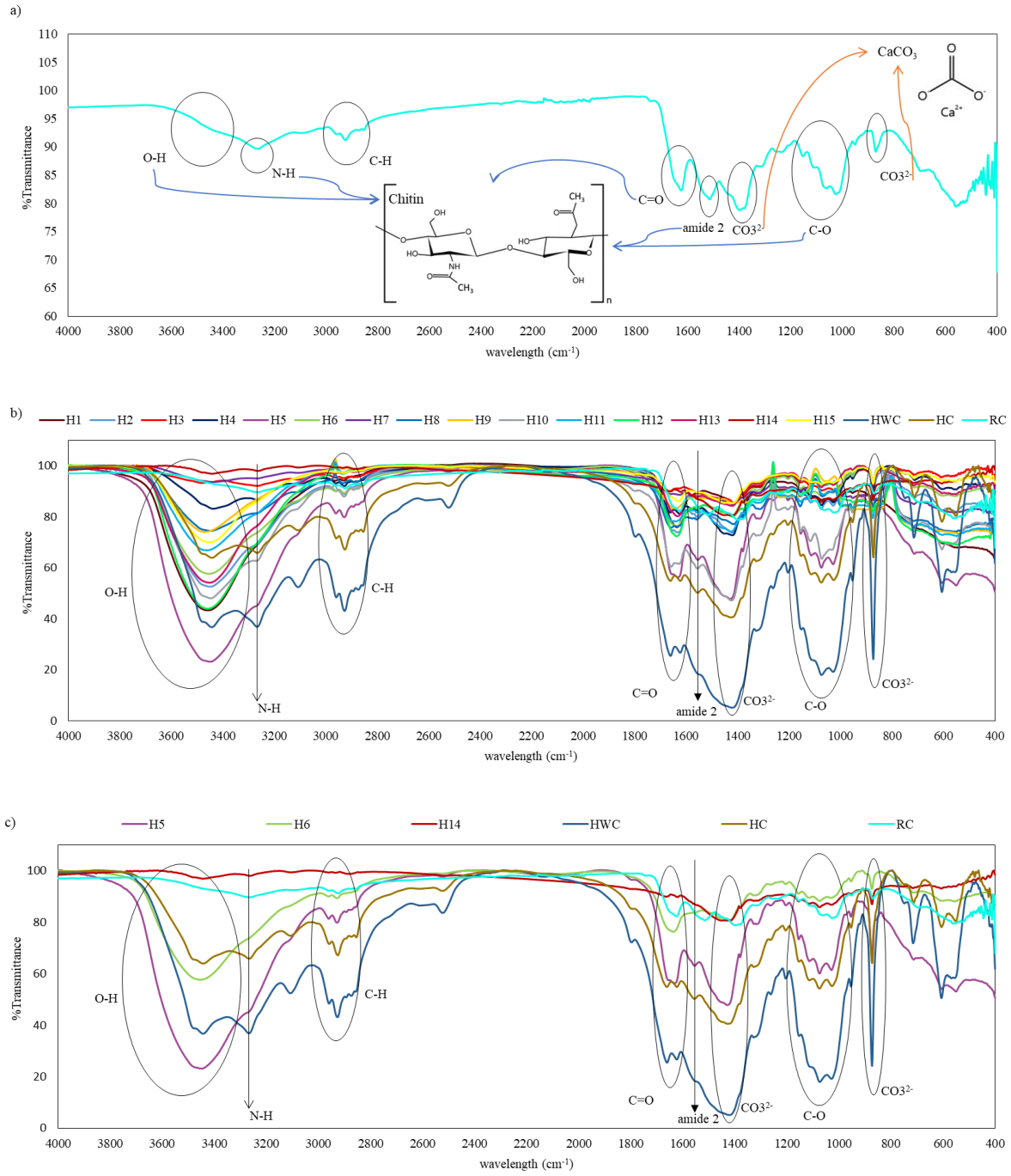

Figure 3.9. FTIR of a) Raw Crab, b) All Hydrochar, and c) Selected Hydrochar

The hydrochar FTIR can be seen in Figure 3.9 b and c. All hydrochar (including HC and HWC) spectra was similar to RC FTIR spectra. As noted above, FTIR intensities can vary between samples, however as FTIR is not quantitative this does not mean functional groups are increasing

or decreasing. To assess the change in functionality, ratios of different functional groups within the same sample can be compared to ratios in other samples. The ratios of FTIR peaks of O-H/N-H and OH/C-H of the RC and hydrochar were compared to determine if there was difference in surface functionalities and to give an indication of the relative decrease or increase of the functional groups' presence in the RC and hydrochar (Figure 3.10, data in Appendix, Table A4). The ratio of these peaks in the RC was similar to hydrochars produced at 0.5 h residence time regardless of the temperature and water ratio. Compared to RC and 0.5 h hydrochar peak ratios, the 1.75 h and 3 h residence time hydrochars peaks ratios decreased. This shows that 0.5 h residence time was not enough to change surface functionalities in the hydrochar and longer residence time were needed to cause changes in hydrochar surface functionalities. The decreased in peaks ratio in Figure 3.10 as residence time increased showed that increasing residence time led to increase in N-H and C-H functional groups compared to O-H.

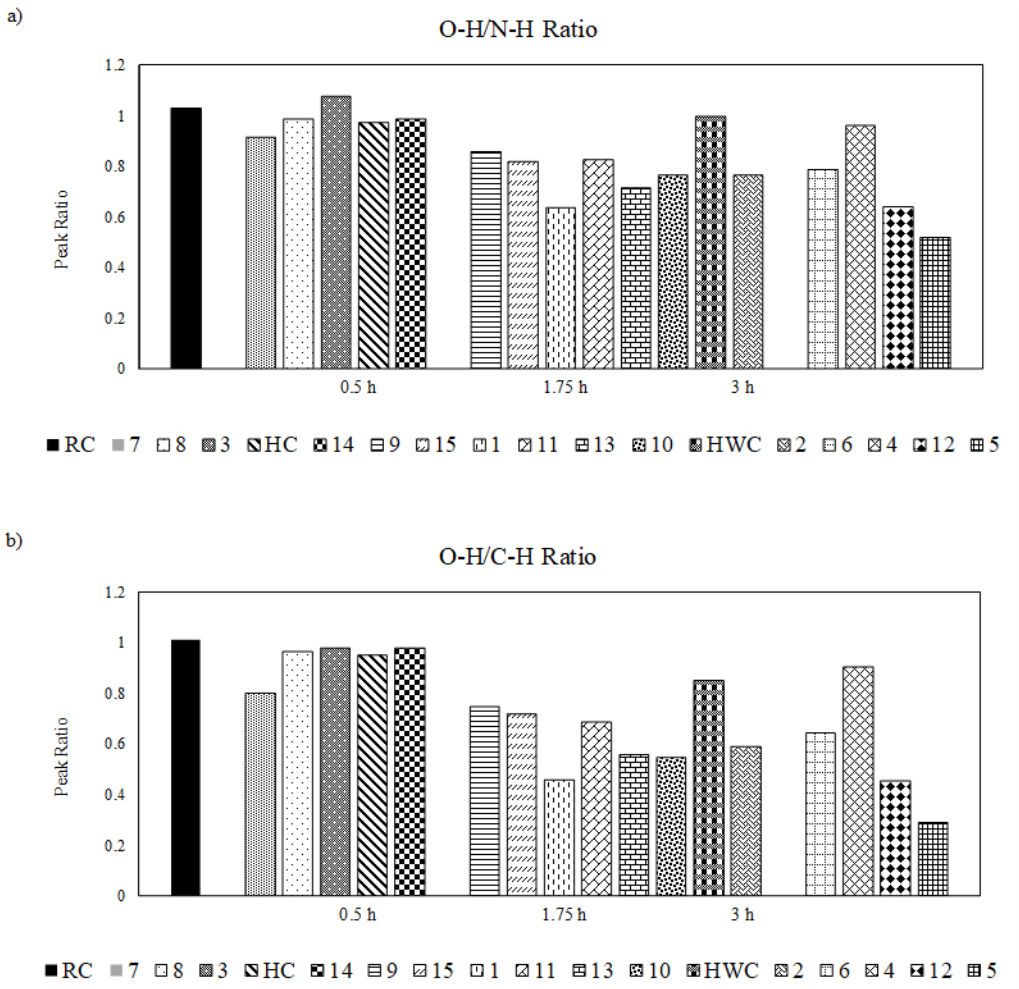

Figure 3.10. Crab Shell and Hydrochar a) O-H/N-H, and b) O-H/C-H FTIR peak ratio.

3.3.3.6. pH

The hydrochar pH was basic, between 7.7-8.6 (Appendix, Table A5) due to the minerals (mainly but not limited to $CaCO_3$) present in the crab shell. Compared to RC, the hydrochar pH was lower, likely due to products from protein hydrolysis to amino acids [69, 70, 71]. However, further investigation/analysis should be done to confirm the compounds present in the crab byproduct hydrochar. From Figure 3.11.a, the hydrochar pH decreased when temperature and residence time increased.

The liquid pH was also basic, from 8.6-9.5. The basic nature of HTC liquid is likely from soluble minerals from the crab shell ($CaCO_3$) or possible HTC products (amino acids such as arginine and lysine and amine from protein degradation [69, 72, 73]). HTC liquid pH at water ratio 2 decreased as residence time increased, but increased with temperature (Figure 3.11.b). The same trend was observed at water ratio 3. However, at water ratio 4, the pH increased with temperature and residence time. The pH increase with temperature and residence time was related to increased mineral solubility/reactivity at the high-water ratio. There was a noticeably high pH value at 9.53 (Figure 3.11.b) at a water ratio of 2.22, which was the HWC. This could be due to the property/composition of moisture in the WC. Initial moisture in the WC could already be saturated in water-soluble minerals (ex., $CaCO_3$). However, when the sample was heated, increased pressure during HTC might increase the $CaCO_3$ solubility, thus, increasing the liquid pH further [54]. If the water/moisture in the crab shell contains NaCl, it also increase $CaCO_3$ solubility in water [54]. Several possibilities might affect the HTC liquid pH. However, this could not be confirmed until further investigation/analysis on HTC liquid.

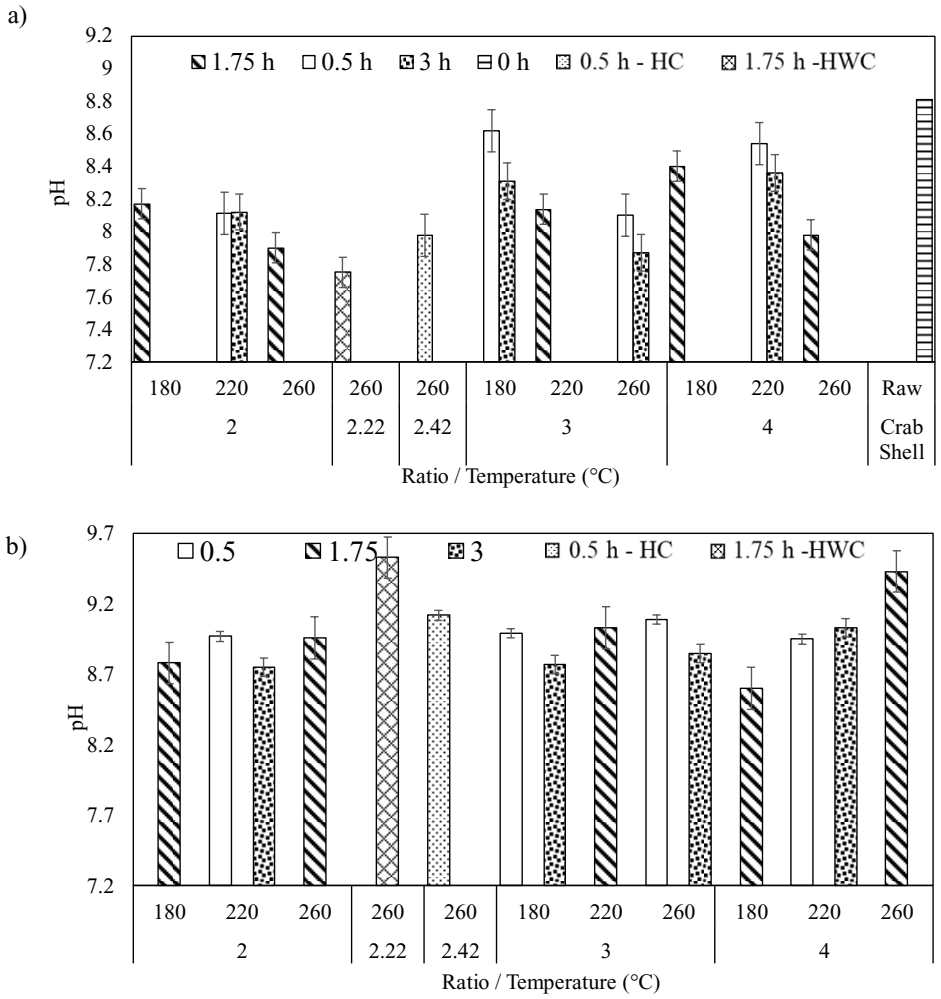

Figure 3.11. a) Crab Shell and Hydrochar pH, and b) HTC Liquid pH as a function of time, temperature, and water ratio.

3.3.3.7. BET Surface Area

The BET surface area of the raw crab shell was 11.48 ± 0.05 m^2/g and after HTC, the hydrochar surface area increased to values between 13.47 - 26.67 ± 0.14 m^2/g (Figure 3.12). The hydrochar surface area increase when increasing temperature and residence time up to maximum surface area of ~26 m^2/g at 260 °C and 0.5 h. The surface area decreased at 260 °C at residence times greater than 0.5 h. As will be outlined below in the DoE this shows the negative impact of higher process intensity (high temperature and long residence times) on surface area, likely as a result of pore collapse, deformation, melting, and fusion at higher process intensity [25, 40, 74]. The same trend was observed on other feedstocks HTC, such as sewage sludge, pulp and paper

mill sludge, and macroalgae at higher temperatures and longer residence times [25, 31, 36, 40]. The HTC conditions effect on the hydrochar surface area will be discussed further in DoE section 3.4.6.

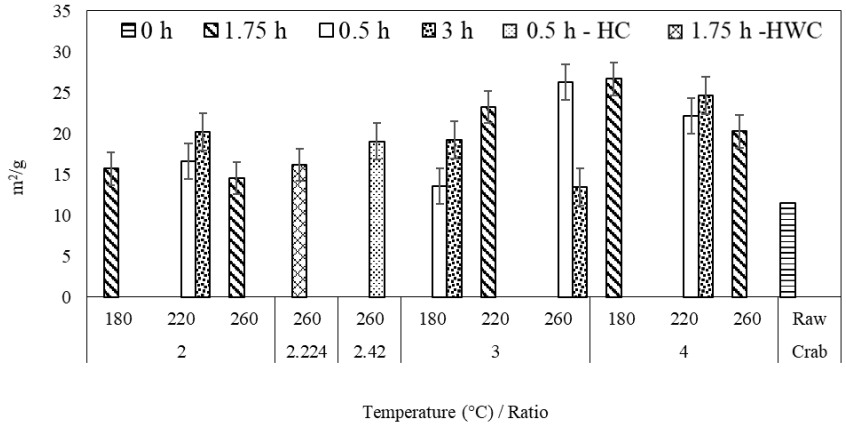

Figure 3.12. BET Surface Area of Crab Shell and Hydrochar as a function of time, temperature, and water ratio.

The surface area of wet crab HTC hydrochar (HWC) at water ratio 2.22, 260 °C, and 1.75 h was 16.17 m^2/g. It should be noted the particle size of WC was larger compared to the RC. However, it did not appear to impact surface area as dried crab HTC hydrochar at water ratio 2, 260 °C, and 1.75 h (H10) was 14.53 m^2/g. Additionally, grinding HWC to < 2 mm resulted in a similar surface area, 17.42 m^2/g. The crab shell hydrochar surface area was slightly higher or similar compared to other crab/crustacean shell hydrochar (4.03-26.8 m^2/g) [40, 41, 43]. However, crab shell hydrochar surface area was lower compared KOH activated crab shell hydrochar (2109 m^2/g) [33, 44]. Despite the low surface area, studies studied hydrochar from crustacean shells as an adsorbent and showed promising results, this is due to its transformation into a more porous material and increased functional groups [23, 43, 45].

3.3.3.8. Ultimate Analysis

The ultimate analysis of raw crab shell and hydrochar graphs (wt%, db) are summarized in Table 3.4 and in Figure 3.13. Consequently, the ultimate composition discussed in this section will refer to C, H, and N wt%, db.

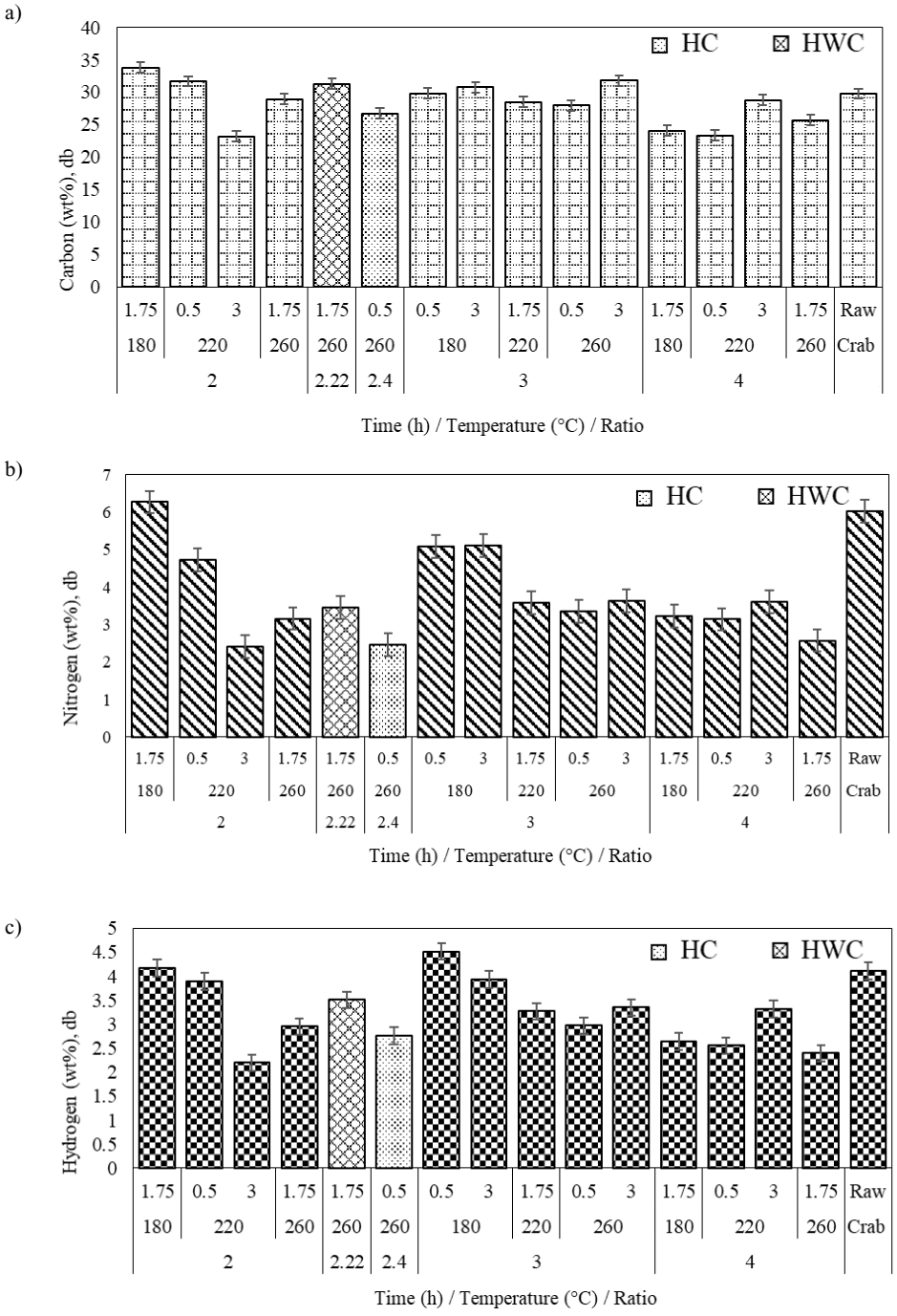

Figure 3.13. Crab shell and hydrochar a) carbon content – dotted grid, b) nitrogen content – diagonal stripes, and c) hydrogen content – checker board dry ash free basis, as a function of time, temperature, and water ratio; HC elemental composition - dots and HWC elemental composition - diamond grid.

Overall (with few exceptions discussed below), the hydrochar carbon content was approximately the same or slightly slower than the feedstock, however this is difficult to assess as lack of reaction as hydrochar carbon can be "lost" due to dissolution of CaCO3 or "gained" due to polymerization. Nitrogen content was lower compared to feedstock (Table 3.2). The hydrogen content was lower in the hydrochar except at the lowest temperature studied at water ratio 2 (180 °C). The decrease in nitrogen content is likely due to protein hydrolysis [75]. Chitin thermal degradation and/or hydrolysis was considered negligible due to low HTC temperatures. In related work, chitin was observed to initiate thermal degradation at 300 ℃ and in a subcritical water study chitin was observed to react/degrade at 283 ℃ [55, 76]. Aida et al. (2014) showed limited (less than 6 %) chitin degradation in HTC experiments at 220 °C and 20 min, these values increased to 50% at 400 °C [77]. Protein reacts at lower temperature than chitin, between 150-310 ℃ [32]. Protein hydrolysis also had been studied using various feedstocks, such as: shrimp shell, blue mussel, abalone viscera, and tuna skin, showed that protein degradation in subcritical water environment had initiates at 120-150 ℃ [71, 78, 79, 80, 81].

Direct comparison of the hydrochar carbon and RC is complex as outlined in the DE section 3.4.1, the dominating reactions (hydrolysis vs polymerization etc.) shift depending on the temperature/time/water ratio. At a water ratio of 2 as the reaction intensity increased from 180 °C and 1.75 h to 220 °C and 3 h, the carbon content decreased from 33.79 to 23.32 wt% db, however a further temperature increases to 260 °C resulted in an increase in carbon up to 31.31wt% for 1.75 h (Figure 3.13.a). As the water ratio increased to 3, increases of temperature between 180 to 220 °C and time from 0.5 h to 3 h had little impact on carbon content (~29-30 wt% db). At 260 °C and 3 h there was a slight increase in carbon, but within experimental error (31.8wt%) The highest water ratio used (4) showed the most dramatic drop in carbon content relative to the feedstock. Low temperatures and/or short residence times had carbon content between 23.37 wt% (220 °C and 0.5 h) and 24.09 wt% (180 °C and 1.75 h). As the temperature increased to 260 °C, the carbon content increased with residence time from 25.21wt% at 1.75 h to 28.8 wt% at 3 h. The increase in carbon content possibly due to protein polymerization [75], which would be favoured at higher temperatures and residence times, while the decrease is likely due to minerals/ $CaCO_3$ dissolution in water [70]. These reactions may be occurring simultaneously, which could explain why there is little change in carbon in some of the operating regimes. The DE section below breaks the interactions between temperature, time and water ratio and a fuller discussion is provided there.

At a water ratio of 2 the nitrogen content decreased as temperature increased from 180 to 220 °C from feedstock nitrogen levels at the lowest temperature and time studied (180 °C and 1.75 h) to 2.42 wt% at 220 °C and 3 h, a 60% drop, and then leveled off as temperature increased to 260 °C and 1.75 h (Figure 3.13.b). At fixed water ratio of 3, at 180 °C the nitrogen was approximately 15 % less than the feedstock at all residence times studied. At temperature 220 °C and above the nitrogen was ½ that of the feedstock (between 3.33-3.73 wt%). At a water ratio 4 the hydrochar nitrogen content was again approximately ½ the feedstock value, as low as 2.58 wt% at the highest temperature studied (260 °C and 1.75 h). The nitrogen was much more sensitive to temperature at temperatures 220 °C and above, which makes sense given protein thermal degradation/hydrolysis at temperatures above 180 °C. As with the nitrogen the interaction between the operating conditions are outlined more completely in DE.

At fixed water ratio 2 the hydrochar hydrogen decreased at temperatures greater than 180oC and/or residence times greater than 30 min, below these limits the hydrochar hydrogen resembled the feedstock. Similar observations occurred at a water ratio of 3. At a water ratio of 4 the hydrogen was approximately 40% of the feedstock at all temperatures and times studied except for the one run at 3 h where the hydrogen was 20% of the feedstock.

The relationship between HTC conditions (water ratio, temperature, and residence time) and the effect on hydrochar elemental composition as a function of temperature, time, and water were complex, hence the breakdown of discussion based on set water ratio. In an attempt to better understand the trends a DE was utilized to understand the interaction of HTC on elemental composition. The effect of HTC conditions on including but not limited to ultimate composition will be further discussed and interactions (if any) will be explained in section 3.4 below.

3.3.4. DE Results

DE runs (H1-15) were analyzed by the Design Expert (DE) software as describe in section 2.2.1. The responses considered were based on the initial data analysis outlined above and included C, H, and N content (wt%, db), yield (wt%, db), ash content (wt%, db), and BET surface area (m2/g). The coding for the inputs/variables were; water ratio, R / A, temperature, T (°C) / B, and residence time, t (h) / C.

3.3.4.1. Carbon Content, C (wt%, db)

The two-factor interaction model was suggested for hydrochar carbon content with predicted R^2 value of -0.2087 and adjusted R^2 value of 0.4358. The negative predicted R^2 value implies that the overall mean may be a better predictor of response than the current model [49]. Despite negative predicted R^2 value, the selected model was significant and lack of fit F value showed there was a 30.23 % chance that the lack of fit could occur due to noise [49]. The R^2 values were deemed adequate to navigate the design space [49]. The hydrochar carbon content (C) showed significant dependency on water ratio and water ratio and residence time interaction. The coded equation:

$$C\ (wt\%, db) = +28.36 - 1.96*A + 0.2075*C + 3.48*A*C \quad (Eq.\ 6)$$

The actual value equation:

$$C\ (wt\%, db) = +48.56267 - 6.82950*R - 8.18600*t\ [h] + 2.78400*R*t\ [h] \quad (Eq.\ 7)$$

Water ratio is a significant factor affecting carbon content. As water ratio increased the carbon content decreased to the lowest carbon content at water ratio 4, which also seen in figure Figure 3.14.b. this is consistent with the previous observations of carbon content, and the decrease in carbon content is likely due to dissolution of carbon from the mineral carbonates ($CaCO_3$) [70].

The interaction between water ratio and residence time is also a significant factor: at low residence times (0.5 h), increasing the water ratio led to a decrease in carbon content and at a residence time of 3 h increasing the water ratio led to increased carbon content (Figure 3.14.b). The water ratio and residence time interaction is the same regardless the temperature. Again, the decrease in carbon content at low residence time is possibly due to carbon dissolution into the water from the mineral carbonates ($CaCO_3$) [70]. Without a more detailed analysis on the liquids, the reasons for the increase in carbon at longer residence times can only be speculated, but could be due to longer times favouring slower reactions which concentrate carbon due to loss of nitrogen (protein hydrolysis and polymerization) [70, 75]. The carbon content relationship with water ratio and time is also clearly demonstrated in the response plot (Figure 3.14.a). Most studies (sewage sludge, pulp and paper sludge, macroalgae, and pretreated crustacean shell) showed the drivers for carbon content increase in the hydrochar are temperature and residence time, i.e., process intensity [20, 21, 24, 26, 27, 28, 31, 35, 36, 38, 39, 42, 46]. In our study, due to the high $CaCO_3$ content, the

water ratio-residence time interaction is most significant factor affecting the carbon content. At the same time, the temperature was deemed insignificant and removed from the model equation. The lack of significance of temperature is likely due to the higher temperatures required to degrade chitin and combination of temperature and water content to impact calcium carbonate (combined the chitin and calcium carbonate make up over 50 wt% of the feedstock) whereas lignocellulosic or carbohydrate-protein-based feedstock are dominated by carbohydrates with a lower thermal degradation temperature.

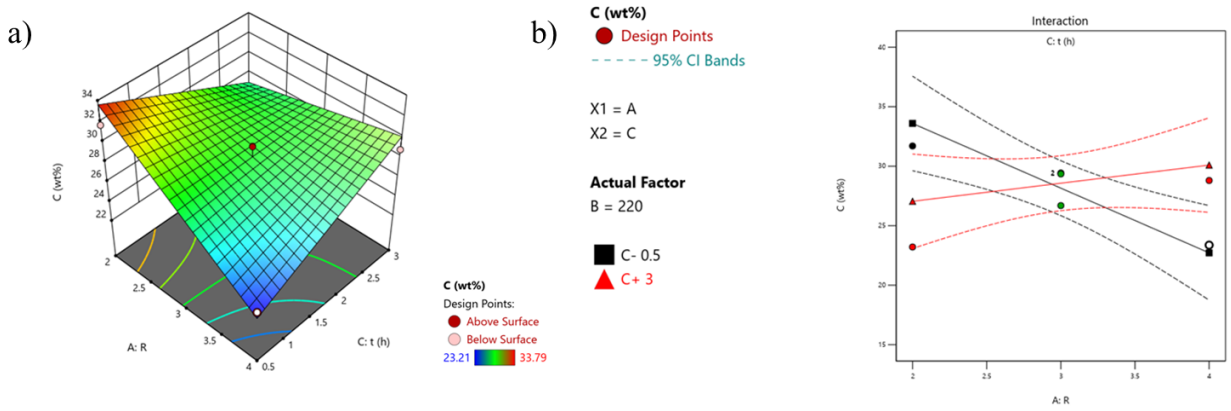

Figure 3.14. C (wt%, db) a) Response Plot of AC interaction, and b) AC Interaction Graph.

3.3.4.2. Nitrogen content

The linear model was suggested for hydrochar nitrogen content with predicted R^2 value of 0.1951 and adjusted R^2 value of 0.4474. Predicted R^2 more than 0.2 lower than adjusted R^2 this indicates there are too many insignificant terms in the model [49]. The selected model was deemed significant and F value showed there was a 6.34 % chance that the lack of fit could occur due to noise [49]. The R^2 values were deemed adequate to navigate the design space [49]. The nitrogen content (N) showed significant dependency on temperature. The coded equation:

$$N\ (wt\%, daf) = +3.80 - 0.5050*A - 0.8713*B \quad (Eq.\ 8)$$

The actual value equation:

$$N\ (wt\%, daf) = +10.11021 - 0.505000*R - 0.021781*T\ [°C] \quad (Eq.\ 9)$$

The bulk of HTC studies highlight the importance of temperature on nitrogen in the hydrochars for lignocellulose/protein/lipid-based biomass such as sewage sludge, pulp and paper sludge, and macroalgae [20, 21, 24, 26, 27,28, 31, 35, 36, 46]. The DE and experimental observations (section 3.3.8) show this same trend for this high ash/chitin material, where temperature was the most significant factor in nitrogen decrease (Figure 3.15). This is not unsurprising given the protein hydrolysis occurring [78, 79, 80, 81]. In a study on subcritical water treatment of shrimp, the increased of protein content in the liquid hydrolysate which as temperature increased from 140 – 260 °C [71]. Residence time had the same impact, increasing the protein in hydrolysate as residence time increased from 10 min up to 40 min at all temperature. Protein hydrolysis to amino acids was also observed by increasing in hydrolysate amino acid as temperature and residence time increased [71]. This indicates that the liquid product may have applications in animal feed etc.

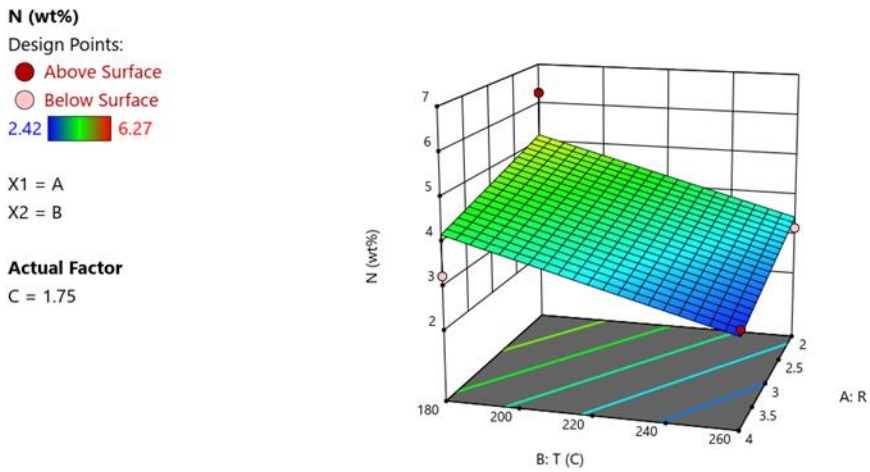

Figure 3.15. N (wt%, db) Response Plot at C = 1.75 h.

3.3.4.3. Hydrogen Content

The two-factor interaction model was suggested for hydrochar hydrogen content with predicted R^2 value of -0.0464 and adjusted R^2 value of 0.4513. The negative predicted R^2 value implies that the overall mean may be a better predictor of response than the current model [49]. The selected model was significant and lack of fit F value showed there was a 38.68 % chance that the lack of fit could occur due to noise [49]. The R^2 values were deemed adequate to navigate the

design space [49]. The hydrogen content (H) showed significant dependency on temperature and water ratio and residence time interaction. The coded equation:

$$H\ (wt\%, db) = +3.25 - 0.2875*A - 0.4500*B - 0.1450*C + 0.6175*A*C \quad \text{(Eq. 10)}$$

The actual value equation:

$$H\ (wt\%, db) = +9.38267 - 1.15200*R - 0.011250*T\ [°C] - 1.59800*t\ [h] + 0.494000*R*t\ [h] \quad \text{(Eq. 11)}$$

As noted above in the experimental section temperature does have an influence on hydrogen content (Figure 3.16.a-c). Increasing temperature showed a decrease in the hydrogen content. A more pronounced decrease in hydrogen content at all temperatures was shown at high water ratio (4) – short residence time (0.5 h) and low water ratio (2) – long residence time (3 h) compared to low water ratio – short residence time.

The water ratio and residence time effect interaction on hydrogen content was shown in Figure 3.16.d. The effect of the interaction was: at low residence time (0.5 h), increasing the water ratio led to a decrease in hydrogen content. In comparison, increasing the water ratio at a high residence time (3 h) increased hydrogen content. The water ratio and residence time interaction is the same regardless of the temperature.

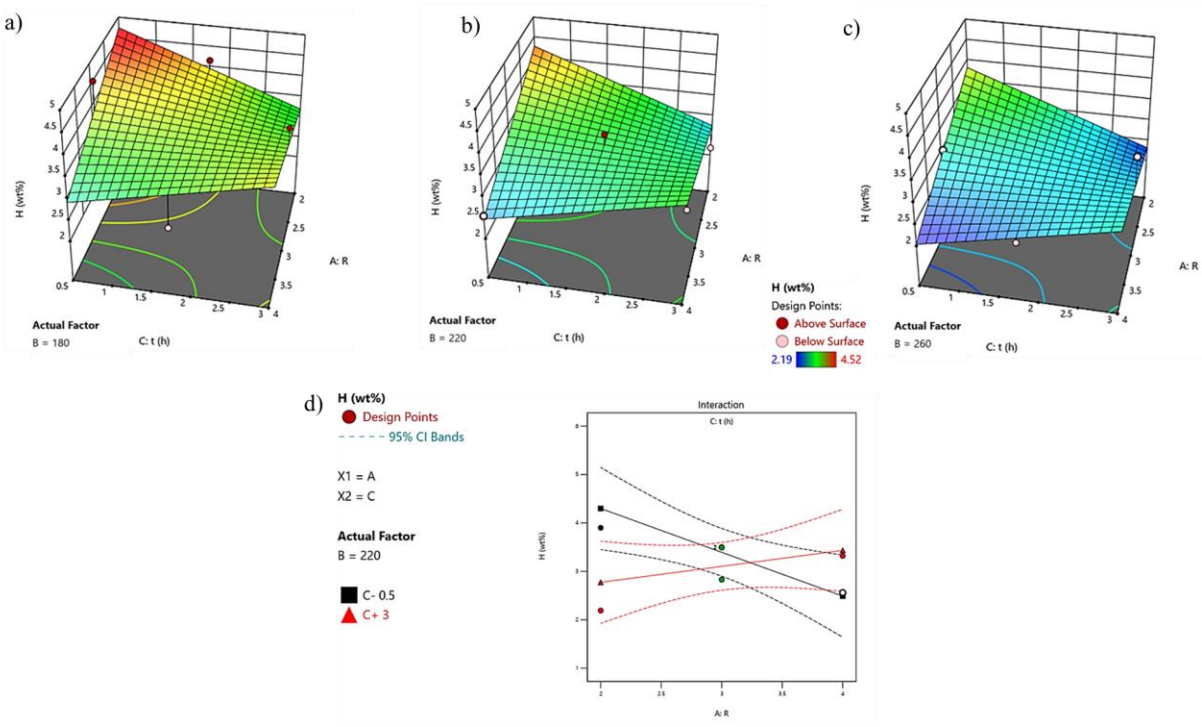

Figure 3.16. H (wt%, db) Response Plot at a) B = 180 °C, b) B = 220 °C, and c) B = 260 °C; and d) AC Interaction Graph.

3.3.4.4. Yield (wt%)

A linear model was suggested for prediction of yield, with a predicted R^2 value of 0.8002 and an adjusted R^2 value of 0.8789. The selected model was significant [49]. The lack of fit F value showed there was a 7.40 % (low probability, < 10%) chance that lack of fit occurred due to noise, which led to a significant amount of variance [49]. The R^2 values were deemed adequate [49]. The yield (wt%) showed significant dependency on water ratio and temperature. The coded equation:

$$\text{Yield} = +70.79 - 3.87*A - 4.44*B - 0.8725*C \quad \text{(Eq.12)}$$

The actual value equation:

$$\text{Yield} = +107.99833 - 3.86500*R - 0.110875*T\ [°C] - 0.698000*t\ [h] \quad \text{(Eq. 13)}$$

The DE analysis showed that the water ratio and temperature significantly reduced yield (wt%). This result is consistent with the observation discussed in section 3.2. The decrease in yield reflects the increased conversion of biomass to hydrochar. Nitrogen was the main contributor to

the conversion (protein hydrolysis reactions). The contour and response plot also shows the effect of water ratio and temperature on yield (wt%) (Figure 3.17).

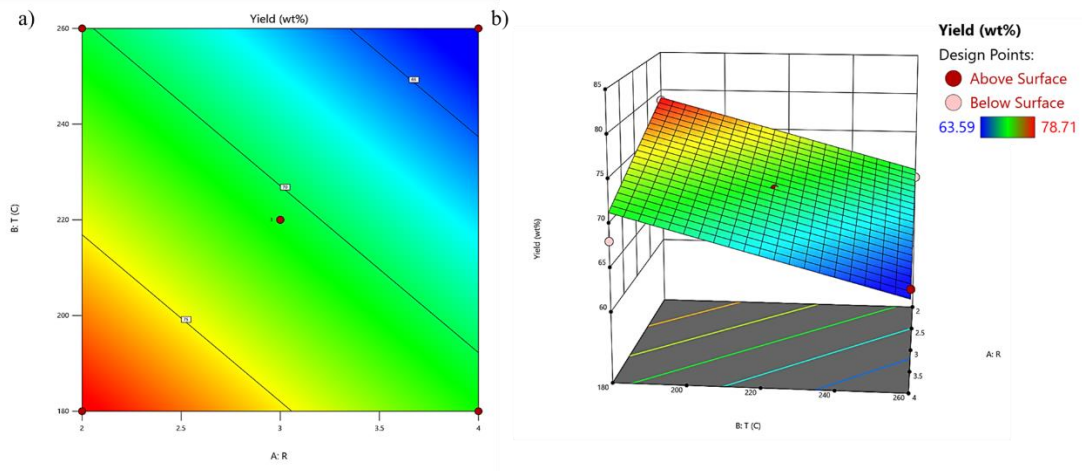

Figure 3.17. a) Contour Plot, and b) Response Surface of Hydrochar Yield Model.

3.3.4.5. Ash Content (wt%, db)

As with yield, a linear model was suggested for ash content, with a predicted R^2 value of 0.7226 and an adjusted R^2 value of 0.8065. The selected model was significant [49]. The lack of fit F value showed a 17.62 % chance that lack of fit occurred due to noise [49]. The R^2 values were deemed adequate [49]. The ash content (wt%) showed significant dependency on water ratio and temperature. The coded equation:

$$\text{Ash} = +38.57 + 1.37*A + 3.11*B + 0.6625*C \quad \text{(Eq. 14)}$$

The actual value equation:

$$\text{Ash} = +16.40208 + 1.37500*R + 0.077813*T\ [°C] - 0.530000*t\ [h] \quad \text{(Eq. 15)}$$

Hydrochar ash content was increased with increasing water ratio and temperature (Figure 3.18). The ash dependency on water ratio and temperature is consistent with the observation discussed in section 3.3.1.

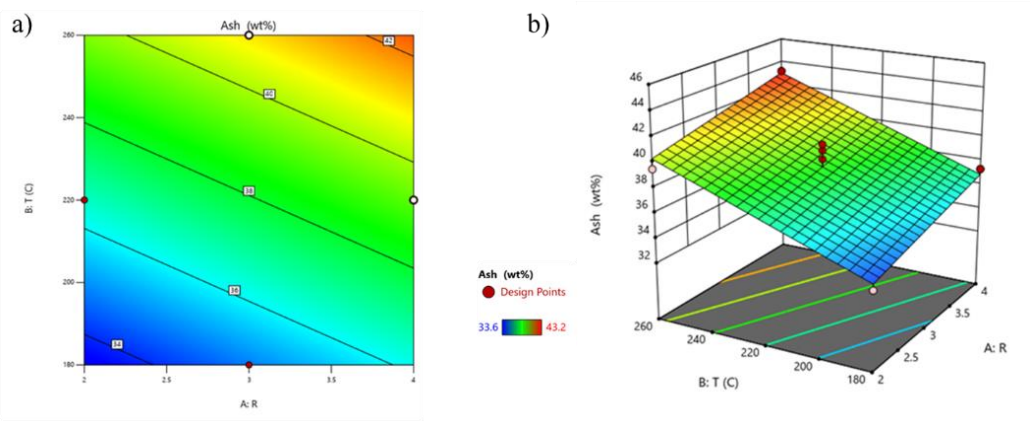

Figure 3.18. a) Contour Plot, and b) Response Surface of Hydrochar Ash Model.

3.3.4.6. BET Surface Area (m^2/g)

Two factor interaction model was suggested for BET surface area with a predicted R^2 value of -0.1926 and an adjusted R^2 value of 0.4104. The negative predicted R^2 value implies that the overall mean may be a better predictor of response than the current model [49]. Despite the negative predicted R^2 value, the selected model was significant and the lack of fit F value showed a 39.27 % chance that the lack of fit could occur due to noise [49]. The R^2 values were deemed adequate to navigate the design space [49]. The BET surface area (m^2/g) depended significantly on water ratio and temperature and residence time interaction. The coded equation:

$$\text{BET surface area } (m^2/g) = +20.21 + 3.33*A - 0.0750*B - 0.1362*C - 4.62*B*C \quad \text{(Eq. 16)}$$

The actual value equation:

$$\text{BET surface area } (m^2/g) = -24.74217 + 3.32625*R + 0.159825*T\ [°C] + 20.21900*t\ [h] - 0.092400*T*t\ [°C*h] \quad \text{(Eq. 17)}$$

The increase in water ratio significantly increased BET surface area (m^2/g) (Figure 3.19.a-c). There was no significant impact of temperature or residence time, however, there was an interaction between temperature and residence time. This interaction validates the observations from section 3.3.7. The plot (Figure 3.19.d) demonstrates the increasing surface area at low residence times and increasing temperature, reaching a maximum and then decreasing as temperature increased to 260 °C and time to 3 h.

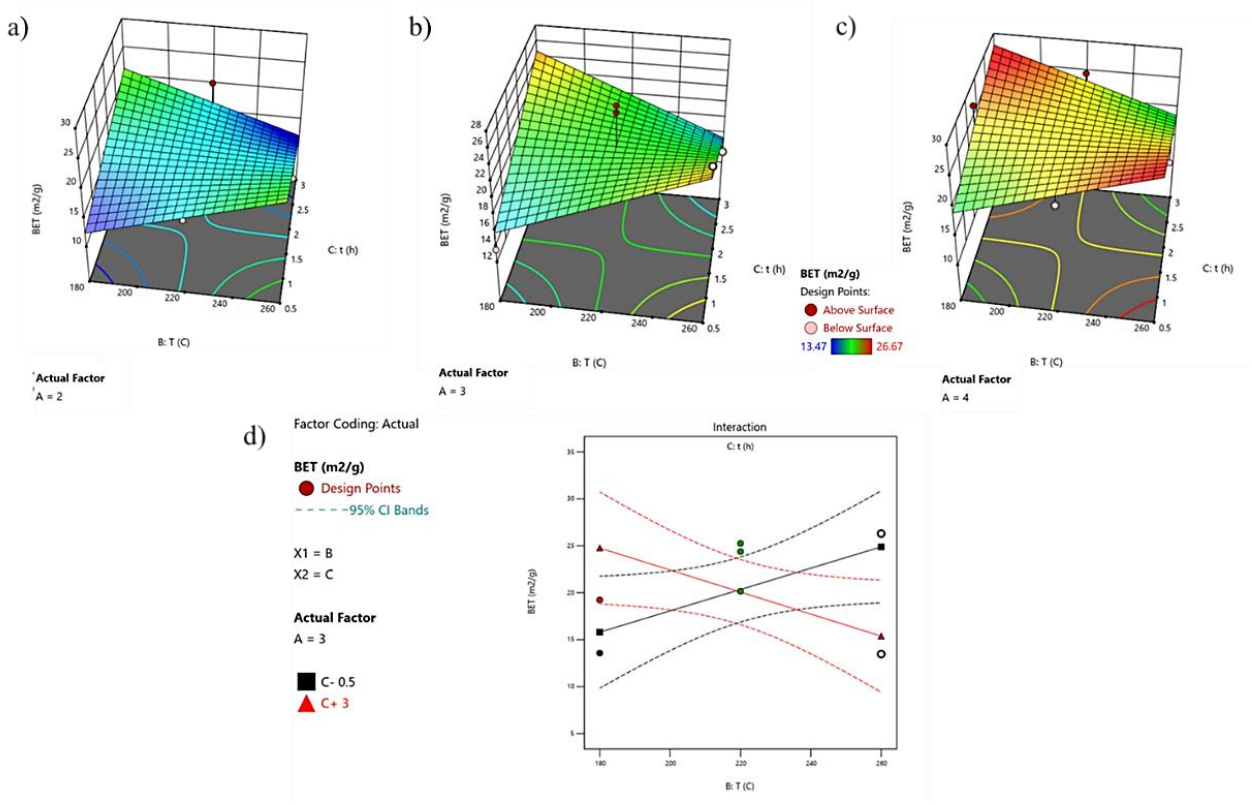

Figure 3.19.BET Surface Area Response Plot at a) A = 2, b) A = 3, and c) A = 4; and d) BC Interaction Graph.

Overall, DoE showed a low value of R^2 on the factors and responses studied. However, the purpose on this study was not for prediction, rather to study if there was any effect or relationship between the studied factors on the responses.

3.3.4.7. Model Confirmation

As described in section 3.2, one additional confirmation run generated by DE was conducted to study the modelled responses at different process conditions. The confirmation run was a water ratio of 2.42, a temperature of 260 °C, and a residence time of 0.5 h. Table 3.7. shows the predicted mean, standard deviation, and the predicted value interval with 95 % confidence. All HC response values were within the predicted 95 % confidence interval except the ash content (red font).

The confirmation was also done for the HWC to observe the values of the responses for this experiment. Table 3.5. shows the predicted mean, standard deviation, and the predicted value interval with 95 % confidence. All HWC response values were within the predicted 95 % confidence interval, except the yield on HWC (red font). As previously mentioned, the deviation in HWC data may be due to the different batches of crab used. Overall, HWC data fit into the trends from the DE experiment.

Table 3.7. Confirmation Runs Prediction and Responses Observation (Confidence = 95 %)

HC	Predicted Mean	Predicted Median*	Std Dev	95% PI low	Data	95% PI high
Yield	69.48	69.48	1.64	65.26	66.96	73.69
BET Surface Area	22.95	22.95	3.56	12.89	19.04	33.01
C	31.32	31.32	2.39	25.26	26.72	37.38
N	3.23	3.23	0.78	1.34	2.47	5.11
H	3.47	3.47	0.51	2.12	2.76	4.83
Ash	40.22	40.22	1.25	37.01	37.00	43.43
HWC	**Predicted Mean**	**Predicted Median***	**Std Dev**	**95% PI low**	**Data**	**95% PI high**
Yield	69.37	69.37	1.64	65.29	60.32	73.44
BET Surface Area	17.54	17.54	3.56	8.61	16.17	26.47
C	29.89	29.89	2.39	24.25	31.31	35.53
N	3.33	3.33	0.78	1.41	3.46	5.24
H	3.02	3.02	0.51	1.75	3.51	4.29
Ash	40.61	40.61	1.25	37.51	40.50	43.72

*For transformed responses the predicted mean and median may differ on the original scale [49].

3.4. Conclusion

As an economic driver in Atlantic Canada, snow crab processing produces abundant high-moisture by-products. This biomass can be utilized and reduce waste loading to the environment. In this study, HTC was used for more sustainable waste utilization without drying the high-moisture material. The variation in water ratio, temperature, and residence time was studied. The study was done on the RC and WC to characterize the produced hydrochar. Furthermore, to investigate the factors (water ratio, temperature, and residence time) relationship and effect on the responses (ultimate composition, atomic ratios, yield, ash content, and surface area). The factors' effect on hydrochar yield and ash content was linear.

However, the factors had a more complex effect on the ultimate composition. There was a significant water ratio and residence time interaction observed in carbon and hydrogen content likely due to mineral dissolution and the complex relationship between the mineral dissolution and protein hydrolysis reactions. Nitrogen content was temperature dependent. Further work will focus on analysis of the liquid product for proteins, amino acids, and other compounds to better assess where one mechanism is dominating over another.

RC hydrochar showed a higher surface area than other feedstock hydrochar, but still low compared to other published work in activated hydrochar. The functionalities of hydrochar were similar to the feedstock. The improvement in the surface area might be a potential for adsorbent utilization. The functional group identified from the FTIR might also inform hydrochar affinity to certain adsorbates. From this study, high ash content in hydrochar was an undesirable property in terms of fuel application since it could lead to fouling and slagging similar to macroalgae hydrochar. However, the minerals in the hydrochar could be a potential for soil remediation application. Optimal conditions for HTC will depend on the intended application and the data acquired from this study can be used to determine the optimal conditions in each suitable application.

References

[1] Department of Fisheries and Land Resources, Newfoundland and Labrador, Canada, "Seafood Industry Year in Review 2019," [Online]. Available: https://www.gov.nl.ca/ffa/files/2019-SIYIR-WEB.pdf. [Accessed 12 August 2021].

[2] V. Sieber, M. Hofer, W. M. Brück, D. Garbe, T. Brück and C. A. Lynch, "ChiBio: An Integrated Bio-refinery for Processing Chitin-Rich Bio-waste to Specialty Chemicals," in *Grand Challenges in Marine Biotechnology*, P. H. Rampelotto and A. Trincone, Eds., Springer, Cham, 2018, pp. 555-578.

[3] M. Asunción Lage-Yusty, M. Vilasoa-Martínez and S. Álvarez-Pérez, "Chemical composition of snow crab shells (Chionoecetes opilio)," *CyTA - Journal of Food,* vol. 9, no. 4, pp. 265-270, 2011.

[4] E. M. Aklog, H. Kaminaka, H. Izawa, M. Morimoto, H. Saimoto and S. Ifuku, "Protein/$CaCO_3$/Chitin Nanofiber Complex Prepared from Crab Shells by Simple Mechanical Treatment and Its Effect on Plant Growth," *International Journal of Molecular Sciences,* vol. 17, no. 10, p. 1600, 2016.

[5] T. J. Beaulieu, P. Bryl and M.-É. Carbonneau, "Characterization of enzymatic hydrolyzed snow crab (Chionoecetes opilio) by-product fractions: A source of high-valued biomolecules," *Bioresource Technology,* vol. 100, no. 13, p. 3332–3342, 2009.

[6] W. J. Naczk, K. Brennan, C. Liyanapathirana and F. Shahidi, "Compositional characteristics of green crab (Carcinus maenas)," *Food Chemistry,* vol. 88, no. 3, p. 429–434, 2004.

[7] Y. I. Hajji, O. Ghorbel-Bellaaj, R. Hajji, M. Rinaudo, M. Nasri and K. Jellouli, "Structural differences between chitin and chitosan extracted from three different marine sources," *International Journal of Biological Macromolecules,* vol. 65, p. 298, 2014.

[8] C. Pires, A. Marques, M. Carvalho and I. Batista, "Chemical Characterization of Cancer Pagurus, Maja Squinado, Necora Puber and Carcinus Maenas Shells," *Poult Fish Wildl Sci,* vol. 5, no. 1, p. 1000181, 2017.

[9] B. S. Parthiban, A. Gopalakannan, K. Rathnakumar and S. Felix, "Comparison of the Quality of Chitin and Chitosan from Shrimp, Crab and Squilla Waste," *Current World Environment,* vol. 12, no. 3, p. 670–677, 2017.

[10] H. Ding, L. Lv, Z. Wang and L. Liu, "Study on the “Glutamic Acid-Enzymolysis” Process for Extracting Chitin from Crab Shell Waste and its By-Product Recovery," *Applied Biochemistry and Biotechnology ,* vol. 190, no. 3, p. 1074–1091, 2020.

[11] M. Leffler, "Maryland Marine Notes (Archive) - Maryland Sea Grant - Treasure from Trash: Is There Profit in Crab Waste?," March April 1997. [Online]. Available: https://www.mdsg.umd.edu/maryland-marine-notes-archive.

[12] N. Yan and X. Chen, "Sustainability: Don't waste seafood waste," *Nature,* vol. 524, p. 155–157, 2015.

[13] T. Mahmood and A. Elliott, "A review of secondary sludge reduction technologies for the pulp and paper industry," *Water research (Oxford),* vol. 40, no. 11, pp. 2093-2112, 2006.

[14] T. Wajima and J. F. Rakovan, "Removal behavior of phosphate from aqueous solution by calcined paper sludge," *Colloids and surfaces. A, Physicochemical and engineering aspects,* vol. 435, pp. 132-138, 2013.

[15] Environment and Climate Change Canada, "Canadian: Solid waste diversion and disposal," 20 December 2018. [Online]. Available: https://www.canada.ca/en/environment-climate-change/services/environmental-indicators/solid-waste-diversion-disposal.html. [Accessed 4 October 2021].

[16] M.-M. Titirici, "Green Carbon," in *Sustainable carbon materials from hydrothermal processes*, Wiley, 2013, pp. 1-36.

[17] ipi.ag, "Hydrothermal carbonization: convert waste to energy," [Online]. Available: https://ipi.ag/en/htc-plant_14. [Accessed 13 October 2021].

[18] E. Bevan, J. Fu and Y. Zheng, "Challenges and opportunities of hydrothermal carbonisation in the UK; case study in Chirnside," *RSC Advances,* vol. 10, no. 52, pp. 31586-31610, 2020.

[19] M.-M. Titirici, A. Funke and A. Kruse, "Hydrothermal Carbonization of Biomass," in *Recent Advances in Thermochemical Conversion of Biomass*, 2015, pp. 325-352.

[20] C. Areeprasert, P. Zhao, D. Ma, Y. Shen and K. Yoshikawa, "Alternative Solid Fuel Production from Paper Sludge Employing Hydrothermal Treatment," *Energy & fuels,* vol. 28, no. 2, pp. 1198-1206, 2014.

[21] N. Saha, A. Saba, P. Saha, K. McGaughy, D. Franqui-Villanueva, W. J. Orts, W. M. Hart-Cooper and M. T. Reza, "Hydrothermal Carbonization of Various Paper Mill Sludges: An Observation of Solid Fuel Properties," *Energies,* vol. 12, no. 5, p. 858, 2019.

[22] S. Oumabady, P. S. Sebastian, S. P. Kamaludeen, M. Ramasamy, P. Kalaiselvi and E. Parameswari, "Preparation and Characterization of Optimized Hydrochar from Paper Board Mill Sludge," *Nature Reserach,* vol. 10, no. 1, p. 773, 2020.

[23] C. He, H. Lin, L. Dai, R. Qiu, Y. Tang, Y. Wang, P.-G. Duan and Y. S. Ok, "Waste shrimp shell-derived hydrochar as an emergent material for methyl orange removal in aqueous solutions," *Environment International,* vol. 134, 2020.

[24] D. Kim, K. Lee and K. Y. Park, "Hydrothermal carbonization of anaerobically digested sludge for solid fuel production and energy recovery," *Fuel,* vol. 130, pp. 120-125, 2014.

[25] M. Niinipuu, K. G. Latham, J.-F. Boily, M. Bergknut and S. Jansson, "The impact of hydrothermal carbonization on the surface functionalities of wet waste materials for water treatment applications," *Environmental Science and Pollution Research volume ,* vol. 27, p. 24369–24379, 2020.

[26] A. E. Brown, G. L. Finnerty, M. A. Camargo-Valero and A. B. Ross, "Valorisation of macroalgae via the integration of hydrothermal carbonisation and anaerobic digestion," *Bioresource technology,* vol. 312, pp. 123539-123539, 2020.

[27] N. Patel, B. Acharya and P. Basu, "Hydrothermal Carbonization (HTC) of Seaweed (Macroalgae) for Producing Hydrochar," *Energies,* vol. 14, no. 7, p. 1805, 2021.

[28] Y. Lin, X. Ma, X. Peng, S. Hu, Z. Yu and S. Fang, "Effect of hydrothermal carbonization temperature on combustion behavior of hydrochar fuel from paper sludge," *Applied Thermal Engineering,* vol. 91, pp. 574-582, 2015.

[29] T. Prakoso, R. Nurastuti, R. Hendriansyah, J. Rizkiana, G. Suantika and G. Guan, "Hydrothermal Carbonization of Seaweed For Advanced Biochar Production," *MATEC Web of Conferences,* vol. 156, p. 05012, 2018.

[30] Q. Xu, Q. Qian, A. Quek, N. Ai, G. Zeng and J. Wang, "Hydrothermal Carbonization of Macroalgae and the Effects of Experimental Parameters on the Properties of Hydrochars," *ACS Sustainable Chemistry & Engineering,* vol. 1, no. 9, p. 1092–1101, 2013.

[31] J.-h. Zhang, Q.-m. Lin and X.-r. Zhao, "The Hydrochar Characters of Municipal Sewage Sludge Under Different Hydrothermal Temperatures and Durations," *Journal of Integrative Agriculture,* vol. 13, no. 3, pp. 471-482, 2014.

[32] I. C. Kantarli, M. Pala, Y. Yildirim, J. Yanik and M. H. Abreu, "Fuel characteristics and combustion behavior of seaweed-derived hydrochars," *Turkish journal of chemistry,* vol. 43, no. 2, p. 475–491, 2019.

[33] G. Zeng, S. Lou, H. Ying, X. Wu, X. Dou, N. Ai and J. Wang, "Preparation of Microporous Carbon from Sargassum horneri by Hydrothermal Carbonization and KOH Activation for CO2 Capture," *Journal of Chemistry,* 2018.

[34] X. Liu, Y. Zhai, S. Li, B. Wang, T. Wang, Y. Liu, Z. Qiu and C. Li, " Hydrothermal carbonization of sewage sludge: Effect of feed-water pH on hydrochar's physicochemical properties, organic component and thermal behavior," *Journal of hazardous materials,* vol. 388, pp. 122084-122084, 2020.

[35] A. Shrestha, B. Acharya and A. A. Farooque, "Study of hydrochar and process water from hydrothermal carbonization of sea lettuce," *Renewable energy,* vol. 163, pp. 589-598, 2021.

[36] A. Méndez, G. Gascó, B. Ruiz and E. Fuente, "Hydrochars from industrial macroalgae “Gelidium Sesquipedale” biomass wastes," *Bioresource technology,* vol. 275, pp. 386-393, 2019.

[37] S. Kannan, Y. Gariepy and G. S. V. Raghavan, "Optimization of Enzyme Hydrolysis of Seafood Waste for Microwave Hydrothermal Carbonization," *Energy & fuels,* vol. 29, no. 12, pp. 8006-8016, 2015.

[38] S. Kannan, Y. Gariepy and G. S. V. Raghavan, "Optimization and Characterization of Hydrochar Derived from Shrimp Waste," *Energy & fuels,* vol. 31, no. 4, pp. 4068-4077, 2017.

[39] S. Kannan, Y. Gariepy and G. S. V. Raghavan, "Conventional Hydrothermal Carbonization of Shrimp Waste," *Energy & fuels,* vol. 32, no. 3, pp. 3532-3542, 2018.

[40] R. Wu, Y. Li, X. Pang, Z. Hu and X. Jian, "Insight into evolution of chemical structure and mineralogy to reveal the mechanism of temperature-dependent phosphorus release from hydrochars," *Industrial Crops and Products,* no. 185, p. 115101, 2022.

[41] Z. Chen, H. Jia, Y. Guo, Y. Li and Z. Liu, "Nitrogen-doped hydrochars from shrimp waste as visible-light photocatalysts: Roles of nitrogen species," *Environmental Research,* vol. 208, p. 112695–112695, 2022.

[42] S. Mikhail, *Microwave Hydrothermal Carbonization of Lobster Waste,* ProQuest Dissertations Publishing, 2020.

[43] X. Han, Z. Wu, Y. Yang, J. Guo, Y. Wang, L. Cai, W. Song and L. Ji, "Facile Preparation of a Porous Biochar Derived from Waste Crab Shell with High Removal Performance for Diesel," *Journal of Renewable Materials,* vol. 9, no. 8, p. 1377–1391, 2021.

[44] L. Peng, Y. Liang, J. Huang, L. Xing, H. Hu, Y. Xiao, H. Dong, Y. Liu and M. Zheng, "Mixed-Biomass Wastes Derived Hierarchically Porous Carbons for High-Performance Electrochemical Energy Storage," *ACS Sustainable Chemistry & Engineering,* vol. 7, no. 12, p. 10393–10402, 2019.

[45] J. Wu, J. Yang, P. Feng, L. Wen, G. Huang, C. Xu and B. Lin, "Highly efficient and ultra-rapid adsorption of malachite green by recyclable crab shell biochar.," *Journal of Industrial and Engineering Chemistry,* p. 206–214, 2022.

[46] A. M. Smith and A. B. Ross, "Production of bio-coal, bio-methane and fertilizer from seaweed via hydrothermal carbonisation," *Algal Research,* vol. 16, pp. 1-11, 2016.

[47] C. He, A. Giannis and J.-Y. Wang, "Conversion of sewage sludge to clean solid fuel using hydrothermal carbonization: Hydrochar fuel characteristics and combustion behavior," *Applied energy,* vol. 111, pp. 257-266, 2013.

[48] V. Novikov, S. Derkach and I. Konovalova, "Chitosan Technology from Crustacean Shells of the Northern Seas," *KnE Life Sciences,* pp. 65-74, 2020.

[49] Stat-Ease, Inc., "Design Expert V13 - Information," Stat-Ease, Inc., [Online]. Available: https://statease.com/docs/v13/. [Accessed January 2023].

[50] ASTM, "Standard Test Method for Chemical Analysis of Wood Charcoal".

[51] H. J. Burke and F. Kerton, "Sequential Extraction of Valuable Bio-Products from Snow Crab (Chionoecetes opilio) Processing Discards Using Eco-Friendly Methods," *Marine drugs,* vol. 21, no. 6, p. 366, 2023.

[52] L. Dai, F. Tan, H. Li, N. Zhu, M. He, Q. Zhu, G. Hu, L. Wang and J. Zhao, "Calcium-rich biochar from the pyrolysis of crab shell for phosphorus removal," *Journal of environmental management,* vol. 198, no. Pt 1, pp. 70-74, 2017.

[53] S. Kannan, I. Burelle, V. Orsat and G. S. Vijaya Raghavan, "Characterization of Bio-crude Liquor and Bio-oil Produced by Hydrothermal Carbonization of Seafood Waste," *Waste and Biomass Valorization,* vol. 11, no. 7, pp. 3553 - 3565, 2020.

[54] B. Coto, C. Martos, J. Peña, R. Rodríguez and G. Pastor, "Effects in the solubility of CaCO3: Experimental study and model description," *Fluid phase equilibria,,* vol. 324, pp. 1-7, 2012.

[55] Z. Sebestyén, E. Jakab, A. Domán, P. Bokrossy, I. Bertóti, J. Madarász and K. László, "Thermal degradation of crab shell biomass, a nitrogen-containing carbon precursor," *J Therm Anal Calorim,* vol. 142, p. 301–308, 2020.

[56] D. Saravanan and P. N. Sudha, "Batch Adsorption Studies for the Removal of Copper from Wastewater using Natural Biopolymer," *International Journal of ChemTech Research,* vol. 6, no. 7, pp. 3496-3508, 2014.

[57] S. R. K. Raut, S. S. Rohiwal, A. P. Tiwari, A. Gnanamani, S. Pushpavanam, S. G. Nanaware and S. H. Pawar, "In vitro biocompatibility and antimicrobial activity of chitin monomer obtain from hollow fiber membrane," *Designed Monomers and Polymers,* vol. 19, no. 5, p. 445–455, 2016.

[58] D. Hopkins, "Adsorption of Copper by Crab Shell Biochar," St. John's, 2021.

[59] J. Coates, "Interpretation of Infrared Spectra, A Practical Approach," in *Encyclopedia of Analytical Chemistry*, R. Meyers, Ed., Chinchester, John Wiley & Sons Ltd, 2000, p. 10815–10837.

[60] A. Krutof, H. Bamdad, K. Hawboldt and S. MacQuarrie, "Co-pyrolysis of softwood with waste mussel shells: Biochar analysis," *Fuel (Guildford),* vol. 282, p. 118792, 2020.

[61] A. Krutof, "Enhancement of fast pyrolysis oil fuel properties through co-pyrolysis and improved analysis," Memorial Univeristy of Newfoundland, St. John's, 2019.

[62] J. Kumirska, M. Czerwicka, Z. Kaczyński, A. Bychowska, K. Brzozowski, J. Thöming and P. Stepnowski, "Application of spectroscopic methods for structural analysis of chitin and chitosan," *Marine Drugs,* vol. 8, no. 5, pp. 1567-1636, 2010.

[63] M. H. Derkani, A. J. Fletcher, M. Fedorov, W. Abdallah, B. Sauerer, J. Anderson and Z. J. Zhang, "Mechanisms of Surface Charge Modification of Carbonates in Aqueous Electrolyte Solutions," *Colloids and Interfaces,* vol. 3, no. 4, p. 62, 2019.

[64] M. Osada, C. Miura, Y. S. Nakagawa, M. Kaihara, M. Nikaido and K. Totani, "Effect of sub- and supercritical water treatments on the physicochemical properties of crab shell chitin and its enzymatic degradation," *Carbohydrate polymers,,* vol. 134, pp. 718-725, 2015.

[65] H. U. Rehman, S. Cord-Landwehr, V. Shapaval, S. Dzurendova, A. Kohler, B. M. Moerschbacher and B. Zimmermann, "High-throughput vibrational spectroscopy methods for determination of degree of acetylation for chitin and chitosan," *Carbohydrate polymers,* vol. 302, no. Article 120428, pp. 120428-120428, 2023.

[66] S. Arulvel, A. Elayaperumal and M. Jagatheeshwaran, "Discussion on the feasibility of using proteinized/deproteinized crab shell particles for coating applications: Synthesis and characterization," *Journal of environmental chemical engineering,* vol. 4, no. 4, pp. 3891-3899, 2016.

[67] F. Parker, "Amides and Amines," in *Applications of Infrared Spectroscopy in Biochemistry, Biology, and Medicine*, F. Parker, Ed., Springer US, pp. 165-172.

[68] v. v. The kinetics and mechanisms of amorphous calcium carbonate (ACC) crystallization to calcite, "The kinetics and mechanisms of amorphous calcium carbonate (ACC) crystallization to calcite, via vaterite," *Nanoscale,* vol. 3, no. 1, pp. 265-271, 2011.

[69] X. Zhuang, J. Liu, Q. Zhang, C. Wang, H. Zhan and L. Ma, "A review on the utilization of industrial biowaste via hydrothermal carbonization," *Renewable & sustainable energy reviews, 2022,,* vol. 154, p. 154, 2022.

[70] A. L. Pauline and K. Joseph, "Hydrothermal carbonization of organic wastes to carbonaceous solid fuel – A review of mechanisms and process parameters," *Fuel (Guildford),* vol. 279, p. 118472, 2020.

[71] Z. Liu, M. Matouri, U. Zahid and M. D. Saldaña, "Value-added compounds obtained from shrimp shells using subcritical water with carboxylic acids," *The Journal of supercritical fluids,,* vol. 197, p. 105902, 2023.

[72] M. Vilasoa-Martínez, J. López-Hernández and M. A. Lage-Yusty, "Protein and amino acid contents in the crab, Chionoecetes opilio," *Food chemistry,* vol. 103, no. 4, pp. 1330-1336, 2007.

[73] P. Körner, "Hydrothermal Degradation of Amino Acids," *ChemSusChem,,* vol. 14, no. 22, pp. 4947-4957, 2021.

[74] J. Fang, B. Gao, J. Chen and A. R. Zimmerman, "Hydrochars derived from plant biomass under various conditions: Characterization and potential applications and impacts," *Chemical engineering journal (Lausanne, Switzerland : 1996),* vol. 267, pp. 253-259, 2015.

[75] R. Wang, Z. Lin, S. Meng, S. Liu, Z. Zhao, C. Wang and Q. Yin, "Effect of lignocellulosic components on the hydrothermal carbonization reaction pathway and product properties of protein," *Energy,* vol. 259, p. 125063, 2022.

[76] W. Yang, H. Wang, J. Zhou and S. Wu, "Hydrolysis kinetics and mechanism of chitin in subcritical water," *The Journal of supercritical fluids,,* vol. 135, pp. 254-262, 2018.

[77] T. M. Aida, K. Oshima, C. Abe, R. Maruta, M. Iguchi, M. Watanabe and R. L. Smith, "Dissolution of mechanically milled chitin in high temperature water," *Carbohydrate polymers,* vol. 106, pp. 172-178, 2014.

[78] C. I. Rivas-Vela, S. L. Amaya-Llano, E. Castaño-Tostado and G. A. Castillo-Herrera, "Protein Hydrolysis by Subcritical Water: A New Perspective on Obtaining Bioactive Peptides," *Molecules,* vol. 26, no. 21, p. 6655, 2021.

[79] G. Hao, W. Cao, T. Li, J. Chen, J. Zhang, W. Weng, K. Osako and H. Ren, "Effect of temperature on chemical properties and antioxidant activities of abalone viscera subcritical water extract," *The Journal of supercritical fluids,* vol. 147, pp. 17-23, 2019.

[80] Y.-R. Jeong, J.-S. Park, D. Nkurunziza, Y.-J. Cho and B.-S. Chun, "Valorization of blue mussel for the recovery of free amino acids rich products by subcritical water hydrolysis," *The Journal of supercritical fluids,* vol. 169, p. 105135, 2021.

[81] R. Ahmed and B.-S. Chun, "Subcritical water hydrolysis for the production of bioactive peptides from tuna skin collagen," *The Journal of supercritical fluids,,* vol. 141, pp. 88-96, 2018.

Chapter 4 – Conclusion and Recommendation

This study aims to investigate the effect of hydrothermal carbonization conditions on the crab hydrochar properties, including assessing the properties for suitable application to valorize crab by-products. Crab by-product feedstock mainly consists of chitin, protein, and minerals (calcium carbonate). The XRD of hydrochar produced in this study showed that after HTC, chitin and calcium carbonate were retained in the hydrochar. Trace analysis further confirmed that calcium was the most abundant mineral in the feedstock and selected hydrochar. The carbon content of the hydrochar was lower or approximately the same as the feedstock, likely due to the calcium carbonate dissolution and polymerization reaction occurring simultaneously. On the other hand, the hydrochar nitrogen content was lower compared to the feedstock. There are two possible reasons for decreasing nitrogen content: protein or chitin degradation/hydrolysis. In this study, the decrease in nitrogen content is more likely due to protein reactions since chitin is thermally stable at the temperatures studied in this thesis. The hydrochar ash content is up to 34% higher than feedstock, and the high ash content made the crab by-product unsuitable for fuel application due to possible fouling and slagging during combustion. The hydrochar BET surface area was higher than the feedstock's and increased with temperature and water ratio to a maximum of 26 m^2/g at 260 °C, water ratio 3 and 30 min. However, increasing the time to a maximum of 3 h reduced the surface area due to pore collapse, deformation, fusion, or melting. The FTIR of the feedstock and hydrochar showed the functional groups related to chitin, such as O-H, N-H, C-H, C=O, C-O, N-H bending, and C-N stretching. Furthermore, carbonate ion peaks from CaCO3 were detected in the feedstock FTIR. The results of the FTIR show that hydrochar has similar functional groups as the feedstock. Further, the peaks related to chitin and $CaCO_3$ confirm the presence of both compounds in the feedstock and hydrochar. The confirmation of the functional groups along with the increase in hydrochar surface area indicate that the hydrochar may be suitable for adsorption. For example, the high surface area and oxygen-containing functional groups (e.g., O-H and C=O) show potential for removing organic contaminants from wastewater, including pesticide and dye, through potential mechanism such as pore filling, H-bonding, and ion exchange [103, 104]. Additionally, hydrochar can be utilized for heavy metal removal in soil and wastewater such as Cd^{2+}, Cu^{2+}, and Pb^{2+} via electron exchange with Ca^{2+} [1] and ion exchange or surface complexation or electrostatic interaction with O-H and C=O functional groups [3, 4].

In conclusion, hydrothermal carbonization (HTC) of crab by-product is a relatively simple process that diverts material from landfills/oceans through conversion to value-added products.

Further, carbon that could have formed GHGs is fixed in the hydrochar. There are limited studies of the valorization of crab by-products using HTC, and the bulk of these studies use pre-treatment methods that use hazardous chemicals and could be unsuitable for the remote location of the processing plant. This thesis is the first step in crab by-product utilization by hydrothermal carbonization, where the effect of operating conditions on hydrochar quality and yield was studied. It is crucial to further the study of this area as it shows potential waste management and valorization methods of crab by-product, and it is recommended for:

- Further work to focus on analysis of the liquid product for proteins, amino acids, and other compounds to better assess where one mechanism is dominating over another. Characterization/analysis of the liquid product is also beneficial to assess liquid product utilization or treatment for designing a sustainable process.
- The hydrochar produced in this study has been assessed for potential application, one of them as a bioadsorbent. From existing studies on crab hydrochar or biochar, wastewater pollutant adsorbent applications to explore can be for dye [104], heavy metals [107], or diesel adsorption [108]. In addition to adsorption performance, it is also recommended to include the spent hydrochar regeneration method to increase process efficiency by reducing new adsorbent needs and generating less waste.
- The hydrochar is also asses for potential soil amendment application. Exploring the soil studies area is recommended to determine hydrochar's applicability, including minerals or nutrients (such as N, K, Ca, and Mg) available in the hydrochar (including concentration) needed in soil and hydrochar adsorption affinity to soil pollutants (e.g., heavy metals). [1]
- The HTC was conducted on a laboratory scale without mixing. For process scale-up, it is recommended to conduct mass transfer studies and applicable mixing methods, as both are critical to ensure uniform distribution of the feed and water during HTC. This is important to ensure efficient process and consistent quality of the product.
- It is recommended to do zeta potential analysis for further insight on the charge of the hydrochar for understanding interactions at the solid-fluid and solid-solid interfaces in adsorption application [5, 7].

References

[1] A. Khosravi, H. Zheng, Q. Liu, M. Hashemi, Y. Tang and B. Xing, "Production and characterization of hydrochars and their application in soil improvement and environmental remediation," *Chemical engineering journa,* vol. 430, p. 133142, 2022.

[2] J. Wu, J. Yang, P. Feng, L. Wen, G. Huang, C. Xu and B. Lin, "Highly efficient and ultra-rapid adsorption of malachite green by recyclable crab shell biochar.," *J. Ind. Eng. Chem.,* p. 206–214, 2022.

[3] H. Lu, W. Zhang, Y. Yang, X. Huang, S. Wang and R. Qiu, "Relative distribution of Pb^{2+} sorption mechanisms by sludge-derived biochar," *Water research,* vol. 46, no. 3, pp. 854-862, 2012.

[4] X. Yang, Y. Wan, Y. Zheng, F. He, Z. Yu, J. Huang, H. Wang, Y. S. Ok, Y. Jiang and B. Gao, "Surface functional groups of carbon-based adsorbents and their roles in the removal of heavy metals from aqueous solutions: A critical review," *Chemical engineering journal,* vol. 366, pp. 608-621, 2019.

[5] D. Hopkins, "Adsorption of Copper by Crab Shell Biochar," St. John's, 2021.

[6] X. Han, Z. Wu, Y. Yang, J. Guo, Y. Wang, L. Cai, W. Song and L. Ji, "Facile Preparation of a Porous Biochar Derived from Waste Crab Shell with High Removal Performance for Diesel," *J Renew Mater,* vol. 9, no. 8, p. 1377–1391, 2021.

[7] A. Serrano-Lotina, R. Portela, P. Baeza, V. Alcolea-Rodriguez, M. Villarroel and P. Ávila, "Zeta potential as a tool for functional materials development," *Catalysis today,* vol. 2023, p. 113862, 2023.

APPENDIX A – Supplementary Material

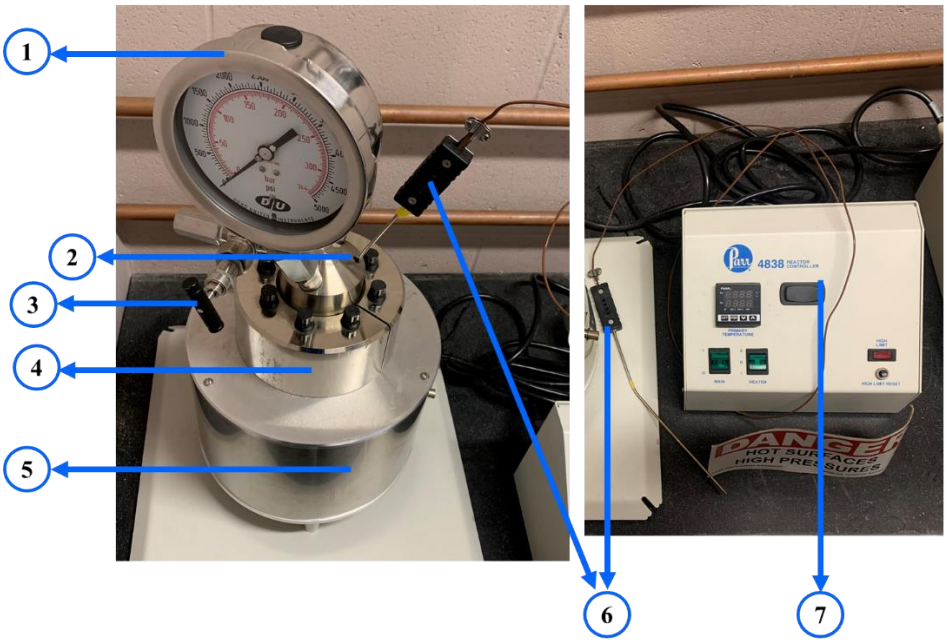

1. Pressure Gauge
2. Thermowell
3. Pressure Relief Valve
4. Reactor
5. Heater
6. Thermocouple
7. Temperature Controller

Figure A1. Reactor Schematic.

Table A1. - Ash content of the hydrochar and compared with ash content on the crab shell basis

Run	R	T	time	g/g crab shell	g/g hydrochar
Raw Crab Shell	-	-	-	0.322	0.322
1	3	220	1.75	0.283	0.392
2	4	260	1.75	0.278	0.432
3	4	220	0.5	0.260	0.366
4	2	220	3	0.305	0.377
5	3	260	3	0.271	0.421
6	3	180	3	0.276	0.348
7	3	180	0.5	0.275	0.358
8	2	220	0.5	0.287	0.361
9	2	180	1.75	0.266	0.336
10	2	260	1.75	0.282	0.395
11	3	220	1.75	0.286	0.399
12	4	220	3	0.291	0.408
13	3	220	1.75	0.290	0.404
14	3	260	0.5	0.282	0.416
15	4	180	1.75	0.266	0.373
HC	2.4	260	0.5	0.281	0.370
HWC	2.22	260	1.75	0.262	0.405

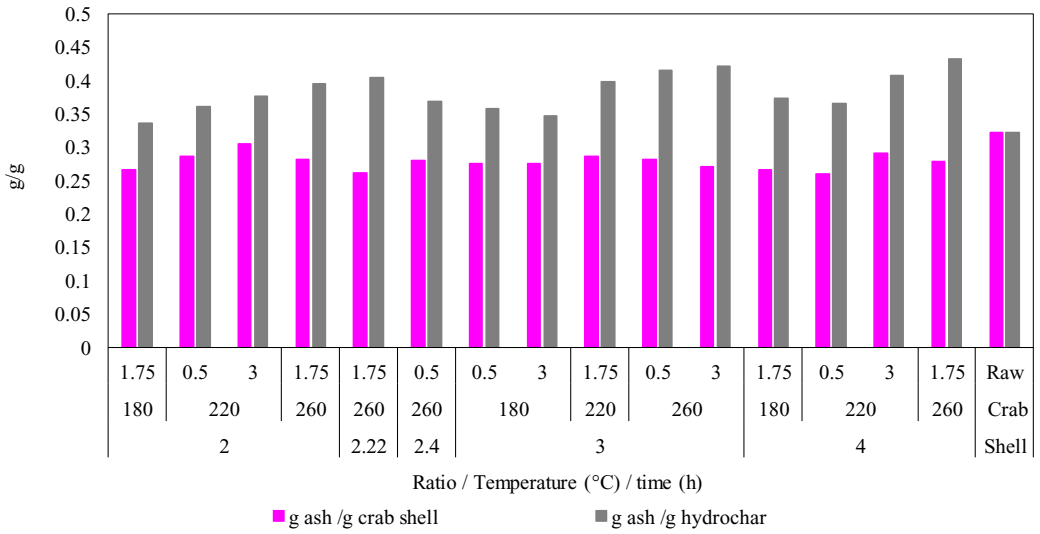

Figure A2. - Ash content of the hydrochar and compared with ash content on the crab shell basis

Table A2. XRD Peak Ratio

				Peak Data		Peak Ratio
Run	R	T	time	Chitin	$CaCO_3$	Chitin/$CaCO_3$
RC	-	-	-	749	583	1.28
1	3	220	1.75	144	192	0.75
2	4	260	1.75	124	192	0.65
3	4	220	0.5	146	148	0.99
4	2	220	3	150	163	0.92
5	3	260	3	99	155	0.64
7	3	180	0.5	143	141	1.01
10	2	260	1.75	107	156	0.69
11	3	220	1.75	178	168	1.06
12	4	220	3	147	132	1.11
14	3	260	0.5	132	174	0.76
16	2.22	260	1.75	101	186	0.54
17	2.42	260	0.5	162	192	0.84

Table A3. H14 hydrochar and liquid trace element comparison (mg/L)

Sample	In Hydrochar	In Liquid
Ca	4012	2570
P	672	1.7
Mg	291.67	76
Na	107	2570
S	107.67	1100
Sr	63	0.11
K	45	1160
Fe	2.99	0.62
Zn	0.81	<0.05
Si	0.83	15.4
Cu	0.58	<0.1
Mn	0.64	0.02
Ba	0.39	<0.05

Table A4. FTIR Peak Ratio

				Peak Data			Peak Ratio	
Run	R	T (°C)	t (h)	O-H	N-H	C-H	O-H/NH	O-H/CH
RC	-	-	-	92.41	89.68	91.23	1.03	1.01
1	3	220	1.75	43.32	68.01	94.29	0.64	0.46
2	4	260	1.75	52.59	68.77	88.91	0.76	0.59
3	4	220	0.5	93.32	86.65	95.21	1.08	0.98
4	2	220	3	83.19	86.65	92.12	0.96	0.90
5	3	260	3	23.16	44.75	79.86	0.52	0.29
6	3	180	3	57.66	73.25	89.35	0.79	0.65
7	3	180	0.5	93.69	95.06	97.14	0.99	0.96
8	2	220	0.5	74.52	81.38	93.22	0.92	0.80
9	2	180	1.75	74.05	86.42	98.88	0.86	0.75
10	2	260	1.75	48.05	62.71	87.98	0.77	0.55
11	3	220	1.75	66.90	80.88	97.27	0.83	0.69
12	4	220	3	43.99	68.78	96.86	0.64	0.45
13	3	220	1.75	54.17	75.80	97.22	0.71	0.56
14	3	260	0.5	96.89	98.04	98.90	0.99	0.98
15	4	180	1.75	70.02	85.48	97.20	0.82	0.72
HC	2.4	260	0.5	63.96	65.86	67.16	0.97	0.95
HWC	2.22	260	1.75	36.72	36.85	43.11	1.00	0.85

Table A5. Hydrochar and Liquid pH

Sample	R	T (°C)	t (h)	Liquid pH	Hydrochar pH
Raw Crab Shell	-	-	-	-	8.81
H1	3	220	1.75	8.88	8.09
H2	4	260	1.75	9.43	7.98
H3	4	220	0.5	8.95	8.54
H4	2	220	3	8.75	8.12
H5	3	260	3	8.85	7.87
H6	3	180	3	8.77	8.31
H7	3	180	0.5	8.99	8.62
H8	2	220	0.5	8.97	8.11
H9	2	180	1.75	8.78	8.17
H10	2	260	1.75	8.96	7.9
H11	3	220	1.75	9.06	8.16
H12	4	220	3	9.03	8.36
H13	3	220	1.75	9.15	8.16
H14	3	260	0.5	9.09	8.1
H15	4	180	1.75	8.6	8.4
HC	2.42	260	0.5	9.12	7.98
HWC	2.22	260	1.75	9.53	7.75